SHEAR STRENGTH OF CORRODED REINFORCED CONCRETE BEAMS

BY

ASHHAD IMAM

A Thesis Presented to the
DEANSHIP OF GRADUATE STUDIES

KING FAHD UNIVERSITY OF PETROLEUM & MINERALS

DHAHRAN, SAUDI ARABIA

In Partial Fulfillment of the
Requirements for the Degree of

MASTER OF SCIENCE

In

CIVIL ENGINEERING

MAY, 2012

KING FAHD UNIVERSITY OF PETROLEUM AND MINERALS
DHAHRAN, 31261, SAUDI ARABIA

DEANSHIP OF GRADUATE STUDIES

This thesis, written by **ASHHAD IMAM** under the direction of his thesis advisor and approved by his thesis committee, has been presented to and accepted by the Dean of Graduate Studies, in partial fulfillment of the requirement for the degree of **MASTER OF SCIENCE IN CIVIL ENGINEERING.**

Thesis Committee

Dr. Abul Kalam Azad (Advisor)

Dr. Shamshad Ahmad (Co-advisor)

Dr. Mohammad Maslehuddin (Member)

Dr. Ahmad Saad Algahtani (Member)

Dr. Salah U Dulaijan (Member)

03 JUN 2012

Dr. Nedal T. Ratrout
Department Chairman

Dr. Salam A. Zummo
Dean of Graduate Studies

4/6/12

Date

DEDICATED

TO

MY FAMILY & FRIENDS

ACKNOWLEDGEMENTS

First and foremost, I thank Allah (azza wajal) for bestowing me with health, patience, and knowledge to complete this work. Acknowledgement is due to the King Fahd University of Petroleum and Minerals for the support given to this research through its excellent facilities and for granting me the opportunity to pursue my graduate studies with financial support.

I acknowledge, with deep gratitude and appreciation, the inspiration, encouragement, valuable time and guidance given to me by Prof. Abul Kalam Azad, who served as my major advisor. Thereafter, I am deeply indebted and grateful to Dr. Shamshad Ahmad, my co-advisor, and Dr. Mohammed Maslehuddin, my committee member, for their extensive guidance, continuous support, and personal involvement in all phases of this research. I am also grateful to my other committee members, Dr. Ahmad S. Al- Gahtani and Dr. Salah U Dulaijan for their constructive guidance, valuable advices and cooperation.

I also acknowledge the sincere and untiring efforts of Mr. Omer and Mr. Imran who assisted me during all stages of my experiments and also helped me in preparing the experimental set-up utilized in this study. Thanks are due to the laboratory personnel Engr Mukarram Khan and Dr. Essa, for their substantial assistance in the experimental work, and also to the department secretaries, Mr. Efren and Mr. Oli for their help and assistance.

I am also indebted to the department chairman, Dr. Nedal T Ratrout and other faculty members for their support. Thanks are due to my senior colleagues at the University, Mr. Shameem and Mr. Ibrahim for their valuable advices. Special thanks are due to Mr. Mohammed Al Osta, Md Imtiaz Hossain, Maaz Farooqui, Syed Abdul Baqi and Amer bin Ziyad who were always there to help me in my work and my sincere appreciation is due to all other housing friends who provided wonderful company and some memories that will last a

lifetime. My deep sense of appreciation is towards Indian community for creating the niche needed for us to nurture our interests and abilities. Finally, I would like to express my deepest gratitude to my mother, father, sisters, brothers, and all other relatives, for their emotional and moral support throughout my academic career and also for their love, patience, encouragement and prayers.

TABLE OF CONTENTS

TABLE OF CONTENTS vi

LIST OF TABLES xi

LIST OF FIGURES xii

THESIS ABSTRACT xv

THESIS ABSTRACT (ARABIC) xvi

CHAPTER 1 1

INTRODUCTION 1

1.1 REINFORCEMENT CORROSION 1

1.2 EFFECT OF REINFORCEMENT CORROSION ON THE PERFORMANCE OF REINFORCED CONCRETE ELEMENTS 3

1.3 NEED FOR THIS RESEARCH 5

1.4 SCOPE AND OBJECTIVES 5

1.4.1 Scope 5

1.4.2 Objectives 6

CHAPTER 2 7

LITERATURE REVIEW 7

2.1 SHEAR STRENGTH OF REINFORCED CONCRETE BEAMS 7

2.2 CORROSION IN REINFORCED CONCRETE ELEMENTS 9

2.2.1 Effect of Corrosion 9

2.2.2 Mechanism of Corrosion in Reinforced Concrete 10

2.2.3 Types of Corrosion in Reinforced Concrete 13

2.3 EFFECT OF CORROSION ON FLEXURAL AND BOND STRENGTH OF REINFORCED CONCRETE MEMBERS……..... 15

2.3.1 Effect of Corrosion on Flexural Strength of RC Members..... 15

2.3.2 Effect of Corrosion on Bond Strength of RC Members 23

2.4 EFFECT OF CORROSION ON SHEAR STRENGTH OF REINFORCED CONCRETE BEAMS.…..……..……..26

2.4.1 Effect of Corrosion on Shear Strength of RC Beams 26

2.4.2 Shear Strength of RC Beams with Exposed or Corroded Longitudinal.....27

2.4.3 Shear Strength of RC Beams with Damaged or Corroded Stirrups 29

2.4.4 Shear strength of RC beams with corroded Longitudinal Steel and Stirrups……..…. 32

2.5 A SYNOPSIS OF PAST WORK.…….……..……...33

2.6 RELIABILITY ANALYSIS OF REINFORCED CONCRETE BEAM 34

CHAPTER 3 37

METHODOLOGY OF RESEARCH 37

3.1 EXPERIMENTAL PROGRAM…… 37

3.2 EXPERIMENTAL VARIABLES…….……37

3.3 TEST SPECIMENS…… 38

3.4 DETAILS OF TEST SPECIMENS…….……...39

3.5 CONCRETE CONSTITUENTS……..... 41

3.6 PREPARATION OF BEAM SPECIMENS……..... 41

3.6.1 Concrete Mix Proportions..... 41

3.7 FABRICATION OF TEST SPECIMENS…….. 42

3.8 DESIGNATION OF BEAM SPECIMENS…….....44

3.9 STRENGTH OF MATERIALS……. 46

3.9.1 Compressive strength of concrete 46

3.9.2 Tensile Strength of Reinforcing Bars 46

3.10 ACCELERATED CORROSION……..…48

3.11 FLEXURAL TEST OF BEAMS…….……..52

3.12 GRAVIMETRIC WEIGHT LOSS……. 57

CHAPTER 4 60

RESULTS AND DISCUSSION 60

4.1 COMPRESSIVE STRENGTH OF CONCRETE.. ……..60

4.2 TENSILE STRENGTH OF STEEL……. 61

4.3 SHEAR STRENGTH OF CONTROL BEAM SPECIMENS 63

4.4 EXPERIMENTAL LOAD DEFLECTION PLOTS 64

4.4.1 Effect of corrosion on load-deflection behavior of beams 66

4.5 EXPERIMENTAL SHEAR CAPACITY OF BEAMS.....67

4.5.1 Control Beams…….. 67

4.5.2 Corroded beams…….……..68

4.6 GRAVIMETRIC WEIGHT LOSS……..……70

4.7 EFFECT OF CHOSEN VARIABLES ON REINFORCEMENT CORROSION……...…73

4.8 EFFECT OF CORROSION ACTIVITY INDEX ON RESIDUAL SHEAR STRENGTH OF CORRODED BEAMS…….. 76

4.9 SHEAR STRENGTH OF CORRODED BEAMS……78

4.10 MODE OF FAILURE OF CONTROL AND CORRODED BEAMS……..82

CHAPTER 5 84

PREDICTION OF RESIDUAL SHEAR STRENGTH 84

5.1 BASIS FOR THE DEVELOPMENT OF THE MODEL……..…….84

5.2 STRENGTH PREDICTION MODEL…….....85

5.2.1 Approach…….. 85

5.2.2 Correction Factor, R_v 86

5.3 COMPARISON OF THE PROPOSED METHOD WITH THE PAST RESEARCH DATA……. 92

5.3.1 Comparison with Rodriguez et al. data 92

5.3.2 Comparison with Juarez et al. data 94

5.4 RELIABILITY ANALYSIS OF REINFORCED CONCRETE BEAMS USING MONTE CARLO SIMULATION…… 96

5.4.1 Monte Carlo Simulation Basics 96

5.4.2 Techniques and steps involved for Monte Carlo Simulation.....97

5.4.3 Normal Probability Distribution 100

5.4.4 Development of Deterministic Safety Model 102

5.5 APPLICATION OF THE PROPOSED MONTE CARLO SIMULATION…….……...104

CHAPTER 6 110

CONCLUSIONS AND RECOMMENDATIONS.....110

6.1 CONCLUSIONS……. 110

6.2 SUGGESTIONS FOR FUTURE RESEARCH…….. 111

REFERENCES.....113

LIST OF NOTATIONS 121

APPENDIX A 123

Load Deflection Curves..... 123

APPENDIX B 134

Applications of the model 134

VITAE 140

LIST OF TABLES

Table 3.1: Test variables and specimens 38

Table 3.2: Weight of Constituents for a Cubic Meter of Concrete 42

Table 3.3: Beam Designations 45

Table 4.1: 28-days Compressive Strength of Concrete, (fc') 60

.Table 4.2: Yield and Ultimate Strengths and Strains of 8 and 20 mm Diameter Steel Bars... 62

Table 4.3: Theoretical Shear Capacity of Control Beams……..…64

Table 4.4: Flexure test results of Control Beams…….….65

Table 4.5: Flexure Test Results of Corroded Beams…….....65

Table 4.6: V_{exu} , V_{thu} and C_c for each group of specimens 68

Table 4.7: Values of $\mathbf{V_{exc}}$, $\mathbf{V_{exu}}$, and *R* for each Group of Specimens 69

Table 4.8: Gravimetric weight loss and their conversion into I_{corr} 72

Table 4.9: $I_{corr}T$ versus ρ Data for all sets of values 74

Table 4.10: $I_{corr}T$ versus R Data for all sets of values 77

Table 4.11: D', $V_{exp,c}$, $V_{th,c}$, and R_f for the Corroded Beams 81

Table 5.1: Values of R_v, $V_{th,c}$, $V_{exp,c}$ and V_{res} 88

Table 5.2: Comparison of the Proposed Model results with Rodriguez et al. [34] data 93

Table 5.3: Comparison of the Proposed Model results with Juarez et al. [71] data…….....95

Table 5.4: Statistical properties of random variables 105

LIST OF FIGURES

Figure 1.1: Effects of Reinforcement Corrosion on Reinforced Concrete Structures 4

Figure 2.1: Effects of corrosion on the load carrying capacity of a reinforced concrete member 10

Figure 2.2: Micro-corrosion cell formation in reinforced concrete……...12

Figure 3.1: Reinforcement Details of Tests specimens……..…40

Figure 3.2: Formwork with cages…….……43

Figure 3.3: Casting of beams……43

Figure 3.4: Moist Curing of concrete beams…….44

Figure 3.5: Arrangement for evaluating the tensile strength of steel bars……..……47

Figure 3.6: Combined set-up for Power supply……48

Figure 3.7: Schematic representation of the Accelerated corrosion test set-up…….……50

Figure 3.8: Two beams in series subjected to accelerated corrosion…….51

Figure 3.9: Set-up for four point bend test of beam specimens……53

Figure 3.10: Flexural strength test using Instron Universal Testing Machine……..…..53

Figure 3.11: Schematic diagram for the modified four point bend test set-up……..….54

Figure 3.12: Four point bend test set-up of beams specimens…….…….....55

Figure 3.13: Control Beam (A2-C) under flexural testing…….……56

Figure 3.14: Control Beam (B1-C) under flexural testing…….…….56

Figure 3.15: Sample of main bars corroded for 6 days (Sample No: B10-6)…….58

Figure 3.16: Sample of stirrups corroded for 6 days (Sample No: B10-6)……58

Figure 3.17: Sample of stirrups corroded for 10 days (Sample No: B5-10)……..59

Figure 4.1: Stress-strain plot for 8 mm diameter steel bar……61

Figure 4.2: Stress-strain plot for 20 mm diameter steel bar……..……62

Figure 4.3: Typical load deflection plot for beams of Group A……66

Figure 4.4: Typical load deflection plot for beams of Group B……67

Figure 4.5: Percentage weight loss versus $I_{corr}T$……..75

Figure 4.6: Failure of a typical Control beam (A2-C)……..…..82

Figure 4.7: Failure of a typical Corroded beam (B8-6)……..…83

Figure 4.8: A close view of crack pattern for control beam (B1-C)……..….83

Figure 5.1: Plot showing variation of R_v versus $I_{corr}T$……..89

Figure 5.2: Plot showing variation of R_v versus $I_{corr}T$ for different A_v/ds……...89

Figure 5.3: Variation of V_r with time for two different corrosion intensity……...……91

Figure 5.4: Comparison of measured V_{exp} and predicted VresV_{res} (Rodriguez Data)…..…..94

Figure 5.5: Schematic showing the basic principle behind Monte Carlo simulation……..….97

Figure 5.6: Flowchart representation of Reliability using Monte Carlo simulation……99

Figure 5.7: Cumulative Probability distribution for $f_c{}'$……...101

Figure 5.8: Cumulative Probability distribution for $I_{corr}T$ ……..……..…...101

Figure 5.9: Determination of critical time for corrosion damage...…….…….103

Figure 5.10: Determination of critical time, t^* for corrosion damage with γ = 1.4……..106

Figure 5.11: Variation of Probability of safety with critical time, t^* at different I_{corr}...…...107

Figure 5.12: Variation of Probability of safety with time for two different γ …….....108

Figure A. 1: Load-midspan deflection plot for Control Specimen A2-C……123

Figure A. 2: Load-midspan deflection plot for Corroded Specimen A3-10……124

Figure A. 3: Load-midspan deflection plot for Corroded Specimen A5-10……124

Figure A. 4: Load-midspan deflection plot for Corroded Specimen A6-10…….125

Figure A. 5: Load-midspan deflection plot for beams (Group A) corroded for 10 days….125

Figure A. 6: Load-midspan deflection plot for Corroded Specimen A7-6.……..126

Figure A. 7: Load-midspan deflection plot for Corroded Specimen A8-6……..….126

Figure A. 8: Load-midspan deflection plot for Corroded Specimen A9-6……...127

Figure A. 9: Load-midspan deflection plot for Corroded Specimen A10-6……..…127

Figure A. 10: Load-midspan deflection plot for beams (Group A) corroded for 6 days….128

Figure A. 11: Load-midspan deflection plot for Control Specimen B1-C……...128

Figure A. 12: Load-midspan deflection plot for two Control Specimens from Group B…129

Figure A. 13: Load-midspan deflection plot for Corroded Specimen B3-10……...129
Figure A. 14: Load-midspan deflection plot for Corroded Specimen B4-10……..…..130
Figure A. 15: Load-midspan deflection plot for Corroded Specimen B5-10……...130
Figure A. 16: Load-midspan deflection plot for Corroded Specimen B6-10……...131
Figure A. 17: Load-midspan deflection plot for beams (Group B) corroded for 10 days…131
Figure A. 18: Load-midspan deflection plot for Corroded Specimen B7-6……..132
Figure A. 19: Load-midspan deflection plot for Corroded Specimen B8-6……..132
Figure A. 20: Load-midspan deflection plot for beams (Group B) corroded for 6 days…..133

THESIS ABSTRACT

FULL NAME	**:**	ASHHAD IMAM
TITLE	**:**	SHEAR STRENGTH OF CORRODED REINFORCED CONCRETE BEAMS
MAJOR	**:**	CIVIL ENGINEERING
DATE	**:**	MAY 2012

Corrosion of reinforcing steel and subsequent concrete deterioration is a major problem faced by the construction industry. However, limited work is available for the estimation of the shear strength of corrosion-damaged members.

In the present work, an effort has been made to develop a model to predict the shear strength of reinforced concrete beams with varying degree of reinforcement corrosion. The experimental variables included: corrosion duration and the cross section of a beam. A total of 20 reinforced concrete beams with different cross sections as (140 x 220 x 1150 mm & 150 x 240 x 1150 mm) were tested, out of which 4 beams were earmarked as control beams that were not subjected to corrosion and the remaining 16 beams were subjected to corrosion by impressed current technique. All the corroded and control beams were tested in four point bend tests. After the bending tests, the beams were broken to retrieve the reinforcing steel in order to assess the gravimetric weight loss.

Results indicated that the product of corrosion current density and corrosion period $I_{corr}T$, is the significant factor affecting the shear strength of a corroded beam. Based on the experimental data, an approach to predict the residual shear strength of corroded beam has been proposed. Monte Carlo simulation was used to determine the probability of failure based on the proposed strength prediction model.

THESIS ABSTRACT (ARABIC)

الاسم: أشهد إمام

العنوان: القص قوة الحزمة تآكل الخرسانة المسلحة

التخصص: الهندسة المدنية

التاريخ: قد 2012

تآكل حديد التسليح واللاحقة تدهور الخرسانة هي المشكلة الرئيسية التي تواجه صناعة البناء والتشييد. ومع ذلك، عمل محدود متاح لتقدير قوة القص من تآكل وتلف الأعضاء.
في هذا العمل، وقد تم بذل جهد لتطوير نموذج للتنبؤ قوة القص للكمرات الخرسانة المسلحة مع درجات متفاوتة من صدأ حديد التسليح. وشملت المتغيرات التجريبية: مدة التآكل وقطاع عريض من شعاع. ما مجموعه 20 الحزم الخرسانة المسلحة مع مقاطع عرضية مختلفة مثل (140 × 220 × 1150 ملم و 150 × 240 × 1150 ملم) تم اختبارها، منها خصصت 4 الحزم والحزم السيطرة التي لم تخضع للتآكل وال 16 المتبقية وتعرض الحزمة للتآكل بواسطة تقنية الحالية أعجب. وجرى اختبار كل الحزم المتآكلة والتحكم في أربعة اختبارات منحنى نقطة. بعد الاختبارات الانحناء، تم كسر الحزم لاسترداد حديد التسليح من أجل تقييم وفقدان الوزن الجاذبية.

وأشارت النتائج إلى أن المنتج من الكثافة الحالية للتآكل والصدأ $I_{corr}T$ فترة، هو عامل مهم يؤثر على قوة القص من شعاع المتآكلة. استنادا إلى بيانات تجريبية، وهو نهج للتنبؤ تم اقتراح قوة القص المتبقية من شعاع المتآكلة. واستخدمت مونتي كارلو محاكاة لتحديد احتمال الفشل استنادا إلى نموذج قوة التنبؤ المقترحة.

درجة الماجستير في العلوم

جامعة الملك فهد للبترول و المعادن

الظهران المملكة العربية السعودية

CHAPTER 1

INTRODUCTION

1.1 REINFORCEMENT CORROSION

Corrosion of reinforcing steel is one of the major worldwide deterioration problems for the reinforced concrete structures. Research in Saudi Arabia and elsewhere in the Middle East indicated that the service life of buildings in the Arabian Gulf is between 10 and 15 years [1]. What could be more frustrating than knowing that corrosion was, in some cases, so severe that concrete damage occurred even before the completion of construction? [2]. While the corrosion of reinforcing steel is not the sole cause of all structural deficiencies, it is a significant contributor and has therefore become a matter of great concern. The highly alkaline environment of good quality concrete leads to the formation of a passive film on the surface of the embedded steel, which protects it from corrosion [3]. In addition, well-consolidated and properly cured concrete with a low water to cement ratio has a low permeability, which minimizes diffusion of corrosion inducing agents, such as chloride, carbon dioxide, moisture, etc. to the steel surface. Further, the high electrical resistivity of concrete restricts the rate of corrosion by reducing the flow of hydroxyl ions from anode to

cathode. At the outset, it must be mentioned that, usually in a properly designed, constructed and maintained structure, there should be little or no problem of steel corrosion during its design life. However reinforcement corrosion occurs either due to carbonation of concrete or diffusion of chloride ions to the steel surface.

When reinforcement corrodes, the strength of a reinforced concrete member is undermined in several ways. Since corrosion products have a greater volume than the parent steel, internal tensile stresses will develop in the concrete at the steel/concrete interface. As a result, the surrounding concrete cracks and will eventually spall away, as corrosion advances. In addition, under tensile stresses developed during corrosion, existing fine and micro cracks in the surrounding concrete tend to enlarge and form a network of interconnected defects, providing increased ionic transport between the surface of concrete and the surface of the reinforcing steel, effectively promoting the corrosion process. Crack growth decreases concrete stiffness and tensile strength, while the formation of a network of cracks increases concrete permeability. Thus, the structural integrity of a reinforced concrete member is increasingly compromised as cracking progresses. As steel is progressively lost to corrosion, its cross-section is reduced, causing a decrease in the member's flexural strength. Furthermore, as corrosion advances, the bond between the steel and surrounding concrete is weakened, thus adversely affecting the load transfer between the two materials. To ensure that reinforced concrete members perform according to their design capacity and design service life, it is important to prevent or delay the occurrence of corrosion [6]. Also engineers are often required to compute the useful service life of a structure with the existing rate of corrosion.

To efficiently rehabilitate corrosion-damaged reinforced concrete structures, the residual strength and failure mechanism of the deteriorated structure must be determined.

For this purpose, a number of studies have been reported in the literature. The majority of the studies till date have been focused on flexural and bond strength of corroded beams [7-9]. Models have been developed by many researchers to determine the residual flexural/bond strength of corroded beams [10-12]. However, there are only a few studies related to the shear strength of corroded beams.

At present, structures are facing corrosion problem after thirty to forty years of their service life. These structures were designed based on codes prevailing three to four decades ago. Recent studies on the size effect on shear strength of concrete members reported that the shear strength of the members designed three to four decades ago was overestimated [14-15]. There are structures in service without stirrups or with minimum stirrups, having a low margin of safety. Besides, a recent literature survey on the shear strength of members constructed without stirrups indicated that there are structures in service with higher probability of experiencing a shear failure [16].

Research is required to study the effect of corrosion of longitudinal and shear reinforcement on the shear behavior of reinforced concrete beams. This study has been designed to address this gap in the knowledge.

1.2 EFFECT OF REINFORCEMENT CORROSION ON THE PERFORMANCE OF REINFORCED CONCRETE ELEMENTS

Where concrete has been carbonated to the depth of the steel reinforcement and a small but uniform amount of moisture is present, the steel is likely to corrode uniformly. This deterioration is often indicated by fine hairline cracks parallel to the direction of the reinforcement throughout the length of the structural component. Fortunately, as corrosion

is fairly uniform, cracking of the concrete cover in normally reinforced or pre-tensioned solid components usually occurs before the steel becomes excessively weak, giving early visual warning of the deterioration.

If chlorides are concentrated near the surface of the steel and water and oxygen are abundantly available, severe pitting corrosion may occur. This reduces the cross-sectional area of the bars at these locations, while the remainder of the bar may be left uncorroded. Structural cracks, or honeycombs, can also create conditions favorable to pitting corrosion by allowing the localized ingress of aggressive agents.

Reinforcement corrosion and concrete spalling cause a reduction in the ultimate capacity, and more significantly, a reduction in the stiffness and ductility of the R.C section primarily due to the loss of the steel/concrete interfacial bond. The effects of reinforcement corrosion on the behavior of reinforced concrete elements are schematically shown in Figure 1.1.

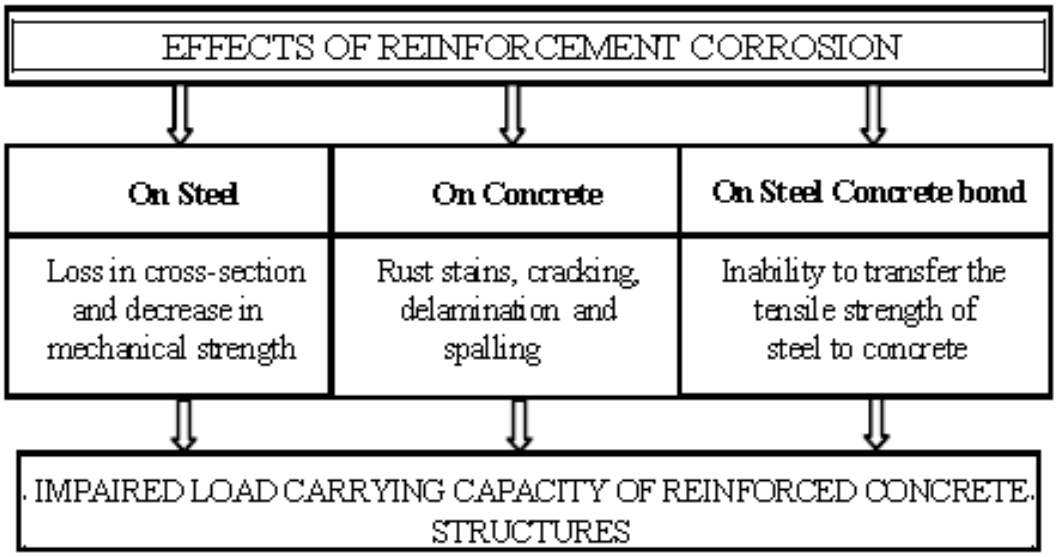

Figure 1.1: Effects of Reinforcement Corrosion on Reinforced Concrete Structures.

1.3 NEED FOR THIS RESEARCH

Limited research has been conducted to study the effect of corrosion of vertical stirrups and longitudinal steel on the shear strength of reinforced concrete beams. In view of the fact that corrosion damage reduces the load carrying capacity of a reinforced concrete element, it is of great interest to develop models that can be used to predict the residual strength of a corroding concrete element. The need for the prediction of the residual shear strength often arises to determine the underlying safety of the corroding members and to decide when the repair or strengthening must be undertaken without any further delay.

This study aims to make a contribution in the area of the prediction of the residual shear strength of corroded reinforced concrete beam by suggesting a predictive model that will be developed through an extended experimental work on beams subjected to different degrees of corrosion damage.

1.4 SCOPE AND OBJECTIVES

1.4.1 Scope

This research program consists of experimental and empirical phases. The experimental phase comprises casting of reinforced concrete beams, corroding of reinforcing steel and testing of 20 RC beams: 16 corroded beams and four control beams. The beams were divided into two groups (i.e. Group A & Group B) based on their cross sections. Each group included 10 beams: two control and eight corroded. The beams were tested under a four-point loading regime. The empirical work includes the development of a model utilizing the experimental data to predict the shear strength of corroded reinforced concrete beam.

1.4.2 Objectives

The general objective of this study was to examine the effect of corrosion of vertical stirrups on the shear behavior of reinforced concrete RC beams. The specific objectives were the following:

(i) To investigate the effect of corrosion on the shear behavior of RC beams with vertical shear reinforcement,

(ii) To cast concrete beam specimens of different sizes reinforced with longitudinal tension bars and two-legged vertical stirrups as shear reinforcement,

(iii) To induce different degrees of reinforcement corrosion in the test specimens using a purpose-built accelerated-corrosion setup,

(iv) To conduct four-point bend tests on the corroded reinforced concrete beam specimens to determine the shear strength and to capture the load-deflection response,

(v) To develop an empirical model to predict the residual shear strength of corroded RC beams,

(vi) To use Monte Carlo simulations to determine the probability of failure based on the proposed strength prediction model.

CHAPTER 2

LITERATURE REVIEW

2.1 SHEAR STRENGTH OF REINFORCED CONCRETE BEAMS

Shear strength in reinforced concrete beams has been the subject of many controversies and debates since the beginning of 20^{th} century. The shear strength of reinforced concrete beams has been extensively studied over the last five decades. A large number of experimental and analytical works has been carried out for the case of slender beams (having a shear span to depth ratio $a/d > 2.5$) with and without shear reinforcement under two-point loading [17].

Transversely loaded reinforced concrete beams may fail in shear before attaining their full flexural strength if they are not adequately designed for shear. Unlike flexural failure, shear failure is very sudden and unexpected, and sometimes violent and catastrophic. A thorough understanding of the different modes of shear failures and the mechanisms involved is necessary to prevent them.

Existing codes and specifications of different countries for reinforced concrete design with regard to shear differ considerably in important aspects. This only reflects the fact that very little is known about the behavior and strength of reinforced concrete

subjected to shearing force in spite of considerable number of tests and theoretical investigations made during more than half a century.

Despite the great research efforts, however, there is still not a simple, analytically derived formula to predict quickly and accurately the shear strength of slender beams. In addition, many of the factors that influence the determination of the required minimum amount of shear reinforcement are not yet known. As a consequence, the current provisions for shear in standard codes, such as ACI, BIS and BS, are still based on empirical or semi empirical considerations. Several experimental studies have been conducted to understand the various modes of failure that could occur due to a possible combination of shear and bending moment acting at a given section [17].

The usual arrangement for investigating shear failure is that of a beam subjected to symmetrically placed two equal concentrated loads 'P' at distance 'a' (shear span) from the supports. It has the advantage of combining two different test conditions, viz, pure bending, that is, no shear force is present between the two loads P, and constant shear force in the two end regions or shear spans.

The failure of beam considered in shear exhibits cracks outside the central section of the beam. Though the bending moment is maximum in the central section, the cause of failure of the beam considered is due to shear force in the end region of the beam where the cracks appeared causing failure. It is to be noted that in the central section there is no shear force present (pure bending). Hence it is felt that the shear force, or the shear stress, must be responsible for such a failure. Thus, the term 'shear failure' is chosen. Later it was recognized that shear stress at failure is far from being constant.

It is believed that the shear failure of reinforced concrete members without stirrups initiates when the principal tensile stress within the shear span exceeds the tensile strength of

concrete. This result in initiation of diagonal crack which later propagates through the beam web. In other words, the diagonal cracking strength of reinforced concrete members depends on the tensile strength of concrete, which in turn is related to its compressive strength.

Studies have shown that shear force is resisted by the combined action of three factors namely, the uncracked concrete in compression region, the aggregate interlocking and the shear acting across the longitudinal steel bars. The shear force across the steel bars is also known as dowel force. The unbalanced shear in excess of the three combined factors is assumed to be resisted by the shear reinforcement. The shear reinforcement is generally provided in the form of vertical stirrups. The stirrups should encircle tension reinforcement and their free ends should be properly anchored in the compression zone of the section so that the vertical legs may resist tension without slipping [17].

2.2 CORROSION IN REINFORCED CONCRETE ELEMENTS

2.2.1 Effect of Corrosion

Corrosion affects the behavior of reinforced concrete members by section loss of the reinforcing bar, cracking and spalling of concrete cover and loss of bond between steel bar and concrete. The pitting corrosion of the reinforcing bar leads to a reduction in the cross-sectional area of the bar resulting in a reduced load carrying capacity. The general corrosion of the reinforcing bar results in cracking and spalling of concrete cover, which causes the loss of bond between the reinforcing bar and the concrete and consequently a reduction in concrete section. Figure 2.1 summaries the effect of corrosion on the load carrying capacity of a reinforced concrete member [13].

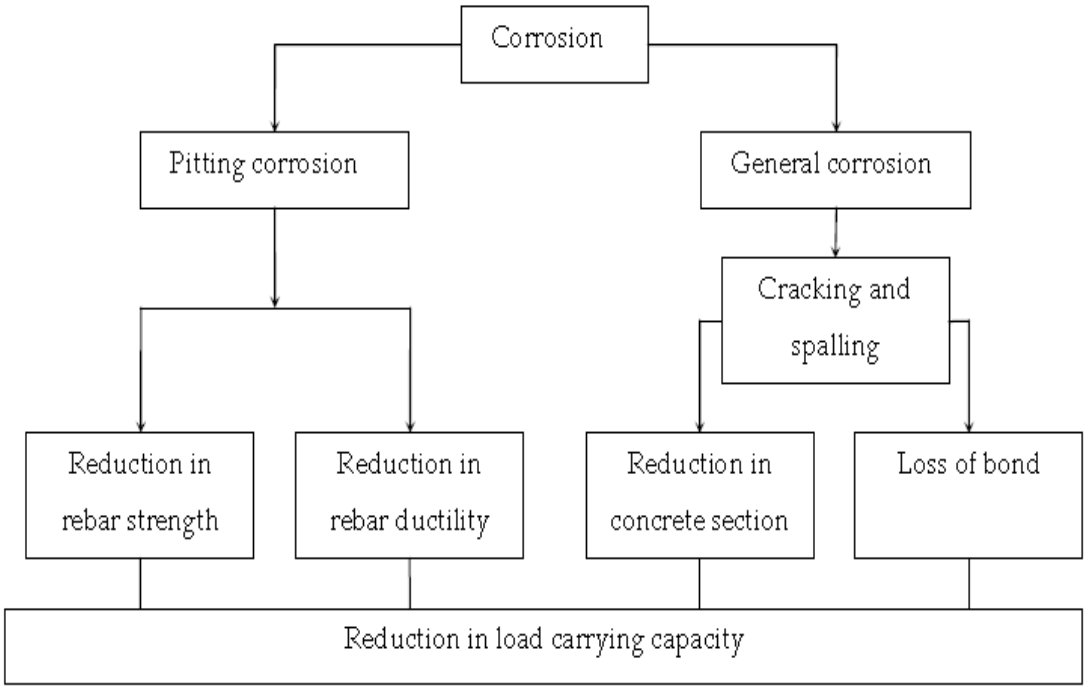

Figure 2.1: Effects of corrosion on the load carrying capacity of a reinforced concrete member.

2.2.2 Mechanism of Corrosion in Reinforced Concrete

Concrete is an alkaline material under normal exposure conditions. The high alkalinity of concrete (pH > 13.5) allows the formation of a passive oxide film on the surface of the embedded reinforcing steel bar, which protects it from corrosion. Once the protective layer around the reinforcing bar is disrupted either by lowering of pH due to carbonation or by ingress of chlorides, corrosion may start [13].

Corrosion of steel embedded in concrete is an electrochemical process in which the energy gained in the conversion of iron ore to steel is released in the form of a direct current. The surface of the corroding steel functions as a mixed electrode that is a composite

of anodes and cathodes electrically connected through the body of steel itself, upon which coupled anodic and cathodic reactions take place. At anodic sites, metal atoms pass into solution as positively charged steel ions (anodic oxidation) and the excess of electrons flow through the metal to cathodic sites where an electron acceptor like dissolved oxygen is available to consume them (cathodic reduction) to generate hydroxyl ions. The electrons created in the anodic reaction must be consumed elsewhere on the steel surface establishing the corrosion reaction. The process is completed by the transport of ions through the aqueous phase, leading to the formation of corrosion products at the anodic sites either soluble (e.g. ferrous chloride) or insoluble (e.g. rust, hydrated ferric oxide). The different behavior of the same metal at two different locations is usually found due to variations arising either during the manufacturing, storage or transportation stages. Anodic and cathodic sites are electronically connected as they exist on the same rod and they are ionically connected by concrete pore water functioning as an aqueous medium, i.e., a complex electrolyte. Hence a reinforcement micro-corrosion cell is formed which can be seen in the below Figure 2.2, [18].

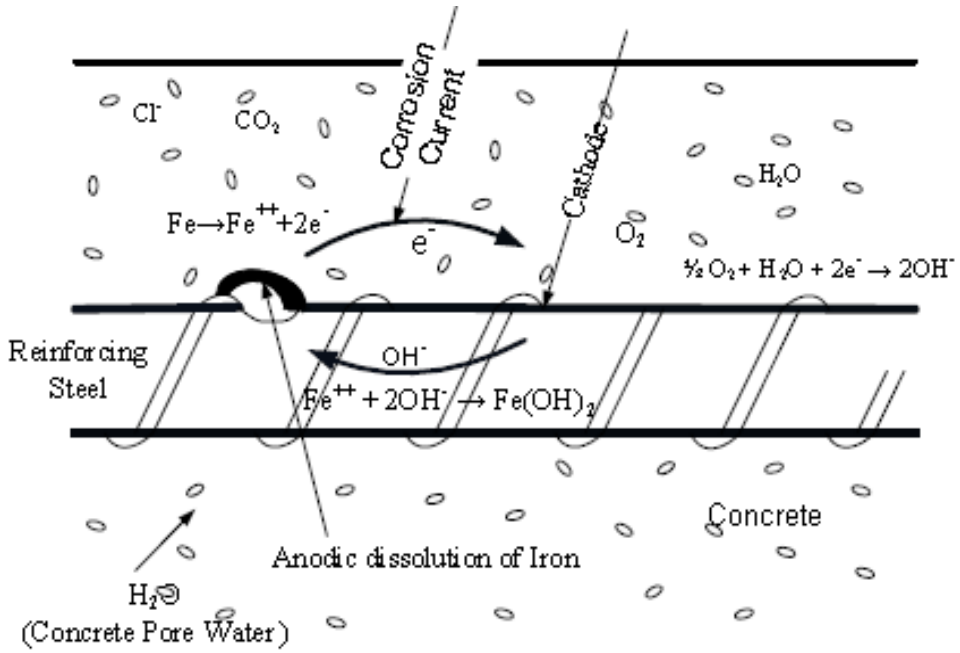

Figure 2.2: Micro-corrosion cell formation in reinforced concrete.

The electrochemical mechanism of corrosion of steel can be summarized with the following three partial processes:

i. Oxidation of iron (anodic process) liberates electrons in the metallic phase and gives rise to the formation of iron ions ($Fe \rightarrow Fe^{2+} + 2e^{-}$).

ii. Reduction of oxygen (cathodic process) consumes the electrons produced at the anodic site, and it produces hydroxyl ions ($2e^{-} + H_2O + \frac{1}{2}O_2 \rightarrow 2(OH)^{-}$) electrons coming from anodic sites + moisture + oxygen → hydroxyl ions.

iii. Finally, the $(OH)^{-}$ ions flow back to the anode through the concrete to complete the circuit.

The rate of this transfer depends on the temperature, moisture content, ionic concentration and electrical resistivity of concrete. The $(OH)^-$ ions at the anode then combine with the Fe^{2+} cation to form a fairly soluble ferrous hydroxide, $Fe(OH)_2$:

$$Fe^{2+} + 2(OH)^- \rightarrow Fe(OH)_2$$

If sufficient oxygen is available, this product can be further oxidized to form insoluble hydrated red rust. This rust can have a volume 2 to 14 times that of the parent iron from which it is formed. The rust product can exert tensile stresses of the order of 4000 psi, which is 10 times the tensile strength of concrete. This excessive pressure causes the concrete cover to crack. Then it spalls at an advanced stage of corrosion process leading to a reduction in the cross sectional area of the structural member. In addition to loss of cover concrete, a reinforced concrete member may suffer structural damage due to the loss of bond between steel and concrete and loss of rebar cross-section [62].

Hence, oxygen and moisture are the most important ingredients for reinforcement corrosion to occur, and the ingress of these elements through the concrete must be controlled to avoid corrosion.

2.2.3 Types of Corrosion in Reinforced Concrete

2.2.3.1 General Corrosion

General corrosion is normally associated with both chloride ingress and carbonation of concrete. The iron oxide compound formed during general corrosion is usually known as brown rust. These compounds have relatively greater volume than the metal itself and exert expansive pressure onto the surrounding concrete. This leads to the cracking and spalling of

the concrete cover around reinforcing bar before excessive loss of cross-sectional area of the reinforcing bars. Structures experiencing general corrosion of their reinforcing bar have reduced structural capacity due to reduction in bond strength between the reinforcing bar and surrounding concrete, [21].

2.2.3.2 Pitting Corrosion

Pitting corrosion is regarded as localized corrosion. It is only associated with chloride ingress and not with carbonation induced corrosion. The compounds formed during pitting corrosion are different than those formed in general corrosion. These compounds have lesser volumetric expansion than the compounds formed during general corrosion. Consequently, there is less tendency of splitting of concrete cover due to pitting corrosion. On the other hand, excessive loss of cross section of the reinforcing bar may occur without any visible signs of deterioration on the surface of these members. Reinforced concrete structures experiencing pitting corrosion exhibit reduced strength and ductility due to the reduction in the tensile strength of reinforcing bar, [21].

2.2.4 Accelerated Corrosion Technique

Accelerated corrosion technique is widely used to corrode reinforced concrete specimens in the laboratory. In this technique, the corrosion process is activated by the chloride salts in the concrete and accelerated by electrochemical polarization of the reinforcing bar embedded in the concrete. Different methods have been used to incorporate salts in the concrete: some researchers added the salts in the concrete mix while others

immersed the specimens in a salted solution. To electrically polarize the reinforcing bar, it is connected to an external power supply in such a way that a positive potential is created on the bar making it the anode in the corrosion cell. To complete the corrosion cell, an external or an internal cathode is used. Galvanized wire mesh, copper or stainless steel plates are used as an external cathode while a stainless steel bar is used as an internal cathode. Different current densities have been used in the literature ranging from as high as 10400μA/cm^2 to as low as 45μA/cm^2 while the highest corrosion rate recorded in field ranged between 10 and 25μA/cm^2 [22]. El Maaddaway and Soudki [22], recommended that the current density in accelerated corrosion must not exceed 200μA/cm^2. This current density induces corrosion of steel reinforcement in a reasonable time and produces corrosion products and cracking patterns similar to those found in the field.

2.3 EFFECT OF CORROSION ON FLEXURAL AND BOND STRENGTH OF REINFORCED CONCRETE MEMBERS

2.3.1 Effect of Corrosion on Flexural Strength of RC Members

A large number of studies have been conducted to investigate the effect of corrosion on bond strength of RC members. The effect of corrosion on flexural strength of RC members is also well understood. Few of the studies conducted in this area are reviewed in the following paragraphs:

Ravindrarajah and Ong [29] investigated the effect of diameter of steel bar, and the thickness of the cover on the degree of corrosion of mild steel bars embedded in mortar.

They found that there is a significant effect of rebar diameter, cover thickness, and specimen size on the corrosion intensity. The intensity of corrosion of reinforcing steel in concrete was found to increase with an increase in the bar diameter. With the increase in the bar diameter the cover thickness reduces and the corrosion resistance decreases. This is expected since larger bar size has lower electrical resistance and smaller cover thickness shortens the diffusion path for the chloride ions. The relationship between the iron loss and cover/bar diameter was found to be linear. For the same diameter of bar, the corrosion intensity of steel increased when the cover thickness was decreased. The surface area of the corrosion specimen through which the chloride ions diffuse was also found to be an important parameter in determining the rate and extent of corrosion of embedded steel in concrete.

Tarek Uddin et al. [30], studied the influence of crack width and type of bars (plain and deformed) on corrosion of steel bars in cracked concrete. Microcell and macro cell corrosions of plain and deformed steel bars were investigated on 100 × 100 × 400 mm, single cracked specimens with crack widths of 0.1 mm, 0.3 mm and 0.7 mm. Electrochemical investigations were also conducted on 150 × 150 × 1250 mm multi cracked specimens with plain and deformed bars. For these specimens, crack widths were varied from 0.1 to 0.4 mm. The results indicate that the corrosion rate of plain bars is less than the corrosion rate of deformed bars.

Ting and Nowak [31] developed a method for the calculation of the effect of reinforcing steel area loss (due to corrosion or other causes like mechanical damage) on the moment carrying capacity of corroded reinforced concrete beams. They developed a numerical procedure using finite difference method by considering various types of concrete members including a solid slab, void slab, rectangular beam, T-beam and box beam.

According to their approach, the reinforcing steel area loss is a linear function of the loss of material. This is in contrast to the results of Uomoto and Misra [35], who found that the deterioration of structures caused by the reinforcement corrosion is not always directly related to the loss of strength of the bars due to a reduction in the cross-sectional area, but some other factors, such as crack formation in concrete and loss of bond could lead to greater reduction in strength of the structure.

Huang and Yang [32] carried out experiments on 32 corroded reinforced concrete beams, of dimensions 15 × 15 × 50 cm, of which 16 had predetermined cracks, so as to study the effect of reinforcing steel area loss on flexural behavior of reinforced concrete beams. The load carrying capacity of RC beams decreased as the corrosion product increased. The percentage reduction in the loading capacity of the RC beam subjected to corrosion was approximated by the calculated loss of rebar diameter. Based on the results, it was found that for a 10% reduction in the loading capacity of an RC beam, the calculated loss of thickness of steel ranged from about 0.2 μm to 1.44 μm. By comparing the loss of steel thickness with the reduction of the stiffness or loading capacity of the RC beams, they concluded that a small loss of thickness may cause a significant reduction in the load carrying capacity for high strength concrete beams or defective beams.

Yoon et al. [33] investigated concrete beam specimens having dimensions 100 mm × 150 mm × 1170 mm, reinforced with a single standard No. 6 (19 mm diameter) Grade 60 reinforcing steel bar. It was found that, for the beams having a degree of corrosion ≥ 3% weight loss of steel, the remaining loading capacity of the beams decreased as the percentage weight loss of the reinforcing steel increased indicating that the loss of the loading capacity might be primarily due to the loss of steel-concrete bond. They also stated that as the degree

of steel corrosion increased, the failure mode of the reinforced concrete beams shifted from a shear failure to bond splitting failure. In fact, the lower the remaining load carrying capacity of a beam, the clearer the steel-concrete bond failure was seen from the flexure testing.

Rodriguez et al. [34] carried out experiments on six different types of reinforced concrete beams of 150 × 200 × 2300 mm. The bending moment capacity of the control beams was about 37 kN-m. After 100 days of accelerated corrosion, the capacity was reduced to 26 kN-m (30% decrease). After 200 days, the capacity was reduced to 20 KN-m (46% decrease). They found that the experimental value of the bending moment at maximum load, in beam with only bottom bars corroded, was close to the calculated value, using the reduced section of the bottom bars. No damage occurred at the top concrete cover because neither the top bars nor the links were corroded in the beam. They concluded that, it is possible to predict a conservative value of either the ultimate bending moment or the ultimate shear force, for high levels of corrosion, by means of using RC conventional models and considering the reduced section of both steel and concrete.

Uomoto and Misra [35] carried out a large experimental work with corroded beams and columns so as to study the load carrying capacity of concrete structures with corroded reinforcement. They concluded that the reduction in the load-carrying capacity of the beams was not caused simply by the reduction in the effective area or the reduction in strength of reinforcing bars, but by the cracks formed by the corrosion process. Weight loss of 1% to 2.4% in the main reinforcing bars (16 mm diameter) corresponded to 4% to 17% of reduction in the load carrying capacity.

Tachibana et al. [36] carried out tests with corroded beams of 200 × 150 × 2000 mm. The beams had no shear reinforcement but were reinforced longitudinally with two 16 mm diameter bottom bars. The results of the loading tests showed that, no corroded and mildly corroded specimens for the current period of 3 days had a normal behavior and failed in flexure with yielding of steel bars. On the other hand, the specimens for the current period of 10 days and 15 days showed deteriorated behavior and failed in a brittle manner, and the reduction in stiffness and the load carrying capacity occurred, and specimens for the current period of 6 days showed intermediate behavior. A 16% loss of capacity in the beams was reported after 15 days of current application. The maximum percentage weight loss of reinforcement was about 5%. With regard to the load carrying capacity of the RC beams with stirrups, they concluded that the reduction in load-carrying capacity of RC beams with stirrups will not be remarkable, as the transmission of shear stress between concrete and reinforcement will be secured through the stirrups even when bond of reinforcement has deteriorated.

Jin and Zhao [37] carried out beam tests to study the effect of reinforcement corrosion on the bending strength of reinforced concrete beams. They observed that with the increase of the bar corrosion, the failure mode of corroded RC beams changed from ductile mode to brittle mode similar to that of under reinforced beams, and the distribution of cracks of corroded RC beams became concentrated instead of scattered. They developed an empirical model for determining the percentage residual flexural strength of the corroded beams in terms of the percentage reinforcement corrosion. They also developed expressions for calculating the reduced steel cross-sectional area, reduced yield strength and reduced bond strength.

Mangat and Elgarf [9] carried out research work on developing a relationship between the degree of reinforcement corrosion and the residual strength of flexural members through an experimental scheme. Up to a degree of corrosion (percentage reduction in reinforcement bar diameter) of 3.75%, there was very little effect of corrosion rate on flexural load capacity. However, at a corrosion degree of 5% and beyond, the flexural load capacity decreased significantly with increasing corrosion rate. The study obtained a 75% decrease in load capacity for a 10% diameter reduction. They found that reinforcement corrosion in concrete has a marked effect on both the flexural load capacity and deflection of beams. Also, the reduction in reinforcing bar cross-section due to corrosion has an insignificant effect on the residual flexural strength of the beams. The reduction in residual strength was primarily attributed to the loss or breakdown of the steel/concrete interfacial bond. A trigonometric function, in terms of the rate of corrosion, corrosion time and bar diameter, was proposed to predict the residual strength of corroded beams.

Cabrera [38] carried out loading tests with six corroded beams having a cross section of 125 × 160 mm. They found that the moment capacity increased almost 20% when the percent mass loss was smaller than 2%. Otherwise, an approximately linear decrease occurred in the moment capacity when the percent of mass loss increased. Maximum reduction of the cross section (9%) at bottom bar caused a reduction of 20% of the ultimate bending moment and an increase of 50% of the deflection at mid-span corresponding to the service load.

Nokhasteh et al. [39] conducted preliminary flexural tests on three simply supported RC beams. The authors developed a two-dimensional finite element model for the damaged beam. The load-central deflection curves derived from the FE analysis showed a decrease in

stiffness of the damaged beams as compared with their undamaged counterparts. They concluded that corrosion of link reinforcement is likely to be more significant than the main bars because: (i) there is less cover to link reinforcement, (ii) stressing due to bending of the bars increases corrosion, and (iii) the links are smaller in diameter.

Aziz [41] investigated the effect of reinforcement corrosion on the flexural strength of a uniformly loaded and simply supported one-way slab. They reported a sharp reduction in the ultimate flexural strength of slabs with up to 20% reinforcement corrosion; thereafter, the strength decreased at a somewhat reduced rate with further increase in reinforcement corrosion. The reduction in the ultimate flexural strength of slabs with 5% reinforcement corrosion was 25%, while it was 60% in the slabs with 25% reinforcement corrosion.

Al-Sulaimani et al. [7] investigated experimentally the effect of corrosion on the flexural strength of RC beams. It was observed that up to 1.5% corrosion level, there was no reduction in ultimate flexural strength, however; there was a reduction in flexural strength with further increase in corrosion levels (12% reduction at 5% corrosion level).

Almusallam et al., [8] carried out an experimental investigation to determine the effect of corrosion on the behavior of corroded slabs. It was observed that corrosion changed the failure mode from flexure in the control slabs to bond-shear failure in the corroded slabs. Reduction in the ultimate flexural strength was also observed; 25% and 60% reduction in ultimate strength for 5% and 25% corrosion level, respectively.

It is noted that researchers have attempted to empirically correlate the residual load carrying capacity of a flexural member with the degree of reinforcement corrosion and other parameters, such as rebar diameter and cover thickness.

A study on prediction of residual flexural strength of corrosion-damaged reinforced concrete beams was carried out by Azad et al. [12]. In this experimental study, 48 reinforced concrete beam specimens were subjected to accelerated corrosion using impressed current and then tested in a four-point bend test to determine their residual flexural strength. The following variables were used: two levels of applied impressed current density, three levels of corrosion period and two different diameters of tension reinforcement with two different concrete cover thicknesses. Important observations made through analysis of the test results are as follows:

(i) The product of corrosion current density (I_{corr}) and the corrosion period (T), $I_{corr}T$, defined in this study as the 'Corrosion Activity Index', is the key measure of corrosion damage. The percentage metal loss and the loss of flexural strength increase with increasing I_{corr} T.

(ii) The effect of reinforcement cover on degree of corrosion at a constant value of $I_{corr}T$ is found to be small,

(iii) At a lower value of $I_{corr}T$, the residual flexural strength of a corroded beam can be predicted with a reasonable accuracy by considering only the reduced cross-sectional area of tension reinforcement. However, at a higher value of $I_{corr}T$, the increasing adverse effect of bond cannot be ignored in determining the residual flexural capacity.

2.3.2 Effect of Corrosion on Bond Strength of RC Members

In the field of reinforced concrete, the bond between concrete and reinforcing bar can be thought of as the property which causes hardened concrete to grip an embedded steel bar and thus prevent the longitudinal sliding of the reinforcing bar through the concrete. This property ensures an effective interaction between steel and concrete. Bond stress can be defined as the force per unit of normal surface area of the reinforcing bar acting parallel to the bar on the interface between the bar and the surrounding concrete.

Bond stress may also be thought as the rate of transfer of load between concrete and steel. In other words, if there is bond stress there will be a change in steel stress and vice versa. Whenever the tensile or compressive forces in a bar change, to maintain the equilibrium, this change in bar force must be resisted at the contact surface between the steel and concrete by an equal and opposite force produced by bond between the reinforcing bar and concrete.

Since the external load is not directly applied to the reinforcement, steel receives its share of the load only from the surrounding concrete. The composite action of concrete and steel as one member is assured only if there exists, a perfect bond between steel and concrete in order to transfer the stresses from concrete to steel. Efficient bond ensures an efficient structural behavior of a reinforced concrete member. The findings of studies conducted to evaluate the effect of reinforcement corrosion on bond strength are discussed in the following paragraphs:

Amleh and Mirza [25] studied the influence of corrosion on bond between the reinforcing steel and concrete using a preliminary series of tests on 14 tension specimens, each 100 mm in diameter and 1-m long and reinforced with one No. 20 bar (19 mm in

diameter). Twelve of the 14 specimens were placed in a tank filled with a 5% NaCl solution. The study was carried out for seven different levels of corrosion, ranging from no corrosion (with no cracks), to extensive corrosion, with a 9-mm longitudinal crack caused by the bursting pressure resulting from the volume expansion of the corrosion products. They have reported a 9% loss of bond strength due to 4% loss of weight from corrosion accompanied by transverse cracks, while a 17.5% weight loss with no transverse cracks before yielding of the bar resulted in 92% loss of bond between the steel and the surrounding concrete.

Fu and Chung [26] have reported that the corrosion of steel rebar in concrete immersed in saturated Ca $(OH)_2$ solution caused the bond strength to increase while the contact resistivity decreased. This behavior persisted until five weeks of corrosion. Further corrosion, beyond five weeks, caused the bond strength to decrease while the contact resistivity continued to increase. This means that slight corrosion (<5 weeks) increased the bond strength, whereas severe corrosion (>5 weeks) decreased the bond strength.

Auyeung et al. [27] in their study on bond behavior of corroded reinforcement have reported that when the mass loss of the reinforcement due to corrosion reaches approximately 2%, concrete cracks along the bar. A small amount of corrosion increases both the bond strength and bond stiffness, but the slip at failure decreases considerably. However, they reported that when the mass loss exceeds 2%, bond stiffness decreases considerably. Therefore, failure of specimens with corroded bars can be expected to be much more brittle compared to control specimens with uncorroded bars. Even when there is extensive corrosion with considerable cracking of concrete, bond is not completely destroyed. Measurable bond strength exists even when the mass loss approaches 6%. This

partially explains the fact that structures with extensively corroded reinforcement sometimes sustain considerable loads.

Cabrera and Ghoddoussi [28], investigated the effect of reinforcement corrosion on bond strength. They studied two types of specimens, i.e., pullout test specimens and beam test specimens. The pullout tests were carried out on 150 mm concrete cubes with 12 mm diameter reinforcing bars centrally embedded in the cube. The beam specimens were 125 × 160 × 1000 mm, reinforced with two 10 mm plain top bars, two 12 mm bottom bars and plain links of 8 mm at 40 mm spacing, as a web reinforcement along the shear span of 384 mm. In order to obtain corrosion in a reasonable time, a voltage of 3 V was impressed through the specimen bottom bars up to 40 days. Maximum reduction of the cross section (9%) at bottom bar caused a reduction of 20% of the ultimate bending moment, and an increase of 40% of the deflection at mid-span corresponding to the service load.

Hence it can be said that the effect of corrosion of the reinforcing steel bars on the bond strength of reinforced concrete members has been investigated by many researchers and is relatively well understood. The majority of the studies reported that the bond strength increases initially with an increase in corrosion level until concrete cracks and then the bond strength starts decreasing with a further increase in the corrosion level (Al-Sulaimani et al., [7]; Almusallam et al., [8]; Bhargava et al., [11] and Ouglova et al., [23]).

It is reported in the literature that the bond strength of unconfined steel bars is significantly lower than that of the confined steel bars at the same corrosion level (Fang et al., [24]). Models have been developed to predict the residual bond strength of RC members [10-11].

2.4 EFFECT OF CORROSION ON SHEAR STRENGTH OF REINFORCED CONCRETE BEAMS

The effect of corrosion on shear strength of RC members is not very well understood against the bond strength or flexural strength and models need to be developed in this area. A number of studies have been reported in the literature to investigate the effect of corrosion on shear strength of reinforced concrete beams. However, majority of these studies did not incorporate actual corrosion instead corrosion effects were simulated in different ways. A review of these studies is presented in the following sections with a critical evaluation of their applicability to corrosion effects on shear strength of reinforced concrete beams.

2.4.1 Effect of Corrosion on Shear Strength of RC Beams

Rodriguez et al. [34] carried out an extensive research work to investigate the effect of corrosion on the load carrying capacity of reinforced concrete beams. The test variables included the level of corrosion, reinforcement details (ratio of tensile reinforcement (2-10mm or 2-12mm or 4-12 mm bars), ratio of compression reinforcement (2-8mm or 4-8mm bars), spacing of stirrups (6mm stirrups at 85mm or 150mm or 170mm c/c) and anchorage condition) and the interaction between the corrosion and loading. It was concluded that the mode of failure changes from bending to shear after the corrosion of the reinforcement in beams with usual reinforcement and that pitting corrosion of the shear stirrups was the most influencing factor in the reduction of the load carrying capacity of corroded beams.

Val [42] conducted reliability analysis to investigate the effect of general and pitting corrosion on the flexural and shear behavior of reinforced concrete beams. Different

corrosion rates were considered in the reliability analysis. The results of the analysis showed that higher corrosion rates ($\geq 1\mu A/cm^2$) had a significant effect on the behavior of corroded beams and that at these corrosion rates pitting corrosion (especially pitting corrosion of stirrups) had a more pronounced effect on the behavior of the test beams as compared to those with general corrosion. The results also showed that, in case of pitting corrosion, at higher corrosion rates the shear failure becomes the dominant type of failure.

The above two studies investigated the effect of general and pitting corrosion on the flexural and shear behavior of reinforced concrete beams. The results of these studies indicated that the reduction in shear capacity is higher as compared to reduction in flexural capacity under induced or simulated corrosion effects (especially pitting corrosion effects) as the beams that were designed to fail in flexure, failed in shear when subjected to corrosion effects.

2.4.2 Shear Strength of RC Beams with Exposed or Corroded Longitudinal Reinforcement

Cairns [43] carried out an analytical and experimental research work to study the shear strength of reinforced concrete beams with exposed reinforcement. The variables studied included the beam size and shape and the portion of the span over which the tensile reinforcement is exposed. It was concluded that properly anchored reinforcement significantly contributed to strength of reinforced concrete even if it was exposed over the span and that the shear strength of the beams increased with exposed reinforcement. The author also proposed a method to calculate the shear strength of beams with portion of the reinforcement exposed.

Raoof and Lin [44] carried out an extensive experimental work consisting of 44 small-scale beams and 88 large-scale beams to study the behavior of reinforced concrete beams with exposed tensile reinforcement. Several variables were examined including the extent of removal of steel-concrete bond, the distance of damage from the support, load position relative to the support, the percentage of tensile reinforcement, the depth of concrete removal, the ratio of compression reinforcement, the effect of stirrups and loading arrangement. It was observed that loss in ultimate strength in beams with exposed reinforcement (in absence of shear stirrups) increases with an increase in the percentage of longitudinal reinforcement at a/d between 3.0 and 4.0.

Jeppsson and Thelandersson [45] carried out an experimental study to investigate the reduction in shear capacity of reinforced concrete beams with unbonded longitudinal reinforcement. It was observed that there is a moderate reduction in shear capacity with a significant loss of bond: 33% reduction in load carrying capacity with 80% loss of bond. The author concluded that loss of bond over longitudinal reinforcement is partially compensated by the increased utilization of the stirrups which results in relatively higher residual strengths. The stirrups are very important in beams where longitudinal reinforcement is unbonded because the bond forces redistribute to forces in the stirrups.

Toongoenthong and Maekawa [46] studied the effect of pre-induced damage on the shear capacity of reinforced concrete beams without stirrups. Six different damage conditions were examined. Series 1 consisted of four beam specimens: one control specimen and three specimens subjected to accelerated corrosion causing cracks at three different local locations (case 1-3). Series 2 consisted of two beam specimens: one control specimen and

one specimen with horizontal crack planes produced by inserting a 1mm thick paper plate simultaneously at the three locations studied in series 1 simulating extreme corrosion conditions (case 4). Series 3 (case 5) and series 4 (case 6) were similar to series 2 except for the damage locations: in series 3 the damage was extended to the anchorage zone whereas in series 4 damage was induced over the whole shear span leaving the anchorage zone undamaged. All beam specimens were tested in three-point bending with a shear span to depth ratio of 3.2. The test results showed that a small reduction in shear capacity of beams with local corrosion damage (case 1-3) and a large reduction in shear capacity under extreme simulated corrosion conditions (case 4-5). The reduction in shear capacity under extreme corrosion conditions ranged between 20% (case 4) to 60% (case 5) depending on whether the damage is extended to anchorage zone or not. The author concluded that special attention should be given to the condition of anchorage while assessing the performance of such beams under extreme simulated corrosion conditions.

2.4.3 Shear Strength of RC Beams with Damaged or Corroded Stirrups

Regan and Kennedy [47] investigated the effect of corrosion on the shear strength of reinforced concrete beams. The effect of corrosion was simulated by damage of the stirrups and delamination of the concrete cover. The damage of the stirrups was simulated by removing the end anchorage of the stirrups and using two straight vertical pins except in one beam where U shaped stirrups were used. The delamination of the concrete cover was simulated by exposing the main steel reinforcement during casting of the beam specimens. They observed that the reduction in shear strength were 14-33% for 65-75% loss of stirrup

end anchorage. The authors concluded that the stirrups lacking end anchorage can still contribute to the shear resistance of RC beams.

Toongoenthong and Maekawa [48] investigated the effect of fractured stirrups on the shear strength of reinforced concrete beams. The fractured stirrups were considered the replicas of stirrups damaged by corrosion or alkali-aggregate reaction of concrete. The fractured stirrups were simulated by removing the bond near the edges of stirrup legs. The results showed that the damaged beam experienced 37% reduction in shear capacity compared to the undamaged beam. It was also observed that beams having stirrups without proper anchorage experienced longitudinal cracking along the main reinforcement before inclined cracking, which lead to the ineffectiveness of stirrups.

Higgins and Farrow [49] carried out an experimental work to investigate the shear capacity of conventionally reinforced concrete beams with corrosion damaged stirrups. The main variables examined in this study were the spacing of the stirrups (203 mm, 252 mm, and 305mm) and the level of corrosion (none (A), light (B), moderate(C) and severe (D)). The authors observed that the lightly corroded and control beam specimens failed by shear-compression while the moderate to severely corroded beam specimens failed by fracture of the stirrups. It was also observed that maximum strength loss occurred when the location of pitting corrosion coincided with the location of a diagonal crack. The maximum strength reductions for the rectangular, T and inverted T beam specimens were 30, 26 and 42% respectively. The authors concluded that the inspection of corrosion damaged structures in high shear regions should not be focused on visual distress instead it should be focused on identification of sequential stirrups with reduced stirrup cross sections and that the

conventionally reinforced concrete girders with severely corroded stirrups will behave like girders without stirrups.

Suffern [50] investigated the shear behavior of reinforced concrete deep beams with corroded stirrups. A reduction in strength was observed in most corroded beams; 26% reduction with low corrosion level, 18-53% reduction with medium corrosion level and 41% reduction with high corrosion level which was approximately uniform for all a/d ratios. Stiffness of the corroded beams was also reduced: 30%, 38% and 34% reduction in beams with shear span to depth ratio of 1.0, 1.5 and 2.0, respectively.

Zhao et al. [51] reviewed the existing studies conducted on shear strength of corroded reinforced concrete beams. They reported that shear strength of corroded reinforced concrete beams increases at low corrosion level (up to 10% sectional loss of stirrups) and decreases at higher corrosion levels (when sectional loss of stirrups exceeds 10%). The effect of reduced stirrup cross section on the shear strength is more significant at higher a/d ratios.

They proposed an empirical equation to estimate the residual shear strength of corroded reinforced concrete beams, presented in equation 2.1.

$$V_u = P_v V_{uo} \tag{2.1}$$

Where: V_u is shear strength of RC beams with corroded stirrups; V_{uo} is the shear strength of the same type of RC beam not subjected to any corrosion and P_v is the degradation parameter of shear strength due to corrosion of stirrups. The value of P_v is

expressed as a function of the ratio of the average section loss of the stirrup η_v . The value of P_v can be determined using equation 2.2.

$$P_v = \begin{cases} 1.0 & \eta_v \leq 100\% \\ 1.17 - 1.17\eta_v & \eta_v > 100\% \end{cases} \quad (2.2)$$

2.4.4 Shear strength of RC beams with corroded Longitudinal Steel and Stirrups

Only one study was found in the literature on the effect of corrosion of longitudinal steel and stirrups on shear strength of RC beams.

Xu and Niu [52] carried out an experimental study to investigate the shear behavior of corroded reinforced concrete beams. It was observed that for a given corrosion level, there is a larger reduction in ultimate shear capacity at higher a/d ratios: the reduction in ultimate shear capacity was 10% at a/d=1 and 20% at a/d=2.0 for specimens with 20% corrosion. This study was conducted on very small scale beams and this has a significant influence on the shear strength. Size effect must be considered on any future study on shear strength. Further research is needed to investigate the shear strength of full-scale RC beams subjected to corrosion of both stirrups and longitudinal reinforcement.

2.5 A SYNOPSIS OF PAST WORK

The findings from the past research work were contradictory: Cairns [43] reported that shear strength increases with a loss of bond between the longitudinal reinforcement and concrete while Jeppsson and Thelandersson [45] reported that shear strength decreases with a loss of bond between the longitudinal reinforcement and concrete. This may be possibly because of the different methods used to create the loss of bond in the longitudinal reinforcement. Raoof and Lin [44] revealed that the increase or decrease in shear strength due to corrosion of the longitudinal reinforcement mainly depend on the a/d ratio of the beams. None of the above studies have considered the effects of different levels of corrosion, whereas the corrosion induced degradation is directly associated with the corrosion levels.

The studies carried out by Regan and Kennedy [47] and Toongoenthong and Maekawa [48] simulated the effect of severely corroded stirrups by removing the anchorage of the stirrups. This assumption is applicable for very extreme corrosion conditions. Higgins and Farrow [49] and Suffern [50] investigated the effect of corroded stirrups on shear strength of RC beams with shear span to depth ratios less than 2.0. These studies are only applicable to deep beams. There is no study in the literature that investigated the behavior of reinforced concrete slender beams with corroded stirrups. Further research is required to investigate the behavior of slender beams with corroded stirrups.

The present study aims to make a contribution in the area of the prediction of the residual shear strength of reinforced concrete beam with corroded stirrups by varying different levels of corrosion. Consequently, the present research work has been designed to overcome the shortcomings of the past studies.

2.6 RELIABILITY ANALYSIS OF REINFORCED CONCRETE BEAM

This technique has been used by various researchers to model the variability of structure strength and loading conditions. A lot of research has been conducted for the probabilistic analysis of reinforced concrete beams by considering various parameters, which has a great significance on the reliability and serviceability of the structural components. Some of the studies are mentioned below:

Dimitri, V. [63] examined the effect of corrosion of reinforcing steel on flexural and shear strength, and subsequently on reliability, of reinforced concrete beams. Two types of corrosion were considered general and pitting corrosion, with particular emphasis on the pitting corrosion of stirrups on the performance of beams in shear. Variability of pitting corrosion along a beam is considered and the possibility of failure at a number of the beam cross sections was taken into account. Probabilities of failure were evaluated using Monte Carlo simulation. Uncertainties in material properties, geometry, loads, and corrosion modeling were taken into account. Results show that corrosion of stirrups, especially pitting corrosion, had a significant influence on the reliability of reinforced concrete beams.

Capra et al. [64] presented some numerical simulations of a concrete beam subjected to corrosion. The simulations have been made using a finite element code in which reliability procedures have been implemented using Monte Carlo simulations. In a first [art, a three point bending test has been chosen, taking into account some random material parameters, to compare the ultimate load of the beam provided by the French reinforced concrete code, and analytical limit state equation and finite element simulations. In a second part, the corrosion effects have been taken into account by the use of a random variable related to the

loss of steel section. Numerical simulations have been performed and allowed to describe the evolution of the safety index with time.

Warner and Kabaila [65] have described a method of developing the strength and serviceability of a real structures using Monte Carlo technique. The strength of an idealized axially loaded reinforced concrete column was calculated including the effects of variations in the materials and geometric properties.

Allen [66] has presented a probability distribution of the ultimate moment and ductility ratio for reinforced concrete in bending. The ultimate moment and ductility ratio were obtained using prediction equations and probability distributions of the parameters. The computations were based on the method of using the Monte Carlo technique. The results showed that the probability distributions of ultimate moment and ductility ratio by material properties, duration of loading, steel percentage and geometric properties.

Choi and Kwon [67] performed probabilistic analysis of deflections for reinforced concrete beams and slab using Monte Carlo technique. It was used to assess the variability of deflections with known statistical data and probability distribution of variables. Several results of a probabilistic study were presented to indicate general trends of results and demonstrate the effect of certain design parameters on the variability of deflections.

Arafah [68] presented reliability-based approach for the maximum reinforcement ratio for reinforced concrete flexural members. The study was based on sensitivity analysis of beams at their flexural limit state. The statistical characteristics of strength parameters under the prevailing construction practices in Saudi Arabia were employed. Monte Carlo technique was opted for simulation of sectional behavior. At the maximum reinforcement

and employing local materials (concrete and reinforcement), the probability of brittle flexural failure was found to be higher than that reported in literature.

Kapilesh et al. [70] addressed time-dependent reliability analyses of RC beams affected by reinforcement corrosion. They presented the predictive models for the quantitative assessment of time-dependent damages in RC beams, recognized as loss of mass and cross-sectional area of reinforcing bar, loss of concrete section owing to the peeling of cover concrete, and loss of bond between corroded reinforcement and surrounding cracked concrete. Monte Carlo simulation was used for evaluating the time dependent mean residual area of steel and coefficient of variance associated with steel area and time-dependent mean strength and coefficient of variance associated with the strength, wherein the term strength implies bond strength, flexural strength with and without loss of bond, and shear strength of the considered RC beam. Further by considering variability in the identified basic variables that could affect the time dependent strengths of corrosion-affected RC beams, the estimation of statistical descriptions for the time-dependent strengths was presented for a typical simply supported RC beam.

CHAPTER 3

METHODOLOGY OF RESEARCH

3.1 EXPERIMENTAL PROGRAM

The present study involves casting, corroding and flexure testing of a series of reinforced concrete beam specimens. Beams having different cross sections were subjected to reinforcement corrosion under impressed current of varying time periods to induce loss of metal. Results from the flexure test of corroded beams are used in relating the residual shear strength to corrosion rate, time of corrosion, and beam cross section.

3.2 EXPERIMENTAL VARIABLES

The following variables were used in this experimental program:

i. Two different beam cross sections: 140 × 220 mm and 150 × 240 mm
ii. Two different corrosion durations: 6 days and 10 days under slightly varying impressed current.

3.3 TEST SPECIMENS

A total of 20 reinforced concrete beam specimens were cast to include all variables mentioned in Section 3.2. All tests were repeated twice, including the tests on control specimens. Table 3.1 shows the test variables and the corresponding number of beams cast and tested.

Table 3.1: Test variables and specimens

Variables	**Levels**	**Number of test specimens**		
		T_0	T_1	T_2
C = b×d	2	(C1 + C2) × 2 Repetition = 4 Control Specimens	(C1 + C2) × 4 Repetition = 8	(C1 + C2) × 4 Repetition = 8
T	2			
Total number of specimens		**4 + 8 + 8 = 20**		

The following nomenclature applies to the parameters shown in Table 3.1.

C = cross section of the beam, mm^2

T = impressed corrosion duration, days

3.4 DETAILS OF TEST SPECIMENS

Rectangular reinforced concrete beam specimens of size 140 × 220 × 1150 mm and 150 × 240 × 1150 mm were used for this study. All beams were designed to fail in shear by providing ample vertical shear reinforcement. The reinforcement details of the test specimens are shown in Fig. 3.1. The top and bottom cover were 50 mm. The tension reinforcement consisted of a pair of 20 mm diameter steel bars. The vertical stirrups were of double-legged 8 mm diameter steel bars spaced uniformly at 80 mm centers throughout the length of each beam. Deformed bars were used as reinforcement. While the top two 8 mm diameter anchor bars used to serve as stirrup-holders were epoxy-coated to avoid corrosion, the stirrups were left uncoated so that they would be affected by corrosion along with the tension bars. By allowing the stirrups to corrode, the corrosion damage of the test beams reflects the practical case in which all bars are subjected to corrosion. Two lead wires were used to connect all the stirrups and the bottom bars separately in each of the beam for electrical connection to supply current.

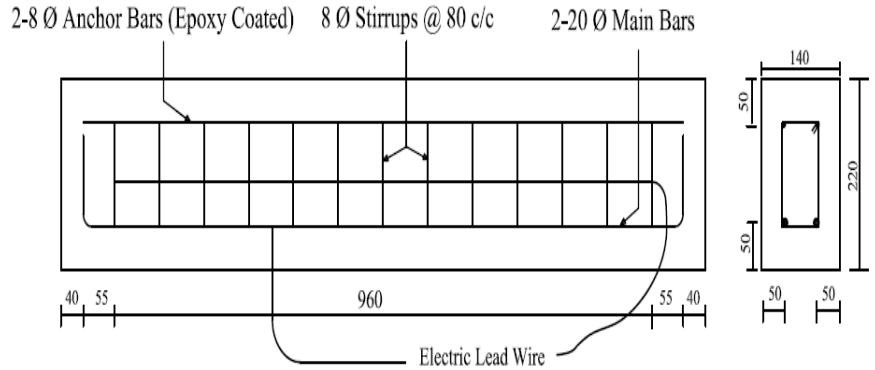

Reinforcement Details of Test Specimen : Group A

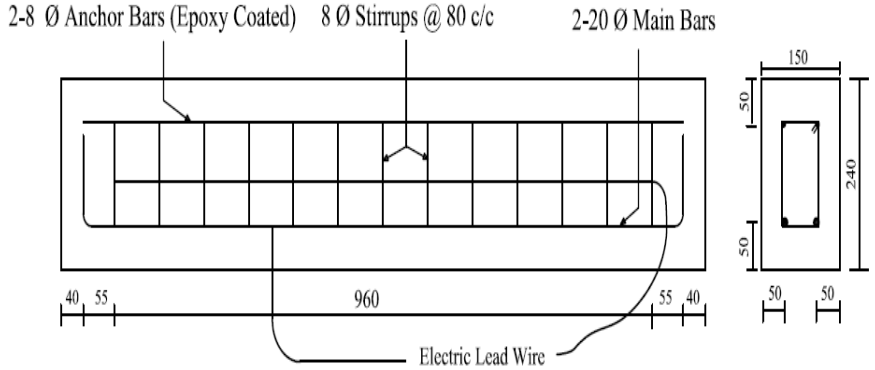

Reinforcement Details of Test Specimen : Group B

Note: All dimensions are in 'mm'

Figure 3.1: Reinforcement Details of Test Specimens.

3.5 CONCRETE CONSTITUENTS

ASTM C 150 Type I Portland cement, which is extensively used in Saudi Arabia, was used in the preparation of concrete specimens. The coarse aggregate for this study was crushed rock processed from the quarries on Riyadh Road with a specific gravity of 2.6. Dune sand with a specific gravity of 2.6 was used as fine aggregate. The absorption values for coarse and fine aggregates were considered as ± 2 %. Potable water was used for mixing and curing of concrete.

3.6 PREPARATION OF BEAM SPECIMENS

3.6.1 Concrete Mix Proportions

Mix design parameters of concrete such as water-cement ratio, cement content, size of coarse aggregate, and coarse to fine aggregate ratio were same for all the concrete mixtures. The following mix proportions were used:

Water-cement ratio = 0.40 (by mass)

Cement content = 370 kg/m^3

Coarse to fine aggregate ratio = 1.46 (by mass)

Max. Size of coarse aggregate used = 10 mm (3/8")

The quantity of each ingredient was calculated on the basis of 1 cubic meter using the above mix design ratios and by taking the density of fresh concrete as 2375 kg/m^3. Calculated weights of the ingredients are shown in Table 3.2.

Table 3.2: Weight of Constituents for a Cubic Meter of Concrete.

Constituents	**Weight (kg)/m^3**
Cement	370
Water	145
Fine Aggregate	754
Coarse Aggregate	1100
Admixture (Sup. Plasticizer)	6
Total	2375

3.7 FABRICATION OF TEST SPECIMENS

The beams were cast in formwork that was made up of wooden frame as shown in Figure 3.2. The formwork was lubricated before casting the concrete for ease of stripping the beams. The reinforcement cages were hung from the top of the formwork in order to provide cover to the main longitudinal reinforcement. All twenty specimens were cast from the same concrete batch. Immediately after casting, the specimens were covered with plastic sheets to avoid moisture loss. Subsequently, the specimens were covered with wet burlap and plastic sheets for curing up to twenty eight days and then the beams were stripped from the formwork and stored in the laboratory. In addition to the beams, six cylinders of 75 × 150 mm were also cast in order to determine the variation in compressive strength of concrete.

Figure 3.2: Formwork with cages.

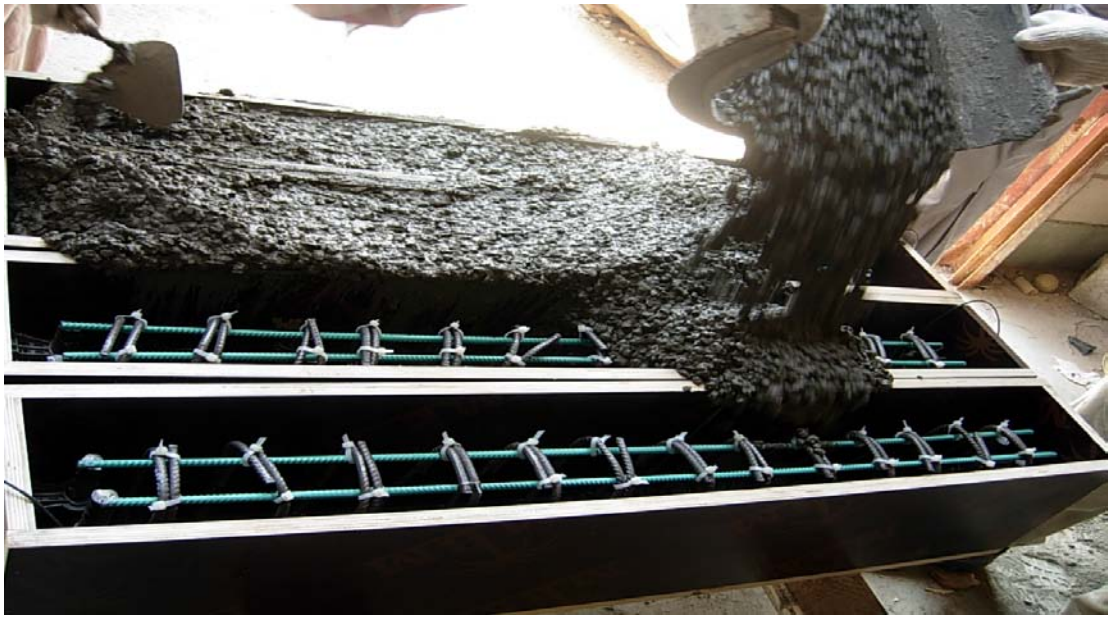

Figure 3.3: Casting of beams.

Figure 3.4: Moist Curing of Concrete beams.

3.8 DESIGNATION OF BEAM SPECIMENS

The 20 beams were divided into two groups, A and B, each group with ten beams. Out of these ten beams, eight were used in accelerated corrosion and the other two were used as 'control beams', which were not subjected to corrosion. Table 3.3 shows the groups and their cross-sectional details. Beams of group A were having a cross section of 140 × 220 mm and the cross section for beams of group B was 140 × 220 mm. For each group, the corroded and the control beams were labeled as shown in Table 3.3. The control beams were used to determine the actual shear strength of the uncorroded state of the beams.

Table 3.3: Beam Designations.

Beam Specimens		Beam Size (b × h) (mm)	Main Steel (No–dia)	Duration, T (days)
Group Designation	**Beam Designation**			
A	A1-C	140×220	2-20 mm	Control Beam
	A2-C			Control Beam
	A3-10			10
	A4-10			10
	A5-10			10
	A6-10			10
	A7-6			6
	A8-6			6
	A9-6			6
	A10-6			6
B	B1-C	150×240	2-20 mm	Control Beam
	B2-C			Control Beam
	B3-10			10
	B4-10			10
	B5-10			10
	B6-10			10
	B7-6			6
	B8-6			6
	B9-6			6
	B10-6			6

3.9 STRENGTH OF MATERIALS

3.9.1 Compressive strength of concrete

The compressive strength of the 75 × 150 mm cylinders f_c' representing the concrete used in beams, have been tested on the 28th day after casting. The test was done in accordance with ASTM C 39. The average value of the six cylinders cast from the batch mix was taken as the applicable value of f_c' for that concrete.

3.9.2 Tensile Strength of Reinforcing Bars

For determination of yield and tensile strength of tension bars, bar specimens of 10 mm and 8 mm diameter were tested in tension in a Universal Testing Machine and the complete load-elongation, hence stress-strain plots were obtained. From the stress-strain plots, yield strength and tensile strength of the bars were determined. An extensometer, of 50 mm gauge length, was used to measure the extension of the bars during the test and a data logger connected to a computer recorded the load and the corresponding extension of the bar as the test progressed. The test arrangement is shown in Figure 3.5.

Figure 3.5: Arrangement for evaluating the tensile strength of steel bars.

3.10 ACCELERATED CORROSION

Sixteen beams, eight beams from each groups, were subjected to accelerated corrosion by impressing a direct current into the longitudinal bars and stirrups. This was achieved through a combined setup developed for this purpose. The set-up consists of a rectifier, variable voltage transformer, AC Voltmeter, DC Voltmeter, DC Ammeter and a transformer. The configuration of this set-up is shown in Figs 3.6.

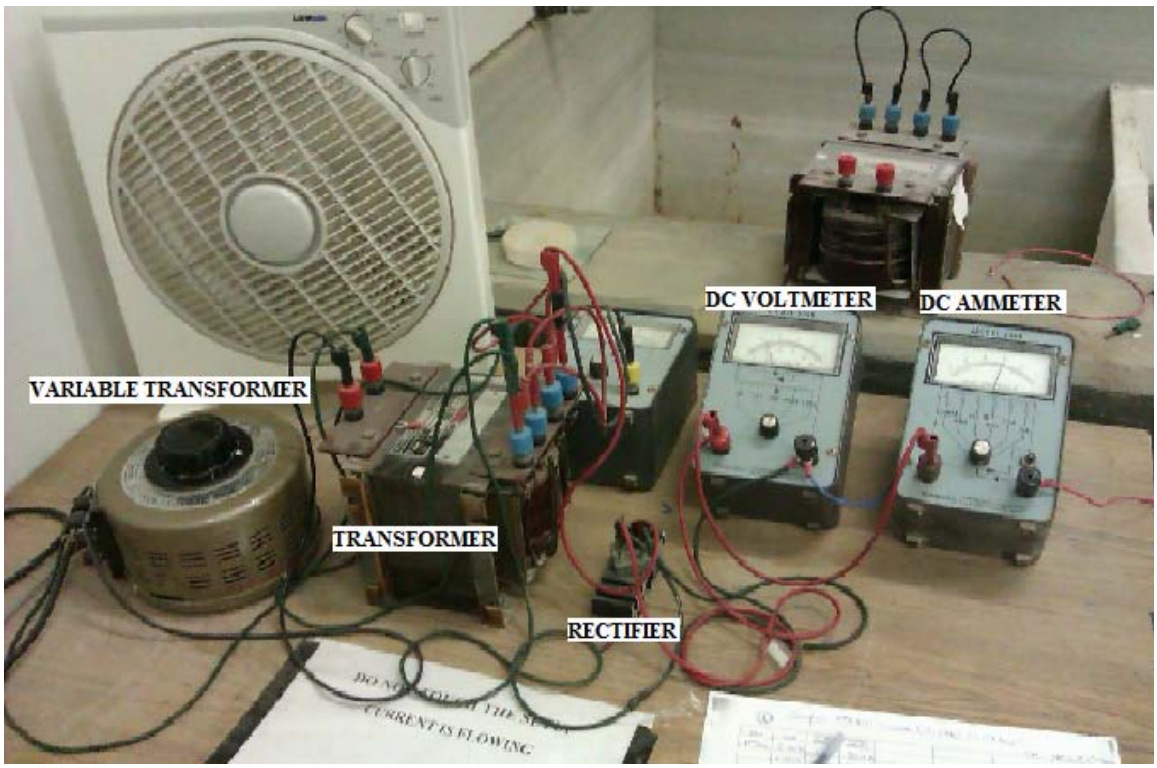

Figure 3.6: Combined set-up for Power supply.

Due to the high voltage requirement the available DC power supply was inefficient to use. Hence in order to use the mean source variable current (AC) and convert it to constant direct current (DC) with the desired current value, this setup was developed. Because of the high voltage provided by the set-up developed, it was possible to connect

two beams simultaneously in series as shown in Fig 3.7. The concrete specimens were immersed upto a depth of 160 mm in 3% sodium chloride solution in a tank such that the base of the specimen was just in contact with water. The direction of the current was adjusted so that the reinforcing steel became an anode and a stainless steel plate placed on the concrete specimen served as a cathode. The stainless steel plate was placed in the tank in such a manner that it covered both the sides of the specimen throughout the length. This arrangement ensured a uniform distribution of the corrosion current along the whole length of the bar. A schematic representation of the test set-up is shown in Fig. 3.7.

Though accelerated corrosion does corrode the bars and leads to crack formation, it differs considerably from the actual corrosion in structures, in rate and characteristics. The corrosion in existing structures is extremely slow and hence; even when the bars corrode and expand; cracks may not always form in surrounding concrete because of concrete creep [35].

Another difference lies in the fact that in Galvanostatic corrosion, the reinforcement is forced to corrode by impressing direct current and this results in all the reinforcing bars becoming anodic to external cathode (in this series of experiments a stainless steel plate). This entails overall corrosion, at an almost uniform rate. This may not be the case in existing structures as pitting corrosion is common.

However, it has been found by some investigators [35], that the cracks formed by accelerated corrosion are quite similar to those formed during exposure tests. This justifies to some extent the choice of the accelerated corrosion induction method to cause a significant amount of corrosion in a short span of time in laboratory tests. Furthermore, accelerated corrosion can induce damage in a very short period of time compared with a very long time sparing over many years that is needed to produce similar corrosion damage.

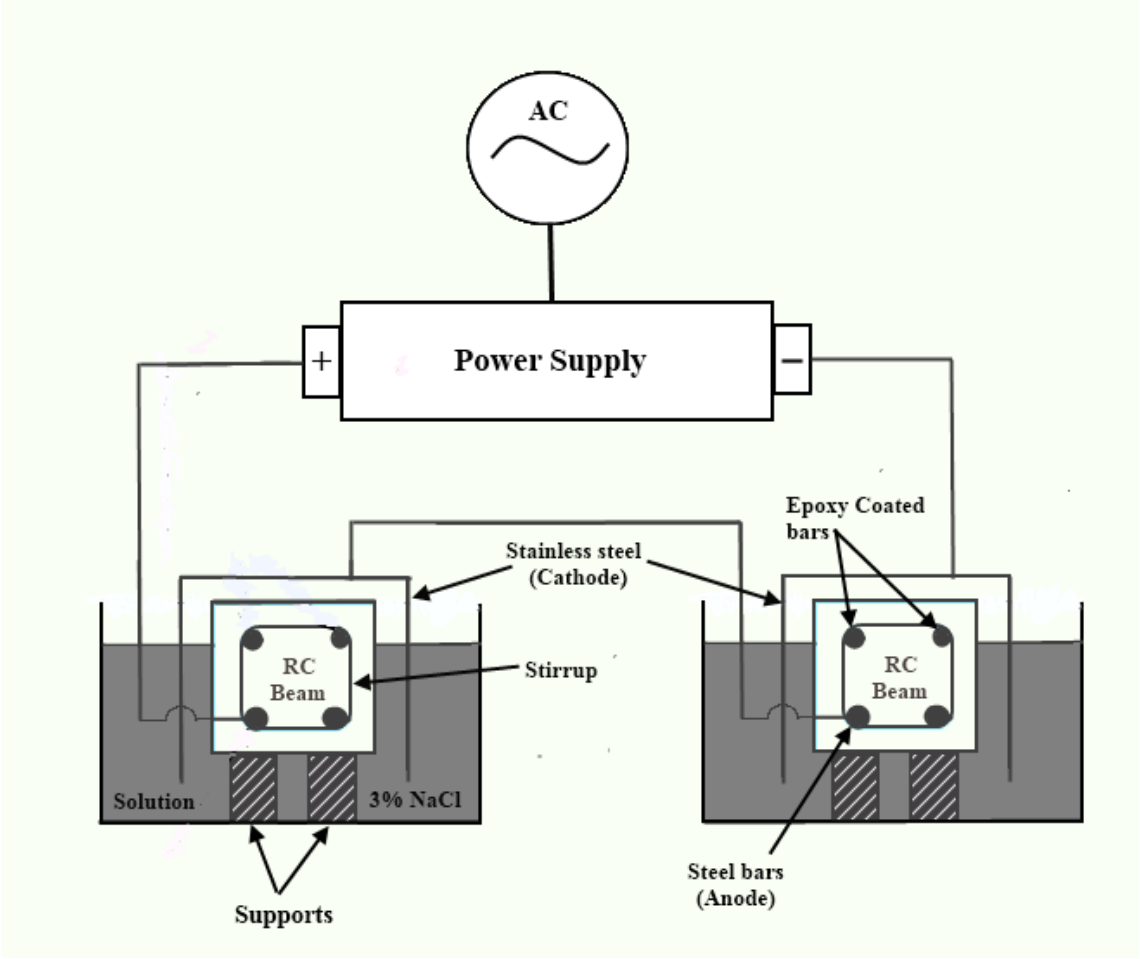

Figure 3.7: Schematic Representation of the Accelerated Corrosion Test Set-up.

It is observed from the previous accelerated corrosion tests on reinforced concrete members that the applied impressed current densities have typically ranged from, as low as 0.1 mA/cm^2 [34] to as high as 4 mA/cm^2 [9]. In this work, corrosion current density in the neighborhood of 2.0 mA/cm^2 was used. Based on the surface area of the bars and stirrups, the required current was calculated as 5.91 Amp and 6.36 Amp for Group A and Group B specimens respectively.

The current supplied to each concrete specimen was checked on a regular basis and any drift was corrected. Typical beam specimens subjected to accelerated corrosion are shown in Fig. 3.8.

Figure 3.8: Two Beams in Series Subjected to Accelerated Corrosion.

3.11 FLEXURAL TEST OF BEAMS

After curing, a set of 4 beam specimens was kept designated as control beams. These four control beam specimens were tested for determining the reference shear strength. The other 16 beam specimens that were subjected to accelerated reinforcement corrosion were tested to determine their residual shear strength.

The beam specimens were tested as simply supported beams under a four point loading system with a total span of 900 mm and a shear span of 300 mm. A schematic representation of the test set-up is shown in Fig. 3.9. The flexure test for all corroded beams in Group A (Table 3.3) was conducted using an Instron Universal Testing Machine of 250kN capacity at a slow loading rate of 1 mm/min. Fig. 3.10 shows test set-up. The load and midspan deflection data for each specimen was recorded using a computerized data acquisition system at pre-determined load intervals till failure. The data so generated was utilized to plot load-deflection curves for each of the tested specimens.

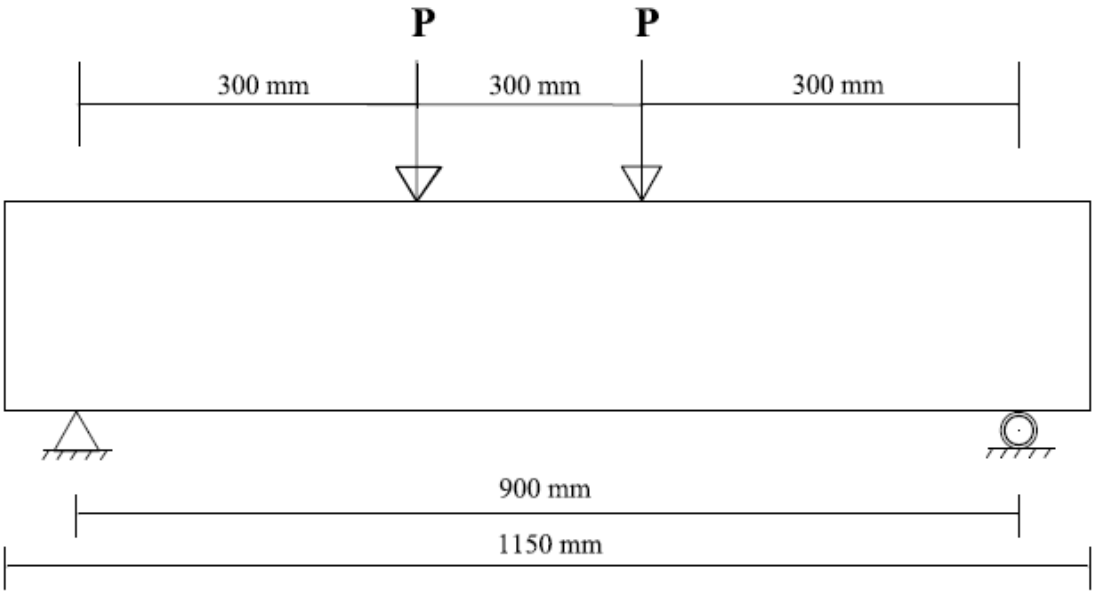

Figure 3.9: Set-up for four-point bend test of beam specimens.

Figure 3.10: Flexural strength test using Instron Universal Testing Machine.

For the tests of Group B beams (Table 3.3), the testing was carried out under a test frame in heavy structure laboratory, as the capacity of Instron machine was found to be insufficient. The test setup is shown schematically in Figures 3.11 and 3.12. Figs 3.13 to 3.14 show a control specimens and specimens corroded for different time periods under flexural test.

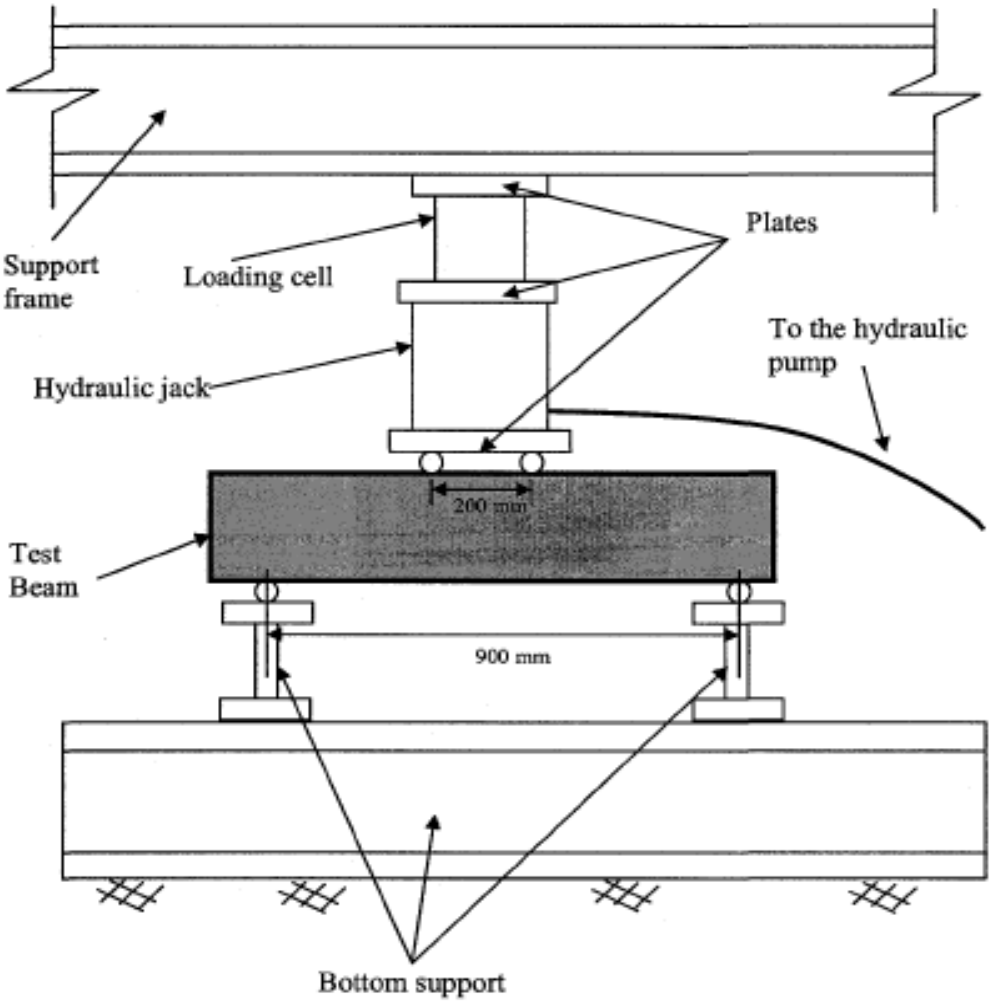

Figure 3.11: Schematic diagram for the modified Four-point Bend Test Set-up.

Figure 3.12: Four-point Bend Test Set-up of Beam Specimens.

Figure 3.13: Control Beam (A2-C) under Flexure Testing.

Figure 3.14: 6-days Corroded Beam under Flexure Testing.

3.12 GRAVIMETRIC WEIGHT LOSS

Following the flexure test on a corroded beam, it was broken to remove the stirrups and tension bars to measure the gravimetric weight loss due to induced corrosion. The bars were cleaned to remove the entire rust product using Clarke's solution and then they were weighed to determine the net weight of steel. Preparation, cleaning and evaluation of weight loss were carried out in accordance with ASTM G1 [44].

The percentage weight loss was calculated as:

$$Percentage\ weight\ loss = \frac{W_i - W_f}{W_i} \times 100 \quad (3.1)$$

Where:

W_i = initial weight of the bar before corrosion

W_f = weight after corrosion

The current was applied through the stainless steel plates covering the entire length of the corroding bar to make the distribution of the current uniform along the length. It was observed after breaking the specimen to expose bars that corrosion in general is non uniform. Samples of corroded steel after evaluating the gravimetric weight loss are shown in Figs. 3.15 to 3.17. These figures reaffirm the general perception that corrosion, in general, is not expected to be uniform throughout the length of the bar, as the loss of steel at some section is considerably higher than that at other sections.

Figure 3.15: Sample of main bars corroded for 6 days (Sample No: B10-6).

Figure 3.16: Sample of stirrups corroded for 6 days (Sample No: B10-6).

Figure 3.17: Sample of stirrups corroded for 10 days (Sample No: B5-10).

CHAPTER 4

RESULTS AND DISCUSSION

4.1 COMPRESSIVE STRENGTH OF CONCRETE

The 28-day compressive strength results of concrete for six 75 × 150 mm cylinders are shown in Table 4.1. All the concrete beams were casted in one batch only. The recorded values of compressive strength varied from 26.71 MPa to 41.65 MPa. An average value of $f_c^{'}$ for 6 cylindrical samples is 33.10 MPa with a standard deviation of 5.10.

Table 4.1: 28-days Compressive Strength of Concrete, $(f_c^{'})$.

Cylinder	$f_c^{'}$ **(MPa)**
01	33.07
02	35.36
03	26.71
04	31.60
05	41.65
06	30.11
Average	**= 33.10 MPa**

4.2 TENSILE STRENGTH OF STEEL

Typical stress-strain curves for the 8 mm and 20 mm diameter steel bars were obtained by plotting the tension test data, and are shown in Figs. 4.1 and 4.2 respectively. The plots correspond to typical stress-strain diagrams of carbon steel, having a sharp yield point and an extended strain-hardening zone. The values of yield and ultimate strengths *(f_y* and f_u) and the corresponding yield and ultimate strains(ε_y and ε_u) for both bars, are shown in Table 4.2.

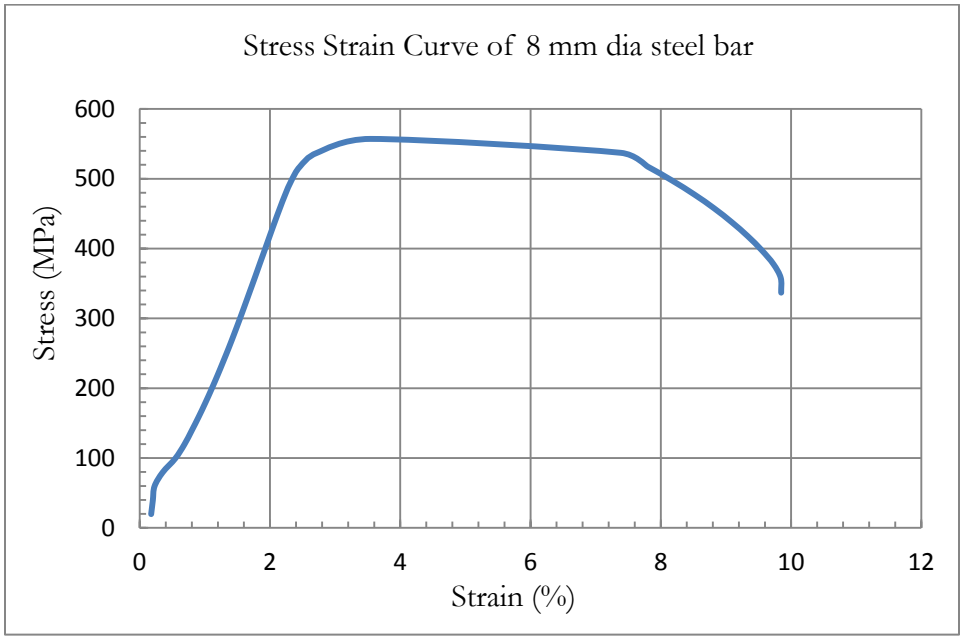

Figure 4.1: Stress-strain plot for 8 mm diameter steel bar.

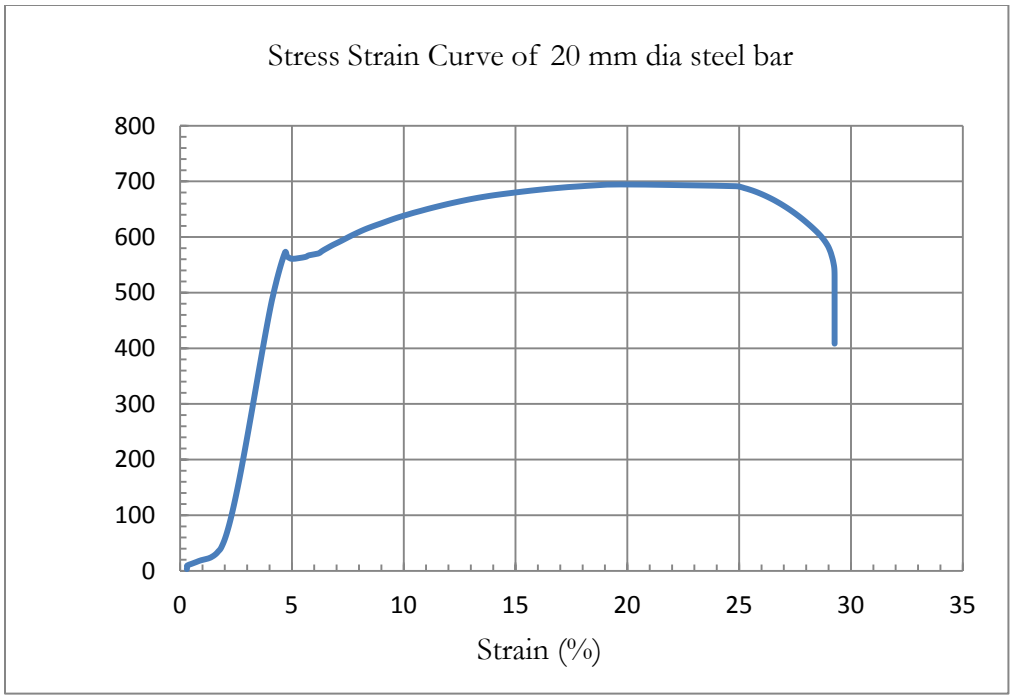

Figure 4.2: Stress-strain plot for 20 mm diameter steel bar.

Table 4.2: Yield and Ultimate Strengths and Strains of 8 and 20 mm Diameter Steel Bars.

Bar diameter (mm)	**Yield Strength, f_y (MPa)**	**Yield Strain, ε_y (mm/mm)**	**Tensile Strength, f_u (MPa)**	**Tensile Strain, ε_u (mm/mm)**
08	520	0.021	560	0.034
20	580	0.048	700	0.235

4.3 SHEAR STRENGTH OF CONTROL BEAM SPECIMENS

The ultimate shear strength capacity of the control beams, termed as $\mathbf{V_{thu}}$, was calculated using the conventional theory from the data gathered about the compressive strength of concrete f_c' indicated in Section 4.1 and tensile strengths of steel f_y , indicated in Section 4.2. The average calculated values of the shear capacity of the two control beams of each group are calculated as:

According to the ACI 318-08 Code provision, design for shear strength is to consider the total nominal shear strength V_n as the sum of two parts,

$$V_n = V_c + V_s \tag{4.1}$$

Where,

V_n is the nominal shear strength;

V_c is the shear strength of the beam attributable to the concrete

V_s is the shear strength attributable to the shear reinforcement

As per ACI-11.2.1.1 provision, V_c is calculated as:

$$V_c = 2\sqrt{f_c'}\, b_w d \tag{4.2}$$

Where, f_c' is in psi

b_w & d is in inch

As per ACI-11.4.7.2 provision, V_s is calculated as:

$$V_s = \frac{A_v f_y d}{s} \tag{4.3}$$

Where, A_v is the area of shear reinforcement within spacing s.

Based on the ACI code provisions, the calculated values of nominal shear strength are shown in Table 4.3.

Table 4.3: Theoretical Shear Capacity of Control Beams.

Beam	**Width of beam (mm)**	**Depth of beam (mm)**	**V_{thu} (kN)**
A1-C	140	220	142.33
B1-C	150	240	160.88

4.4 EXPERIMENTAL LOAD DEFLECTION PLOTS

The failure load, 2P, and the corresponding midspan deflection for each of the beam specimens were recorded using data logger and are presented in Tables 4.4 and 4.5 for control and the corroded beams, respectively.

Table 4.4: Flexure test results of Control Beams.

Beam	a/d ratio	Failure Load, 2P (kN)	Midspan Deflection at Failure Load (mm)
A1-C	1.77	280.2	6.1
B1-C	1.58	297.1	4.7

Table 4.5: Flexure Test Results of Corroded Beams.

Beam	a/d ratio	Failure Load, 2P (kN)	Midspan Deflection at Failure load (mm)
A3-10	1.77	192.14	4.4
A4-10		124.00	2.5
A5-10		163.19	3.5
A6-10		167.05	3.8
A7-6	1.77	177.00	3.8
A8-6		175.15	3.7
A9-6		180.05	3.9
A10-6		205.99	4.4
B3-10	1.58	161.74	3.5
B4-10		206.07	3.8
B5-10		210.00	3.8
B6-10		180.00	3.6
B7-6	1.58	238.20	4.2
B8-6		220.00	4.0
B9-6		140.60	3.0
B10-6		145.20	2.6

4.4.1 Effect of corrosion on load-deflection behavior of beams

Some typical load-deflection curves for both control and the corroded beam specimens are shown in Figures 4.3 and 4.4. These data indicate that reinforcement corrosion has a marked influence on the ductility of the beams. The failure of corroded beam was observed to be as brittle failure. It was evidenced that the stiffness of the beam was not influenced so much due to the reinforcement corrosion. The ultimate deflection of the beams, however, decreased with increasing reinforcement corrosion, leading to a reduction in the ductility of the beams.

To compare the load deflection behavior of some of the beams of each group, load deflection curves of beams of each group are depicted in one plot. Load deflection curves of all beams are presented in Appendix A.

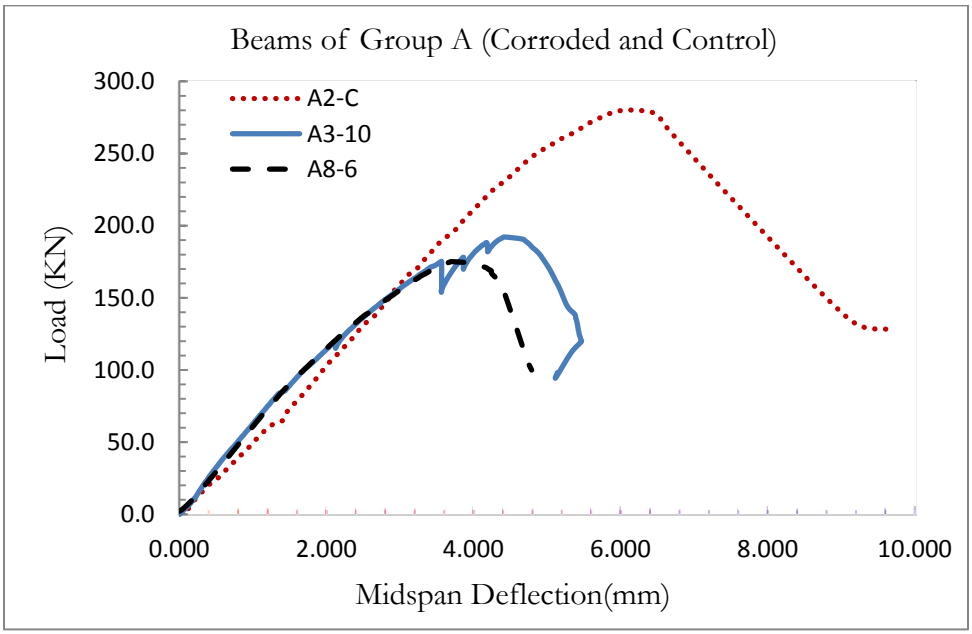

Figure 4.3: Typical Load-deflection Plot for Beams of Group A.

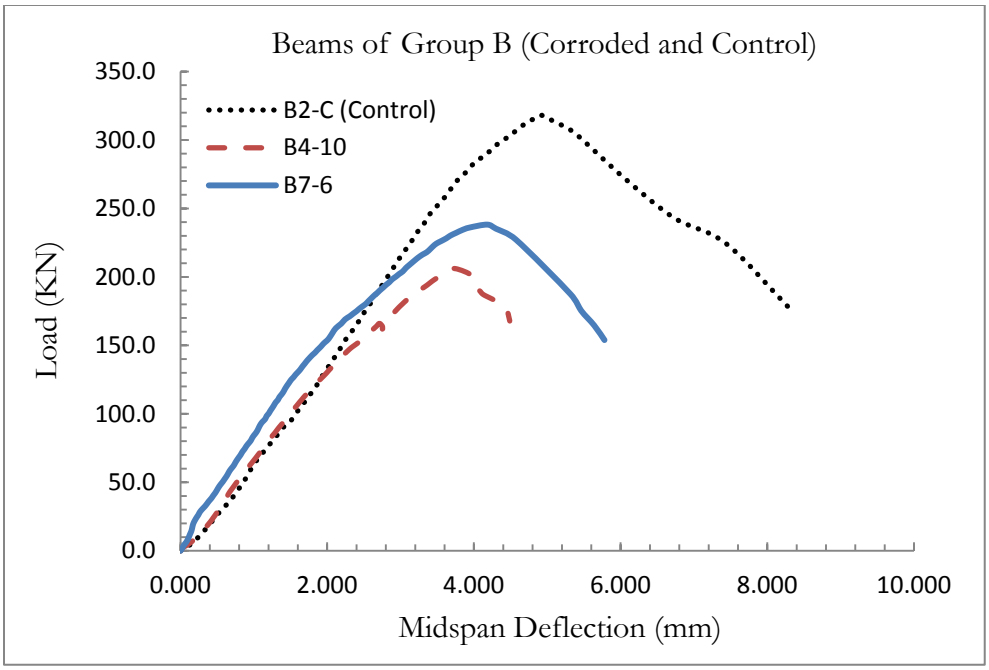

Figure 4.4: Typical Load-deflection Plot for Beams of Group B.

4.5 EXPERIMENTAL SHEAR CAPACITY OF BEAMS

4.5.1 Control Beams

The experimental shear capacity values, V_{exu}, of the control beams of each group (A and B) was calculated from statics as $V_{exu} = P$ kN, where P is the failure load applied to the beam (Fig. 3.10). This value of P equals one-half of the loads applied by hydraulic jack in kN. For each group, the average of the shear capacity values of the two control beams in the group was taken as the representative value of V_{exu} for that group. The experimentally determined values of V_{exu} for each group of control beams are presented in Table 4.6. The ratio V_{exu} / V_{thu} of each group's control beams designated as C_c indicates how good is the theoretical prediction of the beam's capacity, which was calculated in Section 4.3. These values of *Cc* and the corresponding values of both V_{thu} *and* V_{exu} are presented in Table 4.6.

Table 4.6: V_{exu} , V_{thu} and C_c for each group of specimens.

Beam	V_{thu} (KN)	V_{exu} (KN)	$C_c = \frac{V_{exu}}{V_{thu}}$
A1-C	142.33	140.10	0.98
B1-C	160.88	148.55	0.92

From Table 4.6 it can be seen that the values of *Cc* range from 0.92 to 0.98. The result shows that the theoretical shear capacity of the beams predicted by ACI-318 was found to be in close agreement with the experimental results in this experiment. In view of this , all comparisons are made on the basis of the experimental results.

4.5.2 Corroded beams

The experimentally determined values of shear strength of the corroded beams, V_{exc}, (V_{exc} = *P* kN determined from tests) are shown collectively for all beams in Table 4.7.

The ratio of V_{exc} / V_{exu} multiplied by 100, designated as *R,* indicates the residual strength in percentage of the original strength at uncorroded state. From Table 4.7, it is noted that for the beams of Group A with T = 10 days, the value of R varies approximately from 58 % to 69 % with an average R of 62 %. Similarly for Group B with T = 10 days, the value of R varies approximately from 54 % to 77 % with an average R of 69 %. The test results of A4-10, B9-6 and B10-6 were aborted due to accidental experimental mishap.

Table 4.7: Values of $\mathbf{V_{exc}}$, $\mathbf{V_{exu}}$, and *R* for each Group of Specimens.

Beam	**T, (Days)**	$\mathbf{V_{ex,c}}$ **(kN)**	$\mathbf{V_{ex,u}}$**, (kN) (from Table 4.6)**	$\mathbf{R = \frac{V_{ex,c}}{V_{ex,u}} \times 100}$	**Average R**
A3-10	10	96.07	140.10	68.57	62.14
A5-10		81.60		58.24	
A6-10		83.53		59.62	
A7-6	6	88.50	140.10	56.04	64.08
A8-6		87.58		62.51	
A9-6		90.03		64.26	
A10-6		103.0		73.52	
B3-10	10	80.87	148.55	54.44	68.75
B4-10		103.04		69.36	
B5-10		105.00		74.37	
B6-10		90.00		76.81	
B7-6	6	105.00	148.55	80.17	74.52
B8-6		110.00		68.86	

4.6 GRAVIMETRIC WEIGHT LOSS

The weight loss values of the bars were used to calculate the corrosion rate *(J_r),* as follows:

$$J_r = \frac{Weight\ loss(g)}{surface\ area\ of\ bar(cm^2) \times corrosion\ period(year)} \quad (4.4)$$

These values of J_r were used to determine the equivalent corrosion current density values *(I_{corr}),* using the following expression (Ijsseling, 1986 [56]):

$$J_r = \left(\frac{W}{F}\right) I_{corr} \quad (4.5)$$

Where:

J_r = Corrosion rate, in g/cm^2/year

I_{corr} = Corrosion current density mA/cm^2

W = equivalent weight of steel (g)

F = Faraday's constant (A-sec)

Substituting *W*= 55.85/2 = 27.925 g and *F* = 96487 Coulombs (A-sec) in Eq. (4.5) for steel, the following simplified equation for calculating I_{corr} from the value of J_r is obtained:

$$I_{corr} = 0.1096\, J_r \quad (4.6)$$

Where:

I_{corr} is in mA/cm^2

J_r is in g/cm^2/year

The weight loss of bar, per surface area, can be expressed by combining Eqs. (4.4) and (4.5), as follows:

$$\frac{Weight\ loss}{surface\ area\ of\ a\ bar} = \left(\frac{W}{F}\right) I_{corr}T = 0.289\ I_{corr}T \tag{4.7}$$

From the Eq. 4.7 it can be seen that the weight loss of a given bar is directly proportional to $I_{corr}T$ *(W/F* for steel is a constant).

The percentage of weight loss is calculated as follows:

$$\rho = \frac{weight\ loss(g)}{original\ weight(g)} \times 100 \tag{4.8}$$

The calculated values of equivalent I_{corr} from Eq. (4.6) are shown collectively for all corroded beams in Table 4.8.

Table 4.8: Gravimetric weight loss and their conversion into I_{corr}.

Beam	Conversion of weight loss into I_{corr}								
	Gravimetric test results							J_r g/cm²/yr (Eq. 4.4)	I_{corr} mA/cm² (Eq. 4.6)
	I_{app} mA/cm²	T days	Av. length of stirrups (cm)	Av. Surface area of stirrups (cm²)	Av. original wt. of stirrups (g)	Av. wt. loss (g)	ρ % wt. loss		
A3-10	2	10	55.69	139.96	201.42	57.51	28.55	14.99	1.64
A5-10	2	10	55.60	139.74	201.11	60.72	30.19	15.86	1.74
A6-10	2	10	55.89	140.47	202.14	78.27	38.72	20.34	2.23
A7-6	2	6	56.00	140.74	202.59	42.40	20.93	18.33	2.01
A8-6	2	6	56.67	142.43	204.98	45.90	22.39	19.60	2.15
A9-6	2	6	55.74	140.08	201.61	39.09	19.39	16.97	1.86
A10-6	2	6	56.46	141.89	204.23	42.94	21.03	18.41	2.02
B3-10	2	10	61.80	155.32	223.57	65.78	29.42	15.46	1.69
B4-10	2	10	62.45	156.95	225.88	60.52	26.79	14.07	1.54
B5-10	2	10	62.54	157.18	226.21	51.99	22.98	12.09	1.33
B6-10	2	10	62.58	157.28	226.35	65.89	29.11	15.30	1.68
B7-6	2	6	62.89	158.06	227.46	38.21	16.79	14.71	1.61
B8-6	2	6	62.55	157.22	226.26	38.99	17.23	15.09	1.65

The calculated values of equivalent I_{corr} from Eq. (4.6) are shown collectively for all corroded beams in Table 4.8. It is observed that the equivalent I_{corr} values established from gravimetric analysis are not exactly equal to the applied corrosion current density, I_{app}. Similar observations have been reported by other researchers [57-58]. The difference between I_{corr} and I_{app} can be attributed to several factors among which mention can be made of the concrete cover around the bars, quality of concrete, non-uniform corrosion rate along the length of the bars and the diameter of bars.

4.7 EFFECT OF CHOSEN VARIABLES ON REINFORCEMENT CORROSION

The variables chosen in this study include: duration of current application, T and the cross section of beam. As discussed in Section 4.6, a difference exists between the applied current intensity, I_{app}, and the measured corrosion intensity, I_{corr}, in accelerated corrosion tests. In laboratory or field tests on corroded beams, I_{corr} is determined through Galvanostatic or Potentiostatic measurement and it is regarded as the key parameter of corrosion activity. In view of this, I_{corr} , as determined through gravimetric analysis, is taken as the applicable value of corrosion current density for all computations.

From Eq. (4.7), it is noted that the weight loss of a bar is directly proportional to the product $I_{corr}T$, implying that a higher corrosion current density, I_{corr} for a lesser period of corrosion would be as damaging as a lesser value of I_{corr} for a longer corrosion period in terms of metal loss of a corroding bar. The product $I_{corr}T$ has been termed as *'corrosion activity index'* [12].

The values of $I_{corr}T$ and percentage weight loss, ρ of all beams, taken from Table 4.8, are presented in Table 4.9, in two groups with respect to the beam cross section.

The percentage weight loss of stirrups in each beam, ρ, is plotted with respect to $I_{corr}T$ in Fig. 4.5 for each group of data in Table 4.9.

Table 4.9: $I_{corr}T$ versus ρ Data for all sets of values.

Beam	$\boldsymbol{I_{corr}T}$ **(mA-year/cm^2)**	$\boldsymbol{\rho}$ **(% weight loss)**
A3-10	0.045	28.55
A5-10	0.048	30.19
A6-10	0.061	38.72
A7-6	0.033	20.93
A8-6	0.035	22.39
A9-6	0.031	19.39
A10-6	0.033	21.03
B3-10	0.046	29.42
B4-10	0.042	26.79
B5-10	0.036	22.98
B6-10	0.046	29.11
B7-6	0.026	16.79
B8-6	0.027	17.23

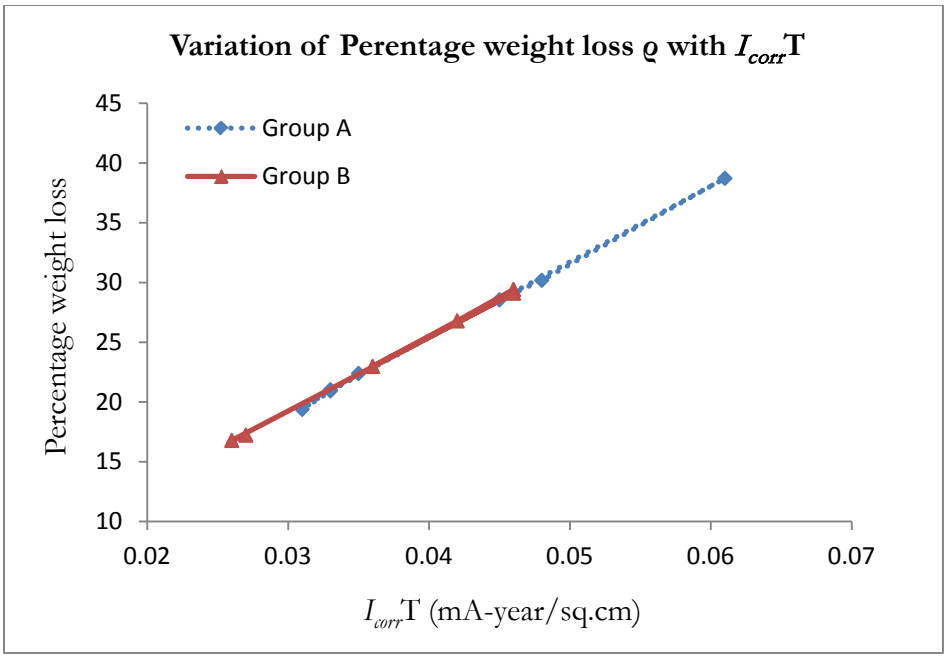

Figure 4.5: Percentage weight loss versus $I_{corr}T$.

It is seen from Fig. 4.5 that the plot of $I_{corr}T$ versus ρ (corrosion activity index versus percentage weight loss of bars) for the two groups of beams shows a linear relationship between $I_{corr}T$ and ρ as expected in view of Eq. (4.6).

4.8 EFFECT OF CORROSION ACTIVITY INDEX ON RESIDUAL SHEAR STRENGTH OF CORRODED BEAMS

Using data from Tables 4.7 and 4.8, Table 4.10 is prepared to list the values of $I_{corr}T$ and the percentage residual strength, *R* for all corroded beams, arranged into two groups with respect to beam cross sections. The results show a considerable amount of scatter, which is not unexpected in accelerated tests due to uncertainties in material properties and the assumption of uniform corrosion. However, the test data points to the fact that R decreases with increasing $I_{corr}T$. With increasing $I_{corr}T$, the metal loss will be higher and this inevitably will reduce the residual shear strength. As an example, for beams of Group B with bigger cross section, the average value of *R* increased from 68.7 % to 74.5 % when $I_{corr}T$ decreased from 0.043 to 0.027 mA-year/cm^2.

Table 4.10: $I_{corr}T$ versus R Data for all sets of values.

Group	Beam	$I_{corr}T$ (mA-year/cm^2)	Average $I_{corr}T$	R (% residual shear strength)	Average R (%)
A (140x220)	A3-10	0.045	0.051	68.57	62.1
	A5-10	0.048		58.24	
	A6-10	0.061		59.62	
	A7-6	0.033	0.033	56.04	64.1
	A8-6	0.035		62.51	
	A9-6	0.031		64.26	
	A10-6	0.033		73.52	
B (150x240)	B3-10	0.046	0.043	54.44	68.7
	B4-10	0.042		69.36	
	B5-10	0.036		74.37	
	B6-10	0.046		76.81	
	B7-6	0.026	0.027	80.17	74.5
	B8-6	0.027		68.86	

4.9 SHEAR STRENGTH OF CORRODED BEAMS

The shear strength of a corroded beam at a given value of $I_{corr}T$ is affected predominately by the following two phenomena:

(i) The loss of metal due to corrosion. The net cross-sectional area of stirrups decreases with the loss of metal and this in turn would reduce the shear capacity of the beam.

(ii) There is a moderate effect on shear strength due to significant loss of bond between reinforcement and concrete from corrosion and crack-induced damage. Past research has shown that reinforcement corrosion leads to degradation of bond, following a small increase in strength at the early stage of corrosion [23-27]. Literature [43-45] shows different observations for shear strength of corroded beam related to the loss of bond.

The yield strength of the corroded steel as reported by Zhang et al. [59], Xi et al. [60], and Jin and Zhao [37], is expected to increase with the corrosion period. However Uomoto et al. [35] and Aziz [41] reported in their study that the yield strength decreases due to the reinforcement corrosion.

In view of the past contradicting findings, the original yield strength of bars has been used in all calculations as the reported change in yield strength for smaller degree of corrosion is not too significant. The shear capacity of corroded beam is first calculated in the same manner as the control beams but using reduced diameter of stirrups, *D*' due to corrosion in place of the original diameter, *D*. Any adverse implication of possible bond loss between reinforcement and concrete from corrosion on shear capacity has been ignored for

this calculation. The reduced diameter *D*' is calculated from the well-known formula for metal loss rate or penetration rate, *Pr*, given as [56]:

$$P_r = \frac{W}{F\gamma_{st}} I_{corr} = \frac{J_r}{\gamma_{st}} \tag{4.9}$$

Where:

P_r = penetration rate cm/year

I_{corr} = corrosion current density mA/cm^2

γ_{st} = density of steel = 7.85 g/cm^3

Jr = instantaneous corrosion rate, in g/cm^2/year

W = equivalent weight of steel = 55.85/2 = 27.925 g

F = Faraday's constant = 96487 Coulombs (Amp-sec)

Equation 4.9 can be simplified as follows:

$$P_r = \frac{W}{F\gamma_{st}} I_{corr} = \frac{27.925}{96487 \times 7.85 \times 1000} \times 24 \times 60 \times 60 I_{corr} = 0.003185 I_{corr} \tag{4.10}$$

The reduction in bar diameter in active corrosion with steady-state corrosion current density I_{corr} for corrosion period *T* is $2P_rT$ and the percentage reduction in diameter of bar is $\frac{2P_rT}{D} \times 100$, where *D* is the original bar diameter.

The reduced net diameter of a corroded bar, D' is then written as:

$$D' = D\left(1 - \frac{2P_rT}{D}\right) \tag{4.11}$$

In terms of cross-sectional area, Eq. (4.11) can be recast for calculating the reduced cross-sectional area $A_v{}'$ of a stirrup as:

$$A_v{}' = A_v(1 - \alpha)^2 \tag{4.12}$$

Where:

A_v is the original cross-sectional area of the shear reinforcement and

$\alpha = 2P_rT/D$, which has been termed as 'metal loss factor' [12].

From Eqs. (4.7) and (4.9), the percentage weight loss ρ can be shown as equal to (2α) times 100.

$$\rho = (2 \times \alpha - \alpha^2) \times 100 \tag{4.13}$$

For small values of P_r, $\alpha^2 \approx 0$. This means that Eq. 4.10 can be simplified as follows:

$$\rho \approx 2\alpha \times 100 \tag{4.14}$$

Using $A_v{}'$ in place of A_v, $V_{th,c}$ values of all corroded beams were calculated using ACI 318 provision i.e. $V_{th,c}$ is equal to the sum of V_c and $V_s{}'$(using reduced diameter of stirrups) as calculated for the control beams. The calculated values of $V_{th,c}$ are presented in Table 4.11 along with the corresponding values of R_f, which is the ratio of $V_{exp,c}/V_{th,c}$.

Table 4.11: D', $V_{exp,c}$, $V_{th,c}$, and R_f for the Corroded Beams.

Beam	**D (mm)**	$\boldsymbol{\alpha}$	$\boldsymbol{I_{corr}T}$ **(mA-year/cm^2)**	**D' (mm)**	$\boldsymbol{V_{th,c}}$ **(kN)**	$\boldsymbol{V_{exp,c}}$ **(kN)**	$\boldsymbol{R_f = \frac{V_{exp,c}}{V_{th,c}}}$
A3-10	8	0.131	0.045	6.95	112.99	96.07	0.85
A5-10	8	0.138	0.048	6.89	111.51	81.60	0.73
A6-10	8	0.178	0.061	6.58	103.64	83.53	0.81
A7-6	8	0.096	0.033	7.23	120.48	88.50	0.73
A8-6	8	0.103	0.035	7.18	119.04	87.58	0.74
A9-6	8	0.089	0.031	7.29	122.02	90.03	0.74
A10-6	8	0.096	0.033	7.22	120.38	103.0	0.86
B3-10	8	0.135	0.046	6.92	127.25	80.87	0.64
B4-10	8	0.123	0.042	7.02	130.13	103.04	0.79
B5-10	8	0.105	0.036	7.16	134.17	105.00	0.78
B6-10	8	0.133	0.046	6.93	127.57	90.00	0.71
B7-6	8	0.077	0.026	7.38	141.09	119.10	0.84
B8-6	8	0.079	0.027	7.37	140.60	110.00	0.78

From the experimental data presented in Table 4.11, it was observed that R_f value is significantly less than 1.0, implying that residual shear capacity cannot be predicted by using only reduced area of shear reinforcement $A_v{}'$.

4.10 MODE OF FAILURE OF CONTROL AND CORRODED BEAMS

Figures 4.6 and 4.7 shows the crack pattern in a control beam and a corroded beam at failure. Typically the cracks originate from the bottom (near the support) and then advances in an inclined manner. All cracks observed are typically diagonal cracks as shown in the below figures. Failure was assumed to occur when the applied load on the beams began to drop, with increasing midspan deflection.

Figure 4.6: Failure of a Typical Control Beam (A2-C).

Figure 4.7: Failure of a Typical Corroded Beam (B8-6).

Figure 4.8: A close view of crack pattern for control Beam (B1-C).

CHAPTER 5

PREDICTION OF RESIDUAL SHEAR STRENGTH

An attempt has been made to utilize the experimental data gathered in this study for proposing a predictive model for the estimation of the residual shear strength of beams that are subjected to reinforcement corrosion.

5.1 BASIS FOR THE DEVELOPMENT OF THE MODEL

The prediction model for the residual shear strength of corroded reinforced concrete beams was developed on the basis of the following observations, as discussed in Chapter 4:

(i) Degree of corrosion increases with increasing corrosion activity index, $I_{corr}T$, and consequently shear strength of a corroded beam decreases with increasing $I_{corr}T$ due to loss of stirrup area.

(ii) The values of R_f, determined on the basis of theoretical shear capacity, calculated using only reduced cross-sectional area $A_v{}'$ from Eq. (4.12), shows that R_f is considerably less than 1.0.

(iii) The effect of crack induced damage and bond slip should be considered in developing a correction factor.

5.2 STRENGTH PREDICTION MODEL

5.2.1 Approach

The following two-step procedure is proposed to predict the residual strength of a corroded beam for which the cross-sectional details, materials strengths and corrosion activity index, $I_{corr}T$ are known:

(i) First, shear capacity, $V_{th,c}$ is calculated using reduced cross sectional area of reinforcement, $A_v{}'$, calculated from Eq. (4.12).

(ii) The computed value of $V_{th,c}$ is then multiplied by an applicable correction factor, R_v to obtain the predicted residual strength of the beam, V_r, as follows:

$$V_r = R_v V_{th,c} \tag{5.1}$$

The value of R_v reflects all other corrosion effects including crack induced damage.

5.2.2 Correction Factor, R_v

The proposed value of R_v is taken as a function of two important variables namely, $I_{corr}T$ and (A_v/ds). The parameter (A_v/ds) is the ratio of shear reinforcement to the effective area within which A_v is present and therefore represents the amount of shear reinforcement.

$$R_v = f\left(I_{corr}T,\ \frac{A_v}{ds}\right)$$

Based on the experimental observations and several trials, R_v is taken in the following empirical form:

$$R_v = 1 - \left\{C \times (I_{corr}T)^x \times \left(\frac{A_v}{ds}\right)^y\right\} \quad (5.2)$$

Where C, x and y are the constants that are determined through a multi-level regression of test data for R_v (Table 4.11).

To find the values of the constants C, x and y, a regression analysis has been done with respect to the following criterion:

The best fitting relationship is obtained in such a way that the predicted values is lower than the actual experimental data in over 85% of the cases (safe prediction) and in the other cases the predicted values should not exceed 15% of the actual strength. Also the whole set of data has been restricted to a condition that not more than 10% of the data should over estimate the actual experimental values. The enforcement of this criterion leads to a prediction that can be relied upon.

Regression analysis of all data yields:

C = 4.52

x = 0.64

y = 0.14

Thus, the proposed equation for R_v is:

$$R_v = 1 - \left\{4.52 \times (I_{corr}T)^{0.64} \times \left(\frac{A_v}{ds}\right)^{0.14}\right\} \quad (5.3)$$

Where,

d = depth of beam in mm

s = spacing of stirrups in mm

A_v = Area of stirrups in mm^2

I_{corr}= corrosion current density in mA/cm^2

T = duration of corrosion in year

The R_v values for all the corroded beams are calculated by substituting $I_{corr}T$, A_v, d and s values in Eq. (5.3). The residual shear strength, V_r, for all the 13 corroded beams are calculated from Eq. (5.1) using the values of $V_{th,c}$ (Table 4.11). The values of R_v, $V_{ex,c}$ and predicted V_r for all the 13 corroded beams are presented in Table 5.1.

Table 5.1: Values of R_v, $V_{th,c}$, $V_{ex,c}$ and V_r.

Beam	$\boldsymbol{R_v}$ **(Eq. 5.3)**	$\boldsymbol{V_{th,c}}$ **(kN)**	**Measured** $\boldsymbol{V_{ex,c}}$ **(kN)**	**Predicted** $\boldsymbol{V_{res}}$ **(kN)**	**% Error** $\boldsymbol{\frac{(V_{ex,c} - V_{res})}{V_{ex,c}} \times 100}$
A3-10	0.69	112.99	96.07	77.9	19
A5-10	0.68	111.51	81.60	75.8	8
A6-10	0.62	103.64	83.53	64.3	23
A7-6	0.74	120.48	88.50	89.2	-1
A8-6	0.73	119.04	87.58	86.9	0
A9-6	0.76	122.02	90.03	92.7	-2
A10-6	0.74	120.38	103.0	89.1	13
B3-10	0.69	127.25	80.87	87.8	-8
B4-10	0.70	130.13	103.04	91.1	11
B5-10	0.73	134.17	105.00	97.9	7
B6-10	0.69	127.57	90.00	88.0	2
B7-6	0.78	141.09	119.10	110.1	7
B8-6	0.78	140.60	110.00	109.7	1

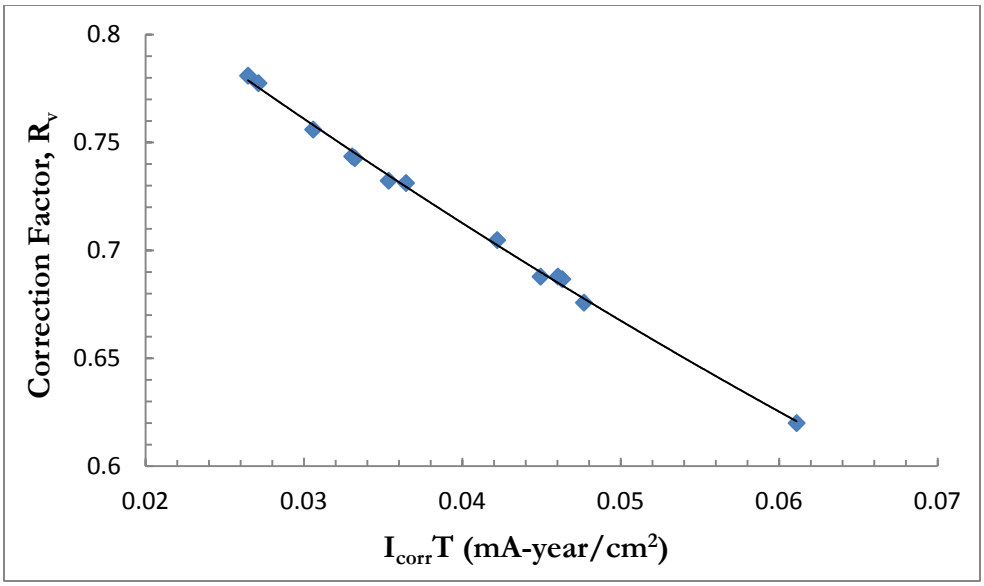

Figure 5.1: Variation of R_v vs. $I_{corr}T$.

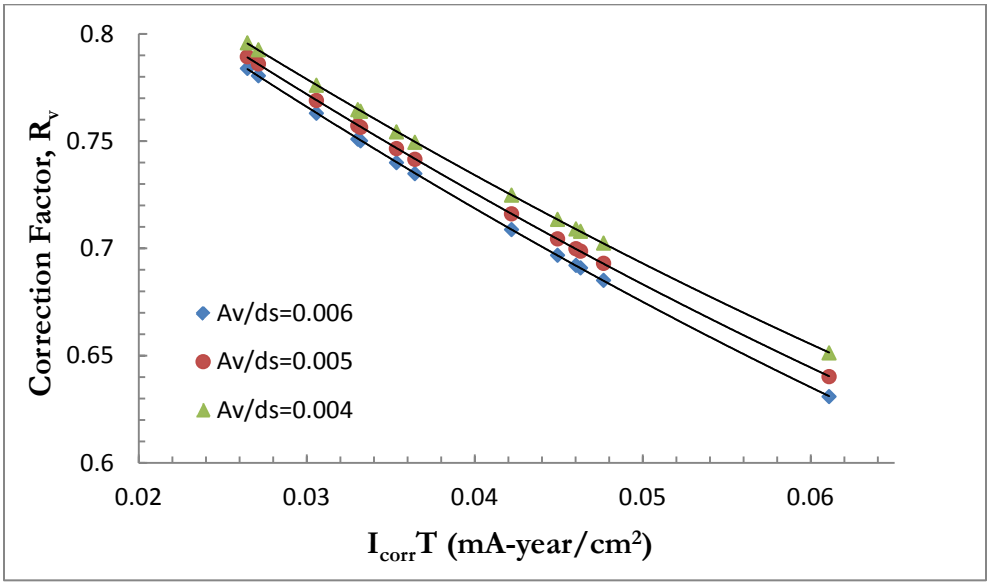

Figure 5.2: Variation of R_v vs. $I_{corr}T$ for different A_v/ds.

From Table 5.1, it is to be noted that out of total 13 predicted values of V_r, 9 values have less than 10% error. About 40% of the data shows an error less than 5%. Based on the experimental values of $I_{corr}T$, the variation of R_v has been depicted in Fig. 5.1. It is observed that the predicted correction factor R_v decreases with an increasing $I_{corr}T$. Similarly for the same $I_{corr}T$, different plots (shown in Fig. 5.2) for varying A_v/ds has been obtained in order to draw the effect of A_v/ds on R_v. The above figure 5.2 reveals that the R_v values are generally lower for the higher values of A_v/ds.

The proposed strength prediction model can be utilized either to find the residual shear capacity of a beam that has suffered corrosion damage or to find the limit of I_{corr} for a given corrosion period that can be permitted for a beam at a lowest level of compromised safety. The latter has practical significance, as I_{corr} can be measured in-situ for a beam to determine the level of corrosion activity. The proposed model allows to predetermine the maximum level of $I_{corr}T$ or I_{corr} for a given *T* at which the residual shear capacity of a beam is expected to reach the minimum safe value.

The utility of the proposed shear strength prediction model can be explained through the various examples shown in Appendix B.

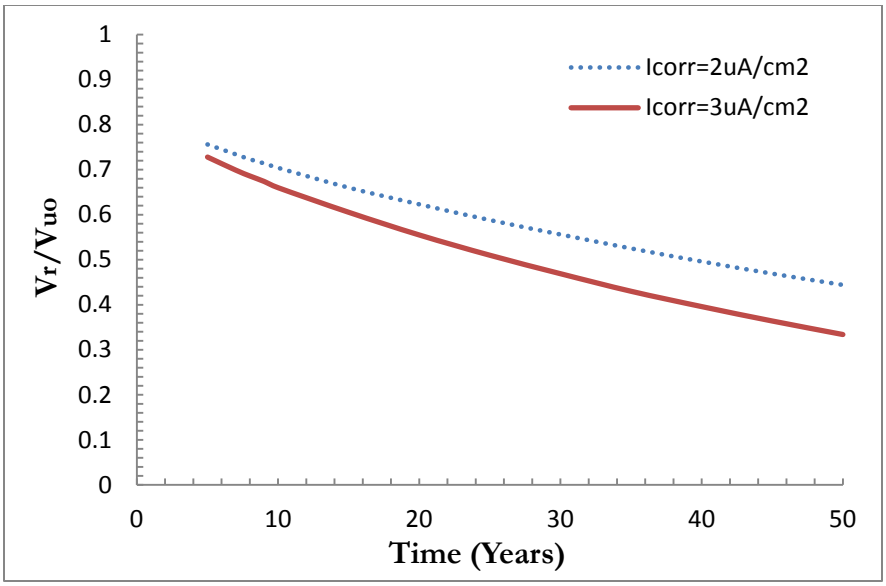

Figure 5.3: Variation of V_r with time for two different corrosion intensity

Figure 5.3 shows the plot of V_r/V_{uo} versus time to demonstrate the declining trend of V_r with time. Two different values of corrosion current density, I_{corr} = 2 μA/cm² and 3 μA/cm² are chosen to show the effect of corrosion on the trend of shear strength. It shows that the shear strength reduction is higher for 3 μA/cm² than the lower corrosion current density, as expected.

5.3 COMPARISON OF THE PROPOSED METHOD WITH THE PAST RESEARCH DATA

To check the general applicability of the proposed model, it is compared with some of the past research work by using those datas into the model. The model has been checked using the data reported by the following researchers:

i. Rodriguez et al., (1997) [34]

ii. Juarez et al., (2011) [71]

The reason for relating to the data of the above researchers is that their data provide complete information on I_{corr}, T, D, the cross-section of the beam and material properties.

5.3.1 Comparison with Rodriguez et al. data

Rodriguez et al. [34], carried out experiments on beams of dimensions 2300 × 200 × 150 mm. Compressive strength varied from 34 MPa to 37 MPa, and the yield strength of the shear reinforcement was 626 MPa. A constant current density of about, 100 $\mu A/cm^2$ was applied to the rebars for a period of time ranging between 100 and 200 days approximately. The details of the comparison are shown in Table 5.2.

A curve is plotted between the experimental shear value as given by Rodriguez et al. [34], and the shear predicted by the proposed model in Fig 5.3.

Table 5.2: Comparison of the Proposed Model results with Rodriguez et al. [34] data.

Beam	**T (days)**	R_v **(Eq. 5.3)**	V_{thc} **(kN)**	V_{exp}**- Rodriguez (kN)**	$V_{pred.}$ **using proposed model (kN)**	**% Error**
B1	104	0.8	46.81	39.8	37.5	5.9
B2	115	0.79	46.16	37.3	36.5	2.1
B3	163	0.74	43.45	27.9	32.1	-15
B4	175	0.72	42.79	31.4	30.8	1.9
B5	108	0.8	47.18	34.6	37.7	-8.9
B6	116	0.79	46.73	34.5	36.9	-6.9
B7	164	0.73	44.02	29.1	32.1	-10.3
B8	175	0.72	43.42	33.9	31.3	7.7
B9	108	0.8	46.57	38.6	37.3	3.4
B10	127	0.77	45.47	36.2	35.0	3.3
B11	154	0.74	43.94	26.6	32.5	-22.1
B12	181	0.72	42.47	28.7	30.6	-6.6
B13	164	0.7	65.3	37.7	45.71	-21.2

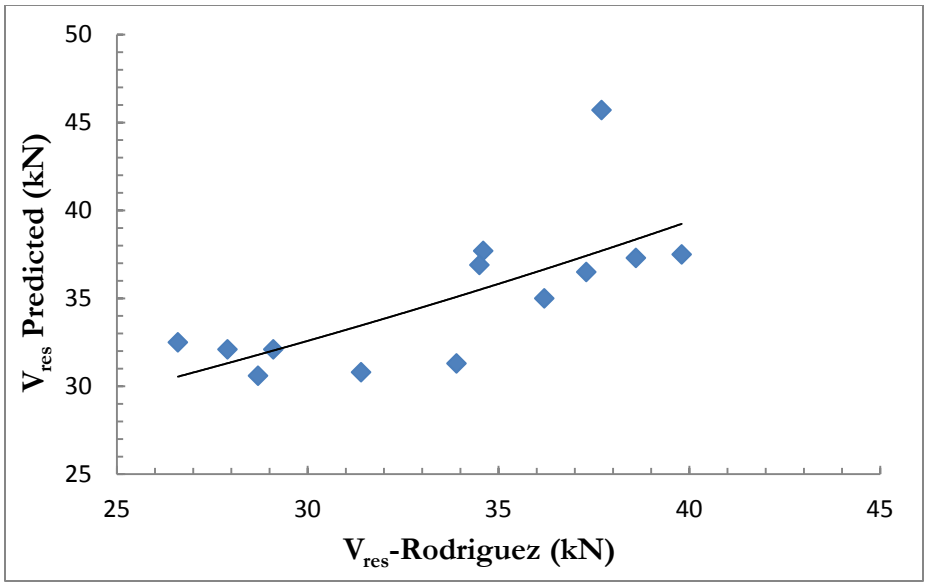

Figure 5.4: Comparison of Measured V_{exp} and the Predicted V_r (Rodriguez Data [34])

From Table 5.2 and Fig. 5.4, it appears that the proposed model can be used to predict with reasonable accuracy. It can be noted that almost 80% of the data are within the range of 10% error which is an acceptable range.

5.3.2 Comparison with Juarez et al. data

Juarez et al. [71], carried out experiments on beams of dimensions 2000 × 350 × 200 mm. Compressive strength for the concrete with a slump of 85 mm was used as 21 MPa and the yield strength of the shear reinforcement was 420 MPa. A constant current density of about, 100 μA/cm^2 was applied to the rebars. The duration of current applied to produce a 20% and 50% loss of shear strength resulting in a moderate and severe level of corrosion, respectively was estimated to be 80 and 120 days. The details of the comparison are shown in Table 5.3.

Table 5.3: Comparison of the Proposed Model results with Juarez et al. [71] data.

Beam	**T (days)**	R_v **(Eq. 5.3)**	V_{thc} **(kN)**	V_{exp}**- Juarez et al. (kN)**	V_{pred} **using proposed model (kN)**	**% Error**
B1	80	0.83	110.3	68	92.1	35
B2	80	0.83	115.9	91	96.8	6.4
B3	120	0.78	104.9	80	81.8	2.3
B4	120	0.78	114.0	86	88.9	3.4
B5	80	0.84	99.2	77	83.5	8.4
B6	80	0.84	92.7	87	77.9	10.4
B7	120	0.79	92.7	80	73.2	8.5
B8	120	0.79	84.9	89	68	23.6

From Table 5.3, it looks that the proposed model predicts good results for the V_r by comparison with the V_{exp} reported by Juarez et al. [71]. It can be noted that six out of eight data points are within the range of 10% error. These results indicate that the model can be used to predict the residual shear strength with an acceptable accuracy.

5.4 RELIABILITY ANALYSIS OF REINFORCED CONCRETE BEAMS USING MONTE CARLO SIMULATION

5.4.1 Monte Carlo Simulation Basics

A Monte Carlo method is a technique for iteratively evaluating a deterministic model using sets of random numbers as inputs. This method is often used when the model is complex, non linear, or involves more than just a couple uncertain parameters. A simulation can involve over 100000 evaluations of the model. It is just one of many methods for analyzing uncertainty propagation, where the goal is to determine how random variation, lack of knowledge, or error affects the sensitivity, performance, or reliability of the system that is being modeled. This method is categorized as a sampling method because the inputs are randomly generated from probability distributions to simulate the process of sampling from an actual population. So, a distribution for the inputs is chosen that most closely matches the actual data or best represents the current state of knowledge. The data generated from the simulation can be represented as probability distributions (or histograms) or converted to error bars, reliability predictions, tolerance zones and confidence intervals. The basic principle behind Monte Carlo simulation is represented in the Figure 5.5.

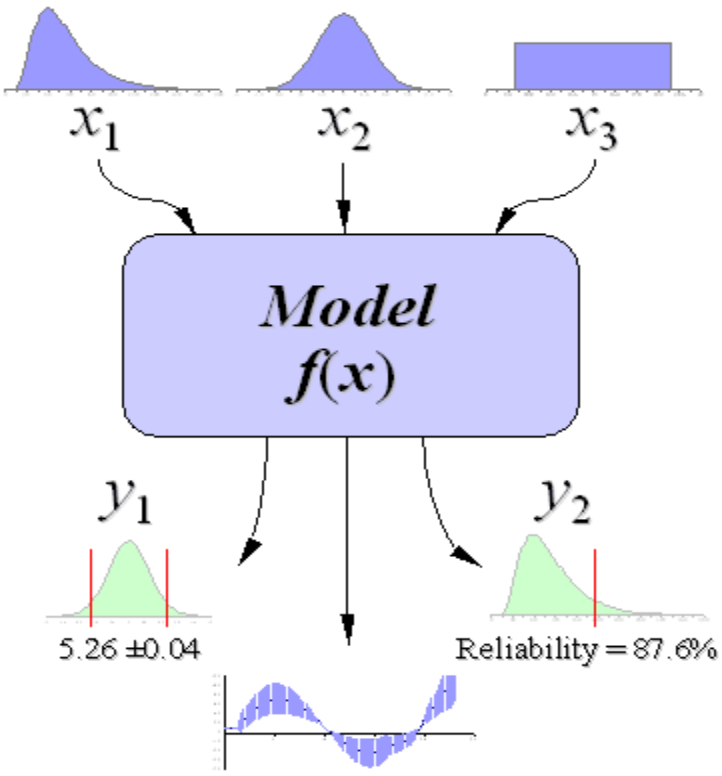

Figure 5.5: Schematic showing the basic principle behind Monte Carlo Simulation.

5.4.2 Techniques and steps involved for Monte Carlo Simulation

Monte Carlo simulation is effective and practical for problems involving random variables with known or assumed probability distributions. This simulation conducts a repeating process using a set of random variables generated in accordance with the corresponding probability distribution. A set of data from Monte Carlo simulation is similar to a set of experimental data if the sample set of data is large and probability distributions are selected properly.

In the present study, the Monte Carlo technique was employed for simulation of the deterministic model based on the random variables selected in order to find the probability of failure in shear. A total of eight parameters were considered as random variables and the distribution for all the eight parameters were assumed to be normal distribution. These include the parameters related to the concrete and steel strength, beam dimensions, area of stirrups (before and after corrosion) and its spacing and corrosion current density. Based on the experimental record and some literature feedback, the statistical data were obtained for the parameters like concrete compressive strength, $f_c^{'}$, yield strength of steel, f_y, and corrosion activity index, $I_{corr}T$. These statistical details will be utilized further in an example to perform the reliability analysis of beam.

The steps in Monte Carlo simulation corresponding to the uncertainty propagation are fairly simple and can be easily implemented in MS EXCEL. General steps to be followed have been shown below:

Step 1: Create a deterministic model, $y = f(x_1, x_2, \ldots., x_q)$

Step 2: Generate a set of random inputs, $x_{i1}, x_{i2}, \ldots., x_{iq}$

Step 3: Evaluate the model and store the results as y_i

Step 4: Repeat steps 2 and 3 for $i = 1\ to\ n$

Step 5: Analyze the results using histograms, summary statistics etc.

The steps for Monte Carlo simulations involved in this study is quite similar as above, but is best represented in the form of a flowchart which is shown in Fig. 5.6:

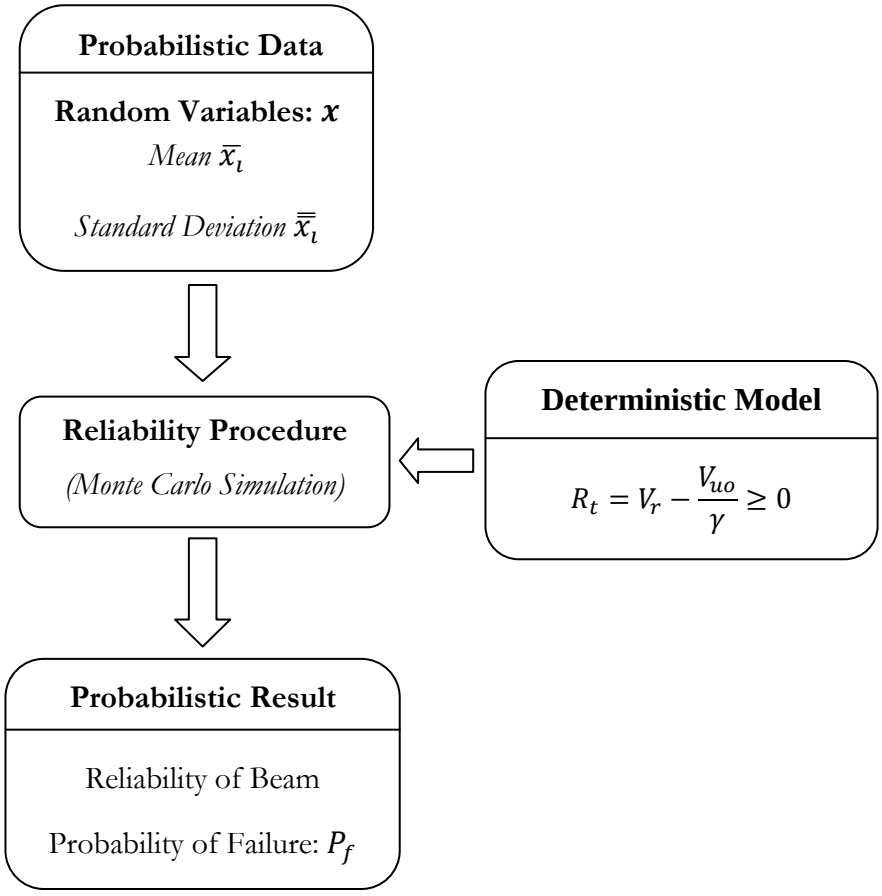

Figure 5.6: Flowchart representation of Reliability using Monte Carlo simulation.

5.4.3 Normal Probability Distribution

The normal, or Gaussian, probability distribution has a bell-shaped curve. It is characterized by its mean mu (μ) and standard deviation sigma (s). The mean describes the location of the curve, the standard deviation describes the shape (how peaked or flat it is). Normal distribution is characterized by a continuous distribution of random variables. Thus continuous distribution is represented by the cumulative distribution function, which gives the probabilities of any random variables less than or equal to the data, i.e. x.

To distinguish between the cumulative distribution function and the probability density function, at first discrete and continuous distributions are defined. With a discrete distribution, the probabilities of a particular value can be computed. Therefore, with a discrete distribution, the probability density function (pdf) determines the probability that a value is exactly equal to x. With a continuous distribution, the probabilities over a range can only be computed. Thus, the cumulative distribution function (cdf) determines the probability that a value in the data set is less than or equal to x.

Based on the experimental data, the normal probability distribution has been plotted in the form of a cumulative frequency distribution for some of the varying parameters. Some of the typical plots for cumulative probability distribution have been shown in Figures 5.7 and 5.8.

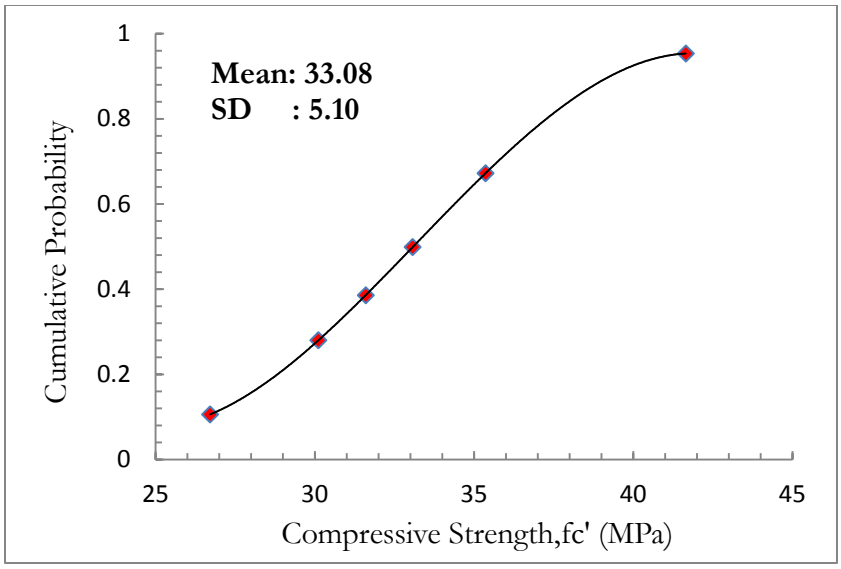

Figure 5.7: Cumulative Probability Distribution for $f_c{}'$.

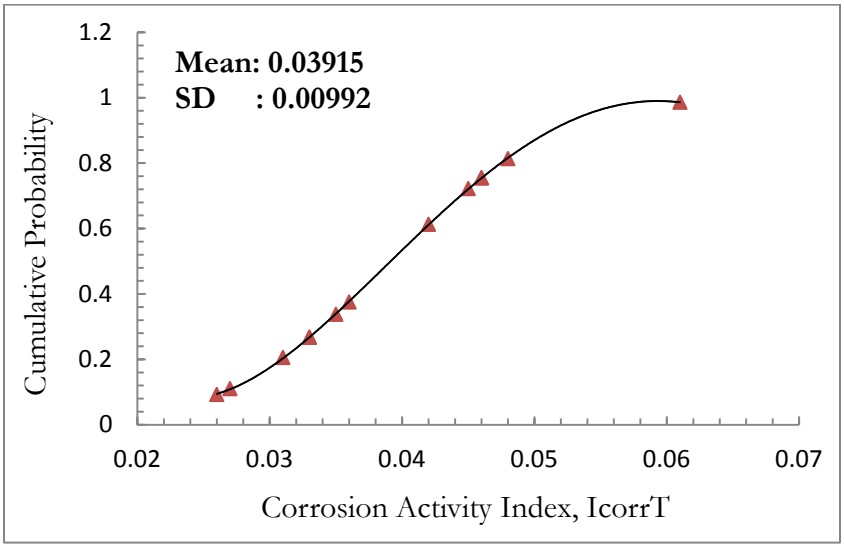

Figure 5.8: Cumulative Probability Distribution for $I_{corr}T$.

5.4.4 Development of Deterministic Safety Model

The original shear strength as per ACI Code provision:

$$V_{uo} = \emptyset(V_c + V_s) = \emptyset\left[2\sqrt{f_c'}\, b_w d + \frac{A_v f_y d}{s}\right] \tag{5.4}$$

The residual shear strength of a corroded beam is predicted as:

$$V_r = \emptyset \times R_v(V_c + V_s') = \emptyset \times R_v\left[2\sqrt{f_c'}\, b_w d + \frac{A_v' f_y d}{s}\right] \tag{5.5}$$

This strength predicted by Eq. (5.5) must be greater or equal to the reduced original strength V_{uo}/γ, where γ is the maximum applicable factor that must be assumed to ensure that the residual strength is not less than the reduced original strength, V_{uo}/γ. Higher the value of γ (γ less than the original factor of safety used in design), less will be the factor of safety. A reasonable value of γ must therefore be assumed to establish a threshold of V_{uo}/γ below which the member's strength can be classified as deficient.

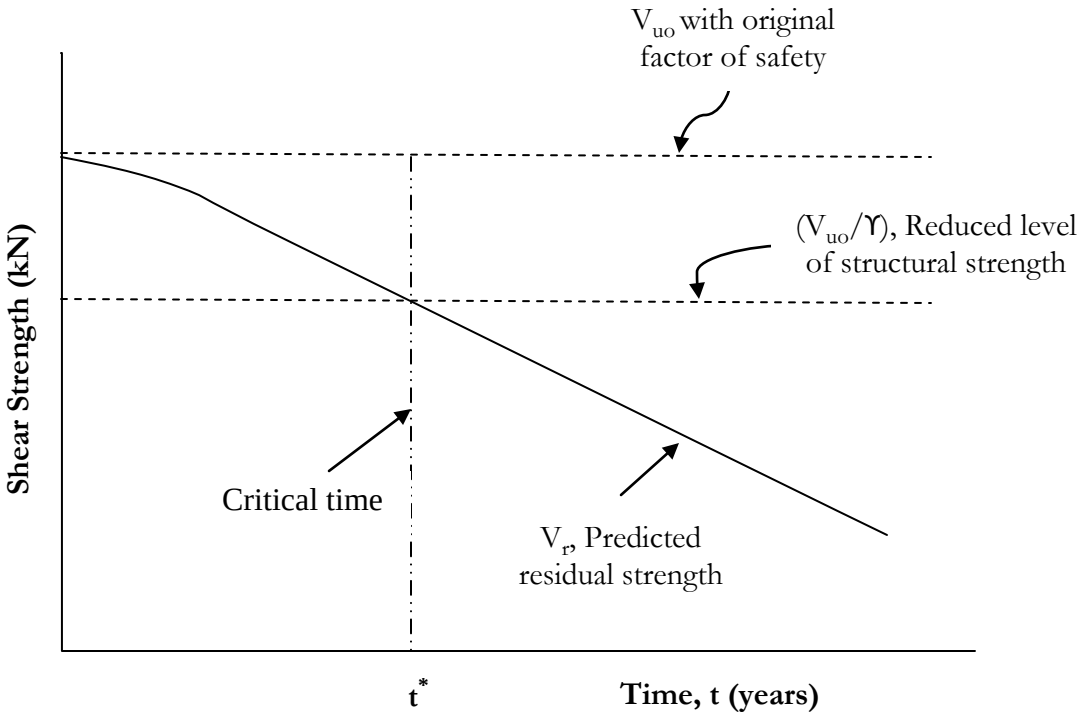

Figure 5.9: Determination of critical time for corrosion damage.

The original shear strength (including factor of safety) V_{uo} has been reduced to a permissible level by choosing a maximum value of a factor γ in order to ensure that the residual shear strength V_r of corroded beam must not exceed this boundary as shown in Figure 5.9. The critical time at which the residual strength is exceeding the reduced level is determined as t^* (Figure 5.9), beyond which the structure is classified as unsafe or dangerous. When time, $t < t^*$, the structure is considered as safe but if $t \geq t^*$, structure is unsafe. Thus, for a structure to be in the safe region, V_r should always be greater and equal to V_{uo}/γ. Based on this concept the deterministic safety model is designed. Therefore, the probability of the prediction with regard to the safety can then be expressed as:

$$R_t = V_r - \frac{V_{uo}}{\gamma} \geq 0 \quad (5.6)$$

This deterministic model has been used in Monte Carlo simulation to find out the probability of R_t satisfying Eq. (5.6).

5.5 APPLICATION OF THE PROPOSED MONTE CARLO SIMULATION

The application of the proposed Monte Carlo simulation for the reliability of corroded beam is demonstrated using the following assumed data:

Effective depth of beam = 220 mm

Width of beam = 160 mm

Diameter of shear reinforcement = 8 mm

Spacing of stirrups = 100 mm c/c

Concrete Compressive strength, $f_c{}'$ = 45 N/mm^2

Yield strength of bar, f_y = 500 N/mm^2

I_{corr} = 1 μA/cm^2

The statistical parameters and its distribution as presented in Table 5.3 are assumed to be valid.

Table 5.4: Statistical properties of random variables

Parameter	Mean	SD	COV	Distribution
$f_c{}'$ (MPa)	45	7.2	0.16	Normal
f_y (MPa)	500	50	0.1	Normal
b (mm)	160	3.84	0.024	Normal
d (mm)	220	5.28	0.024	Normal
$A_v\ (mm^2)$	100.5	5.03	0.05	Normal
s (mm)	100	4.2	0.042	Normal
$A_v{}'\ (mm^2)$	78.52	5.02	0.064	Normal
$I_{corr}T$ $(mA-year/cm^2)$	0.04	0.01	0.25	Normal

Based on the above statistical details for all the varying parameters, Monte Carlo simulation was performed and more than 100000 random variables were generated. The design equation for the reliability analysis used in Monte Carlo simulation has been discussed earlier in Eq. 5.6.

(i) Determination of critical time for corrosion damage

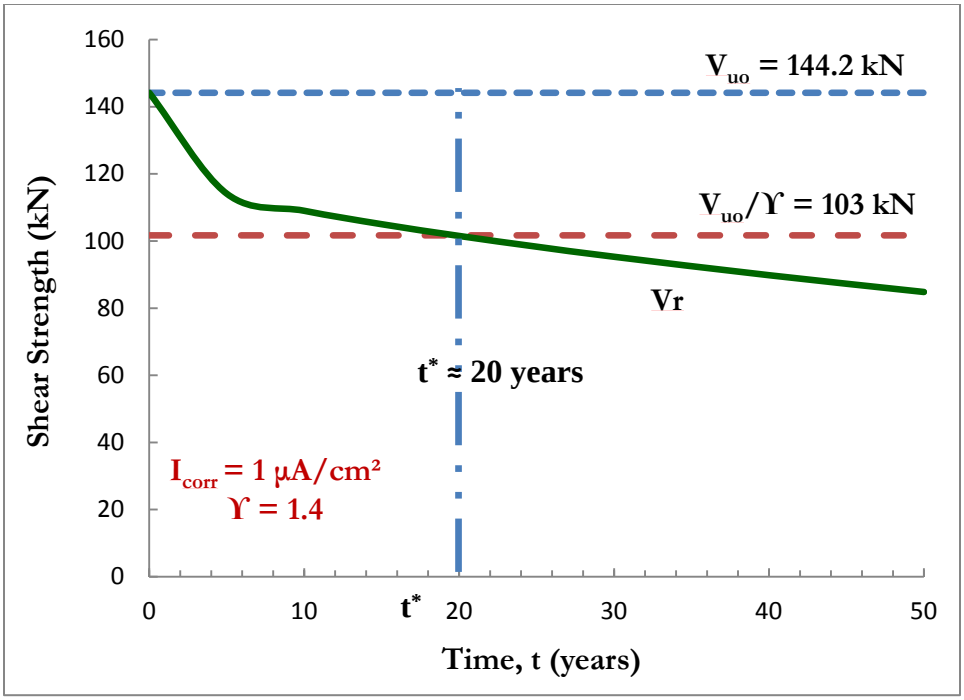

Figure 5.10: Determination of critical time, t^* for corrosion damage with γ = 1.4.

Based on the above assumed data for a beam subjected to corrosion with an intensity of 1 μA/cm², Figure 5.10 is obtained. The original shear strength V_{uo} is calculated as 144.2 kN, which is then reduced to 103 kN by using a factor γ of 1.4. The critical time $t^* \approx 20$ years, is determined up to which the predicted residual shear strength is less than the reduced level of strength, V_{uo}/γ. It can be said that the beam is safe for 20 years beyond which rehabilitation for beam is needed.

(ii) Probability of safety of corroded beam for two different corrosion density

Probability of safety (R_t) from Monte Carlo simulation is expressed as:

$$R_t = \frac{Number\ of\ counts\ satisfying\ the\ design\ equation}{Total\ number\ of\ R_t\ values\ generated}$$

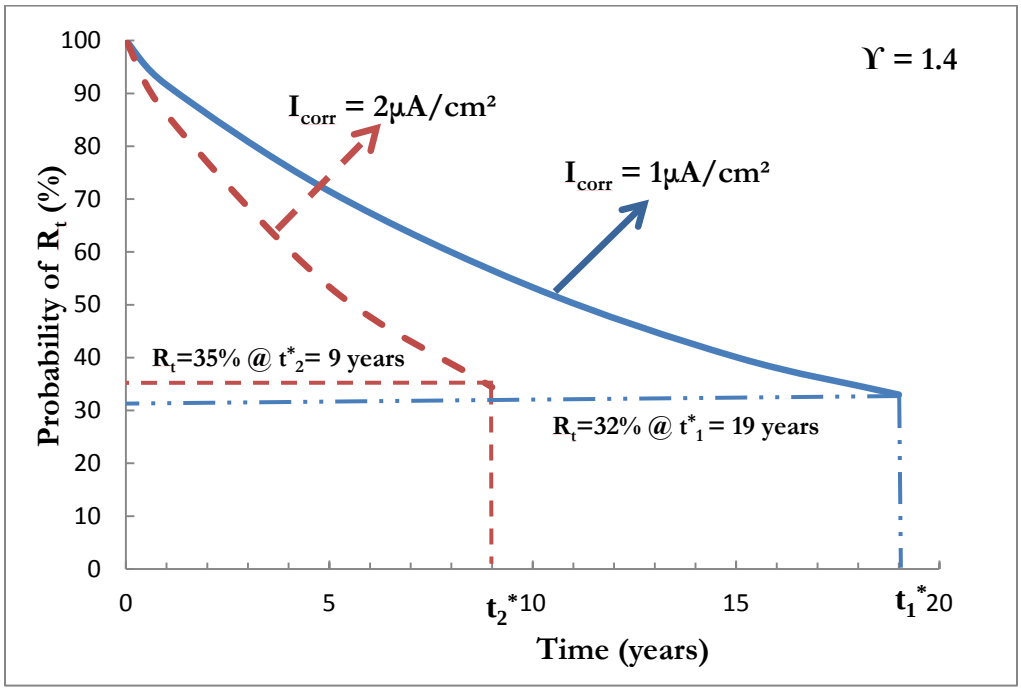

Figure 5.11: Variation of Reliability for critical time t* at two different I_{corr}.

The probability of safety with respect to critical time, t* as shown in Figure 5.11 is obtained for two different corrosion current density, I_{corr} = 1μA/cm² and 2μA/cm² with a constant factor chosen as Υ = 1.4. The critical time, t_1^* for the beam subjected to corrosion with an intensity of 1μA/cm² is obtained as 19 years with R_t of 33%. Similarly, critical time

t_2^* for the corroded beam with I_{corr} = 2μA/cm² is determined as 9 years with 35% probability of safety. It is observed that the probability of safety for beam with I_{corr} =1μA/cm² is approximately 60% at time t = 9 years as compared to the same beam subjected to corrosion with an intensity of 2μA/cm² which reaches its critical time t_2^* = 9 years with 35% probability beyond which the beam is not safe for use. Thus a method has been introduced in order to find the critical period of the corroded members before which some repair or rehabilitation works are to be undertaken to avoid the danger.

(iii) Effect on reliability and critical time due to different factor, ϒ

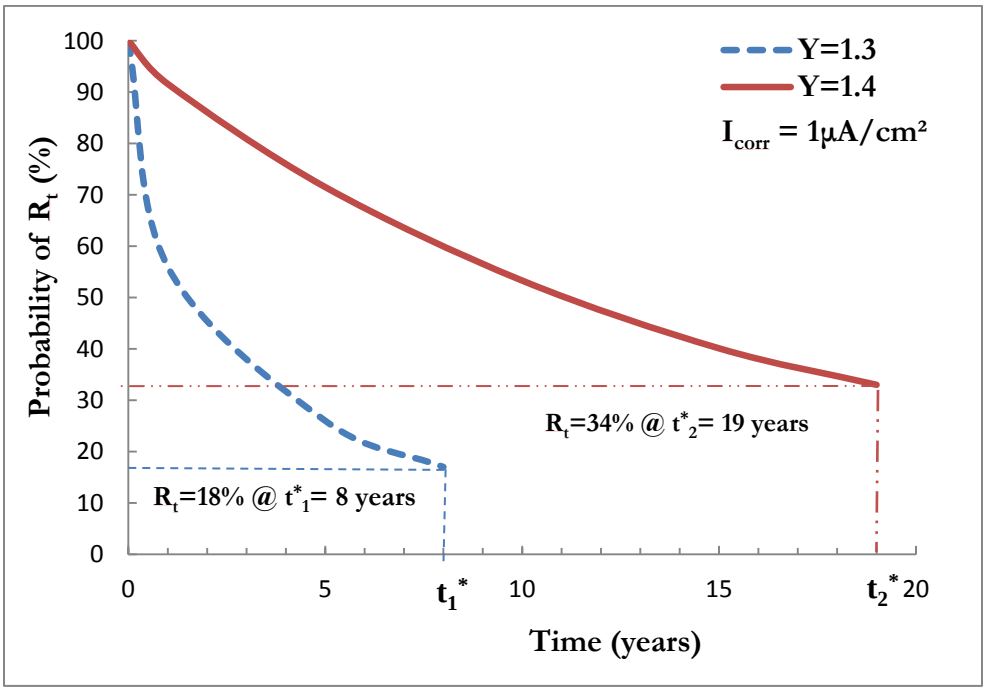

Figure 5.12: Variation of probability of safety for critical time t* for two different ϒ.

The probability with respect to critical time, t* as shown in Figure 5.12 is obtained for two different chosen factor, Υ = 1.3 and 1.4 with a constant corrosion current density, I_{corr} = 1μA/cm². The critical time, t_1^* for the beam strength when reduced to a level of 110.9 kN from the original strength value of 144.2 kN by using a factor Υ of 1.3, is determined as 8 years at which the R_t is obtained as 18%. Similarly, critical time t_2^* for the beam when Υ used as 1.4 for constant I_{corr} is determined as 19 years with a reliability of 34%. It is observed from Fig. 5.12, that the probability of safety for beam with a factor of 1.4 is approximately 62% at time t = 8 years as compared to the same beam when a factor of 1.3 is chosen which reaches its critical time t_2^* = 8 years with 18% probability beyond which the beam is considered as unsafe. Therefore the above plot gives an idea about the value of factor Υ to be chosen should be appropriate enough to obtain a marginal life of a member with regard to its safety.

CHAPTER 6

CONCLUSIONS AND RECOMMENDATIONS

6.1 CONCLUSIONS

In this experimental study, 20 reinforced concrete beam specimens were subjected to accelerated corrosion using impressed current and then they were tested in a four-point bend test to determine their residual shear strength. The following variables were used: two different cross sections of beam and two levels of corrosion period. Based on test data, the following conclusions are drawn:

1. The key parameter for the corrosion damage is the product of corrosion current density and the corrosion period, $I_{corr}T$, defined as the 'Corrosion Activity Index'. It is clear from the results that the both percentage metal loss and the loss of shear strength increase with increasing $I_{corr}T$.
2. Residual shear capacity cannot be determined simply by using reduced $A_v{}'$ alone. The crack induced damage and bond slip must be considered in determining the residual shear strength.

3. Based on the experimental data, an approach has been proposed to predict the residual shear strength of a corroded beam for which $I_{corr}T$, area of shear reinforcement, spacing of stirrups, cross-sectional details and material strengths are known. The proposed approach consists of determination of a correction factor, R_v that should be applied to correct the theoretical shear capacity of a corroded beam, calculated on the basis of reduced cross-sectional area, A_v'. This approach appears to produce satisfactory results within the range of $I_{corr}T$ used in this study.
4. Monte Carlo simulation technique has been used to predict the probability of failure of a beam subjected to a known corrosion current density based on a proposed deterministic model using pre assigned factor of safety.

6.2 SUGGESTIONS FOR FUTURE RESEARCH

The following studies are recommended in order to further strengthen the findings of this study:

1. More tests on larger diameter of shear reinforcement and different widths of beams, different spacing of stirrups has to be conducted in order to obtain a model which shows a strong agreement with the experimental outcomes.
2. More tests are required to find out the maximum level of $I_{corr}T$ below which bond loss can be ignored and the strength prediction can be made simply by using A_v' from Eq. 4.12.

3. In this study, the corrosion of reinforced concrete beams was achieved by using the accelerated corrosion technique. However, in real structures, the corrosion of reinforcement is different in many ways. One of those is the fact that the corrosion product accumulates slowly on the surface of the steel, which is not the case in accelerated corrosion test, as the rust products escape through the cracks. Another difference is that in real situations, corrosion takes place under smaller corrosion current density. It would be desirable to collect data from natural corrosion and to check the validity of the proposed model.

REFERENCES

[1] "*As Solid as Concrete*," Middle East Construction, April/May 1987, pp. 20- 21.

[2] Schutt, W. R., "*Cathodic Protection of New High- Rise Buildings in Abu- Dhabi*," Concrete International, May 1992, pp. 45-46.

[3] Page, C. L., and Treadway, K. W. J., "*Aspects of Electrochemistry of steel in concrete- Nature*," Vol. 297, 1982, pp. 109-115.

[4] Concrete Repair Manual, "*ACI International, BRE, Concrete society, and International Concrete Repair Institute (ICRI)*"; Second edition, Vol. 1, May 2003.

[5] Cabrera, J. G., "*Deterioration of Concrete Due to Reinforcement Steel Corrosion*," Cement & Concrete Composites, 18 (1996), pp. 47-59.

[6] Kimberly, E. K., and Mehta, P. K., "*A Critical Review of Deterioration of Concrete Due to Corrosion of Reinforcing Steel*", Proceedings, Fourth CANMET/ACI International conference on Durability of Concrete, Sydney, Australia, 1997, pp. 535-554.

[7] Al-Sulaimani, G. J.; Kaleemullah, M.; Basunbul, I. A.; and Rasheeduzzafar,(1990) "*Influence of corrosion and cracking on bond behavior and strength of reinforced concrete members*" ACI Structural Journal, 87(2), 220-231.

[8] Almusallam, A. A.; Al-Gahtani, A. S.; Aziz, A. R.; and Rasheeduzzafar, (1996) "*Effect of reinforcement corrosion on bond strength*" Construction and Building Materials, 10(2), 123-129.

[9] Mangat, P.S., and Elgarf, M.S., (1999) "*Flexural strength of concrete beams with corroding reinforcement*" ACI Structural Journal, 96(1), 149–158.

[10] Wang, X., and Liu, X., (2003) "*Bond strength modeling for corroded reinforcements*" Construction and Building Material, 20, 177-186.

[11] Bhargava, K.; Ghosh, A.K.; Mori, Y.; and Ramanujam, S., (2007) "*Models for corrosion-induced bond strength degradation in reinforced concrete*" ACI Structural Journal, 104 (6), 594-603.

[12] Azad, A.K.; Ahmad, S.; and Azher, S.A.; (2007) "*Residual strength of corrosion damaged reinforced concrete beams*" ACI Material Journal, 104(1), 40–47.

[13] Azam, Rizwan (2010), "*Behaviour of Shear Critical RC Beams with Corroded Longitudinal Steel Reinforcement"*, MS Thesis, Department of Civil Engineering University of Waterloo, Ontario, Canada.

[14] Sneed, L.H., (2007) "*Influence of member depth on shear strength of concrete beams*" PhD Thesis, Purdue University, West Lafayette, Indiana, USA.

[15] Sherwood, E.G.; Lubell A.S.; Bentz E.C.; and Collins, M.P., (2006) "*One way shear strength of thick slabs and wide beams*" ACI Structural Journal, 103(6), 180-190.

[16] Collins, M.P., Bentz E.C., and Sherwood, E.G., (2008) "*Where is shear reinforcement required? A review of research results and design procedures*" ACI Structural Journal, 105(5), 590-600.

[17] Dileep Kumar, P.G M.Tech, "*Shear strength of R.C.C beams without web reinforcement*".

[18] Azher, Syed Ayub (January 2005), "*A Prediction Model for the Residual Flexural Strength of Corroded Reinforced Concrete Beam*," M.S Thesis Civil Engineering Department, King Fahd University of Petroleum and Minerals.

[19] West, J., (1999) "*Durability design of post-tensioned bridge substructures*" PhD Thesis, University of Texas at Austin, Texas, USA.

[20] Azad, A.K. and Ahmad, S. (2004), "*Prediction of residual strength of corrosion-damaged reinforced concrete beams*," Final Report SABIC 2002/02, King Fahd University of Petroleum & Minerals (KFUPM), Dhahran, Saudi Arabia.

[21] Federation Internation du Beton (fib), (2000) "*Bond of Reinforcement in Concrete, State-of-Art Report*" International Federation for Structural Concrete, Switzerland.

[22] EL Maaddawy, T. A., and Soudki, K. A., (2003) "*Effectiveness of impressed current technique to simulate corrosion of steel reinforcement in concrete*" Journal of Materials in Civil Engineering, ASCE, 15(3), 41-47.

[23] Ouglova, A.; Berthaud, Y.; Foct, F.; Francois, M.; Ragueneau, F.; and Petre-Lazar, I., (2008) "*The influence of corrosion on bond properties between concrete and reinforcement in concrete structures*" Materials and Structures, 41, 969-980.

[24] Fang, C.; Lundgren, K.; Chen, L.; and Zhu, C., (2004) "*Corrosion influence on bond in reinforced concrete*" Cement and Concrete Research, 34(11), 2159-2167.

[25] Amleh, L., and Mirza, S., "*Corrosion influence on bond between steel and concrete*," ACI Structural Journal, Vol. 96, No.3, May-June 1999, pp. 415- 423.

[26] Fu, X., and Chung, D. D. L., "*Effect of corrosion on the bond between concrete and steel rebar,*" Cement and Concrete Research, Vol. 27, No. 12, 1997, pp. 1811-1815.

[27] Auyeung, Y., Balaguru, P., and Chung, L., "*Bond behavior of corroded reinforcement bars,*" ACI Materials Journal, Vol. 97, No. 2, March-April, 2000, pp. 214-220.

[28] Cabrera, J. G., and Ghoddoussi, P., "*The effect of reinforcement corrosion on the strength of the steel/concrete interface*", Proceedings, International Conference on Bond in Concrete, Riga, Latvia, October 15-17, 1992, pp. 10/11 to 10/24.

[29] Ravindrarajah, R., and Ong, K., "*Corrosion of Steel in Concrete in Relation to Bar Diameter and Cover Thickness*", ACI Special Publication, Volume 100/4, April 1987, pp. 1667-1678.

[30] Tarek Uddin, M., Nobuaki, O., Makota, H., and Tsunenori, S., "*Effect of crack width and bar types on corrosion of steel in concrete*", Journal of Materials in Civil Engineering, Vol. 13, No. 3, May/June, 2001, pp. 194-201.

[31] Ting, S.C., and Nowak, A. S., "*Effect of Reinforcing Steel Area Loss on Flexural Behavior of Reinforced Concrete Beams*," ACI Structural Journal, May-June 1991, pp. 309-314.

[32] Huang, R., and Yang, C. C., "*Condition Assessment of Reinforced Concrete Beams Relative to Reinforcement Corrosion*," Cement and Concrete Composites, 19 (1997), pp. 131-137.

[33] Yoon, S., Wang, K., Weiss W. J., and Shah, S. P., "*Interaction between Loading, Corrosion, and Serviceability of Reinforced Concrete*", ACI Materials Journal, Vol. 97, No. 6, November-December 2000, pp. 637- 644.

[34] Rodriguez, J., Ortega, L. M., and Casal, J., (1997)"*Load carrying capacity of concrete structures with corroded reinforcement*" Construction and Building Materials, 11(4), 239-248.

[35] Uomoto, T., and Misra, S., "*Behaviour of concrete beams and columns in marine environment when corrosion of reinforcing bars take place*," ACI Special Publication SP-109-6, 1988, pp. 127-145.

[36] Tachibana, Y., Maeda, K. I., Kajikawa, Y., and Kawamura, M., "*Mechanical behaviour of RC beams damaged by corrosion of reinforcement*", Third International Symposium on Corrosion of reinforcement in Concrete Construction, Wishaw, UK, 1990, pp. 178-187.

[37] Jin, W.L., and Zhao, Y. X., "*Effect of corrosion on bond behavior and bending strength of reinforced concrete beams*", Journal of Zheijang University (SCIENCE), Vol. 2, No. 3, July-September 2001, pp. 298-308.

[38] Cabrera, J. G., "Deterioration *of Concrete Due to Reinforcement Steel Corrosion*," Cement & Concrete Composites, 18 (1996), pp. 47-59.

[39] Nokhasteh, M. A., Eyre, J. R., and Mcleish, A., "*The effect of reinforcement corrosion on the strength of reinforced concrete members*", Structural Integrity Assessment, Elsevier Applied Science, 1992, pp. 314- 325.

[40] Hognestad, E., Hanson, N. W., and McHenry, D., "*Concrete stress distribution in ultimate strength design*", Proceedings, American Concrete Institute, Vol. 52, 1955-56, pp. 455-479.

[41] Aziz, A.R., "*Reduction in bond and the strength of slabs due to corrosion of reinforcement*", M.S.Thesis, King Fahd University of Petroleum and Minerals, June, 1994.

[42] Val, D, V., (2007) "*Deterioration of strength of RC beams due to corrosion and its influence on beam reliability*" Journal of Structural Engineering, 133(9), 1297-1306.

[43] Cairns, J., (1995) "Strength *in shear of concrete beams with exposed reinforcement*" Proceedings of the Institution of Civil Engineers: Structures and Buildings, 110(2), 176-185.

[44] Raoof, M.,and Lin, Z., (1997) "*Structural characteristics of RC beams with exposed main steel*" Proceedings of the Institution of Civil Engineers: Structures and Buildings, 122(1),35-51.

[45] Jeppsson, J., and Thelandersson, S., (2003) "*Behavior of reinforced concrete beams with loss of bond at longitudinal reinforcement*" Journal of Structural Engineering, 129(10), 1376-1383.

[46] Toongoenthong, K., and Maekawa, K., (2004) "*Interaction of pre-induced damages along main reinforcement and diagonal shear in RC members*" Journal of Advanced Concrete Technology, 2(3), 431-443.

[47] Regan, P. E., and Kennedy Reid, I. L., (2004) "*Shear strength of RC beams with defective stirrup anchorages*" Magazine of Concrete Research, 56(3),159-166.

[48] Toongoenthong, K., and Maekawa, K., (2005) "*Multi-mechanical approach to structural performance assessment of corroded RC members in shear*" Journal of Advanced Concrete Technology, 3(1), 107-122.

[49] Higgins, C., and Farrow, W. C., (2006) "*Tests of reinforced concrete beams with corrosion damaged stirrups*" ACI Structural Journal, 103(1),133-41.

[50] Suffern, C.A., (2008) "*Shear behaviour of disturbed regions in reinforced concrete beams with corrosion damaged Stirrups*" MASc Thesis, University of Waterloo, Waterloo, Ontario, Canada.

[51] Zhao, Y., Chen, J., and Jin, W., (2009) "*Design of shear strengths of corroded reinforced concrete beams*" International Journal of Modeling, Identification and Control,7(2),190-198.

[52] Xu, S., Niu, D., (2003) "*The shear behavior of corroded reinforced concrete beam*" International Conference on Advances in Concrete and Structures.

[53] Xiao-Hui, W., and Xia-La, L., (2008) "*Modelling the flexural carrying capacity of corroded RC beam*" Journal of Shanghai Jiaotong University, 13(2), 129–135.

[54] Al-Gohi, B.H.A. (May 2008), "*Time-dependent modeling of loss of Flexural Strength of Corroding Reinforced Concrete Beams*," M.S Thesis Civil Engineering Department, King Fahd University of Petroleum and Minerals.

[55] A.K. Azad, S. Ahmad and B.H. Al-Gohi, (2010) "*Flexural strength of corroded reinforced concrete beams*" Magazine of Concrete Research, 62, No. 6, 405-414.

[56] Ijsseling, F.P. (1986), "*Application of electrochemical methods of corrosion rate determination to system involving corrosion product layers*," British Corrosion Journal, Vol. 21, No. 2, pp. 95-101.

[57] Yubun, A., Balaguru, P., and Lan, C., "*Bond behavior of corroded reinforcement bars*", ACI Materials Journal, Vol. 97, No.2, March-April 2000, pp. 214-220.

[58] Ballim, Y., and Reid, J. C., "*Reinforcement corrosion and deflection of RC beams- an experimental critique of current test methods*", Cement and Concrete Composites, Vol. 25, 2003, pp. 625-632.

[59] Zhang, P. S., Lu, M., and Li, X.Y., "*Mechanical property of rustiness in reinforcement steel*", Industrial Construction, 25, 1995, pp. 41-44.

[60] Xi, W.L., Li, R., Lin, Z. S., et al., "*Experimental studies on the property before and after reinforcement corrosions in basic concrete members*", Industrial Construction, 27, 1997, pp. 14-18.

[61] Almusallam, A. A., "*Effect of degree of corrosion on the properties of reinforcing steel bars*", Construction and Building Materials, Vol. 15, 2001, pp. 361-368.

[62] Mehta, P. K., (1993). "*Concrete Structures, Properties and Materials*," Prentice-Hall Inc.

[63] Dimitri, V. V., " *Deterioration of Strength of RC Beams due to corrosion and its influence on Beam Reliability*", Journal of Structural Engineering, ASCE, Volume 133, No 9, 2007, pp. 1297-1306.

[64] Capra, B., Bernard, O. and Gerard, B., "*Reliability assessment of reinforced concrete beam subjected to corrosion*", 17th International Conference on Structural Mechanics in Reactor Technology, August 17-22, 2003.

[65] Warner, R.F. and Kabaila, "*Monte Carlo study of structural safety*", American Society of Civil Engineers, Journal of Structural Division, Vol. 94, No ST12, December 1968, pp. 2847-2859.

[66] Allen, D.E., "*Probabilistic study of reinforced concrete in bending*", Technical paper NRC 11139, National Research Council of Canada, Ottawa, 1970.

[67] Choi, B.S. and Kwon, Y.W., "*Probabilistic analysis of reinforced concrete beam and slab deflections using Monte Carlo simulation*", KCI Concrete Journal, Vol. 12, No. 2, 20

[68] Arafah, A., "*Reliability-based criterion for maximum reinforcement ratio of reinforced concrete beam sections*", King Saud University.

[69] Arafah, A. M., "*Statistics for Concrete and Steel Quality in Saudi Arabia*," Magazine of Concrete Research, London, Vol. 49, No. 180, September 1997, pp. 185-194.

[70] Kapilesh, B., Yasuhiro, M., Ghosh, A.K., "*Time-dependent reliability of corrosion affected RC beams—Part 1: Estimation of time-dependent strengths and associated variability*", Nuclear Engineering and Design, 241 (2011) 1371–1384.

[71] Juarez, C.A., Guevara, B., Fajardo, G. and Castro-Borges, P., "*Ultimate and nominal shear strength in reinforced concrete beams deteriorated by corrosion*", Engineering Structures, Vol. 33, 2011, pp. 3189-3196.

LIST OF NOTATIONS

A_v = cross-sectional area of uncorroded stirrup

$A_v{}'$ = cross-sectional area of corroded reinforcement

b = width of beam

R_f = Correction factor $(\frac{V_{exc}}{V_{thc}})$

C_c = $\frac{V_{exu}}{V_{thu}}$

D' = diameter of corroded stirrup

D = diameter of uncorroded stirrup

d = effective depth of beam

s = spacing of shear reinforcement

F = Faraday's constant (96487 A-sec)

$f_c{}'$ = 28-day compressive strength of concrete

h = depth of the beam

f_y = yield strength of reinforcing bar

I_{app} = applied corrosion current density

I_{corr} = actual corrosion current density

$I_{corr}T$ = corrosion activity index

J_r = corrosion rate, i.e. loss of metal per unit surface area per unit time

V_c = shear strength contributed by concrete

V_s = shear strength contributed by shear reinforcement

$V_s{}'$ = shear strength based on reduced diameter of stirrups due to corrosion

V_n = nominal shear strength of beam

V_{exc} = experimental ultimate shear capacity of corroded beams

V_{exu} = experimental ultimate shear capacity of uncorroded beams

V_{res} = predicted residual strength of the beam = $R_v V_{thc}$

V_{thc} = theoretical ultimate shear capacity of corroded beams

V_{thu} = theoretical ultimate moment capacity of control (uncorroded) beams

P_r = penetration rate, i.e. reduction in the rebar diameter per unit time

R = percentage residual strength of a corroded beam

T = corrosion duration

W = equivalent weight of steel (27.9 g)

α = $\frac{2P_r T}{D}$

γ_{st} = density of steel (7.85 g/cm^3)

ρ = percentage weight loss, i.e. degree of corrosion induced through accelerated test.

R_t = reliability of beam

P_f = probability of failure

APPENDIX A

Load Deflection Curves

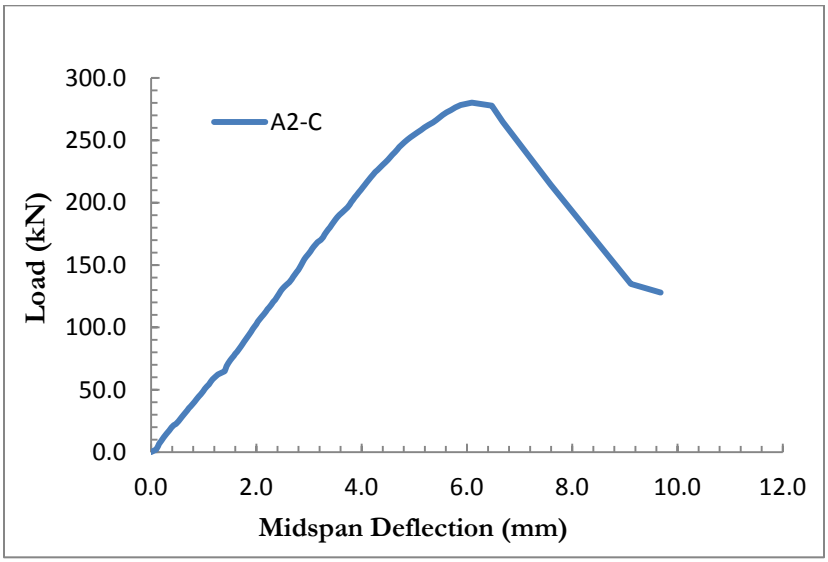

Figure A. 1: Load-midspan deflection plot for Control Specimen A2-C.

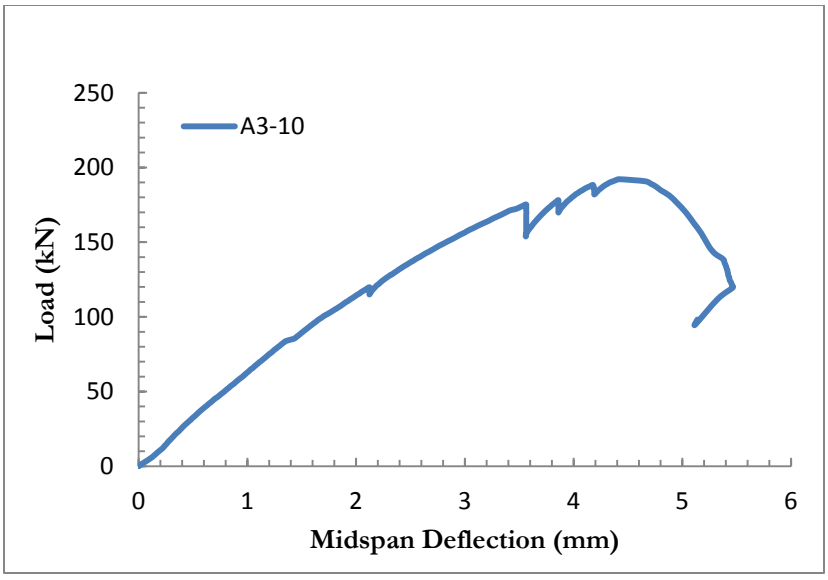

Figure A. 2: Load-midspan deflection plot for Corroded Specimen A3-10.

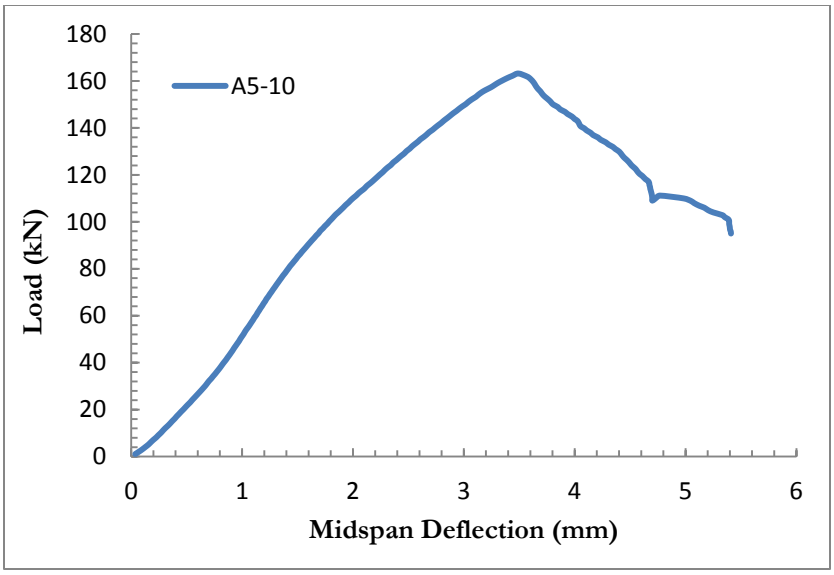

Figure A. 3: Load-midspan deflection plot for Corroded Specimen A5-10.

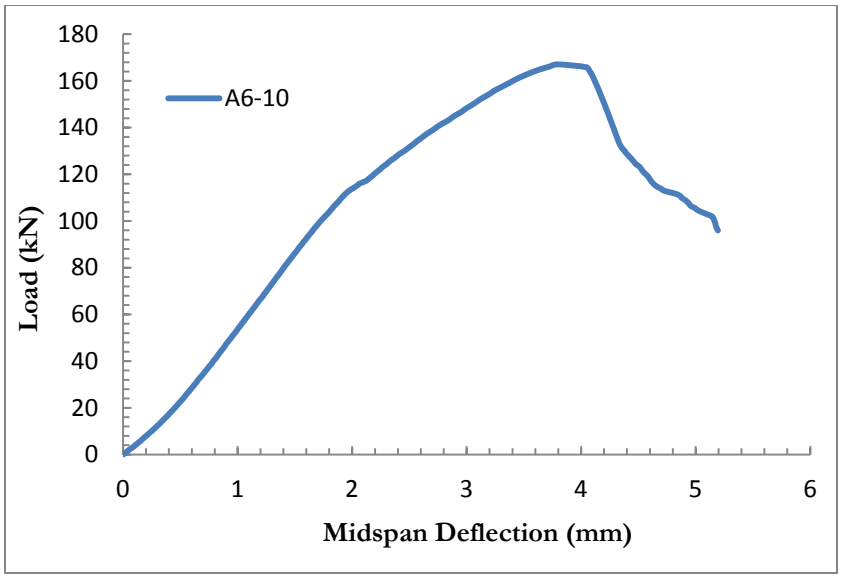

Figure A. 4: Load-midspan deflection plot for Corroded Specimen A6-10.

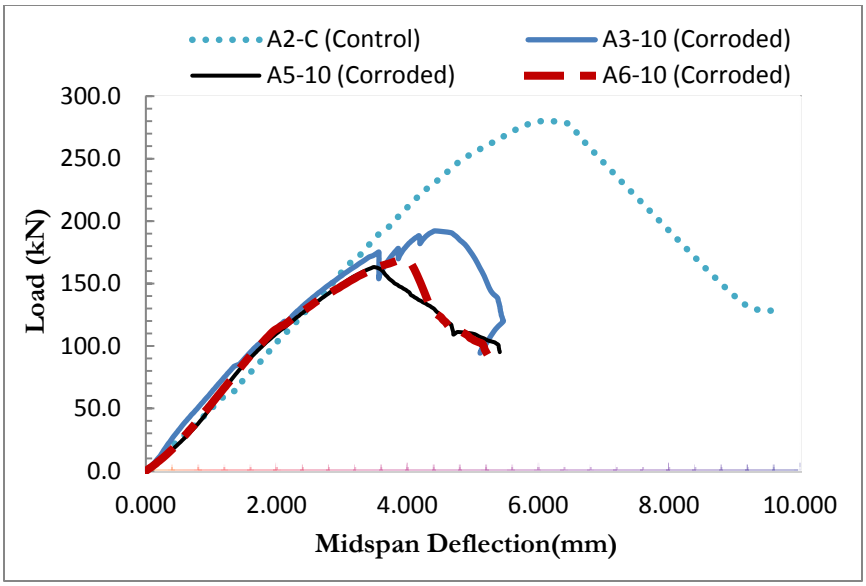

Figure A. 5: Load-midspan deflection plot for beams (Group A) corroded for 10 days.

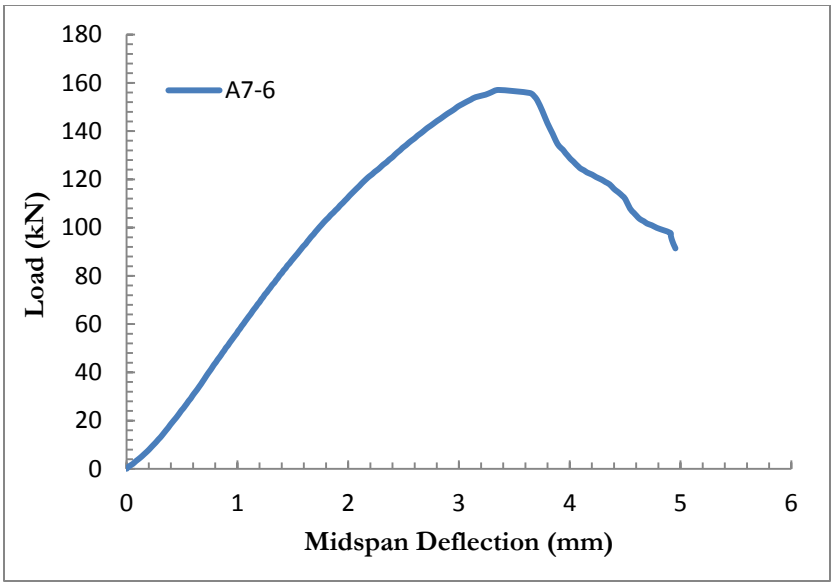

Figure A. 6: Load-midspan deflection plot for Corroded Specimen A7-6.

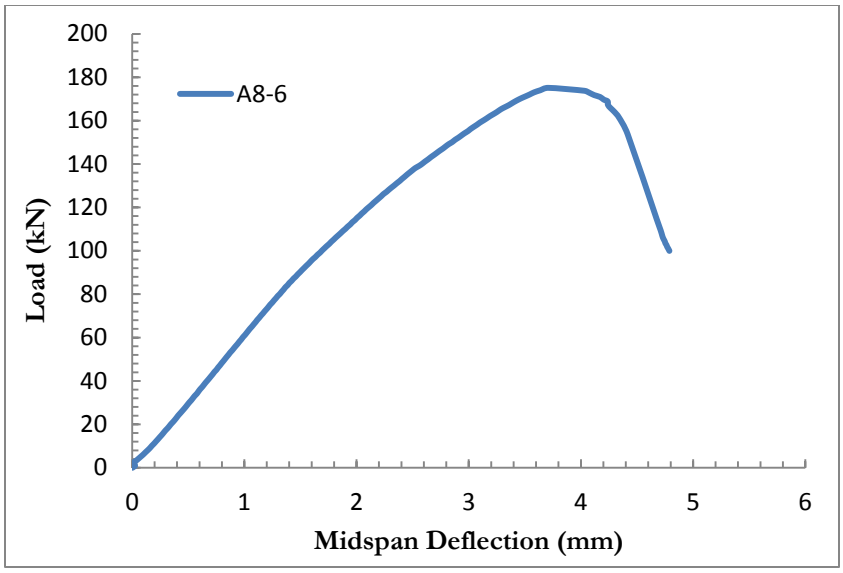

Figure A. 7: Load-midspan deflection plot for Corroded Specimen A8-6.

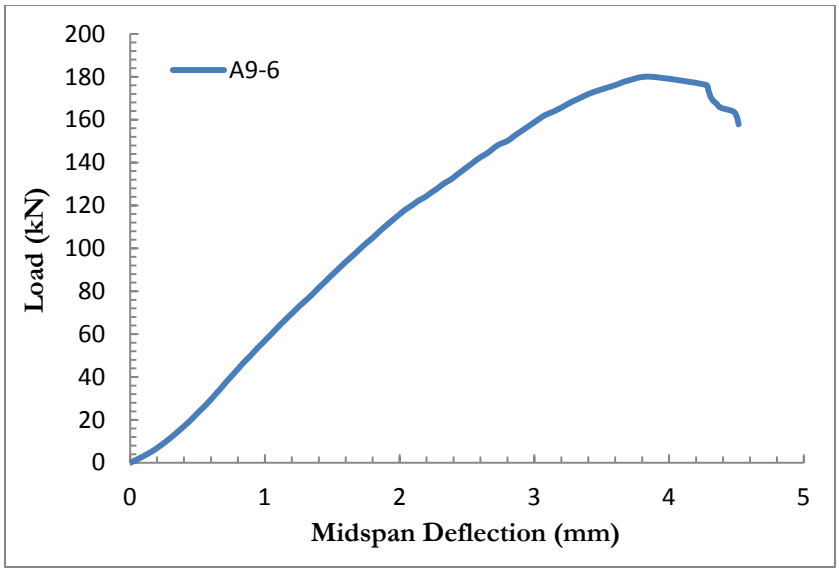

Figure A. 8: Load-midspan deflection plot for Corroded Specimen A9-6.

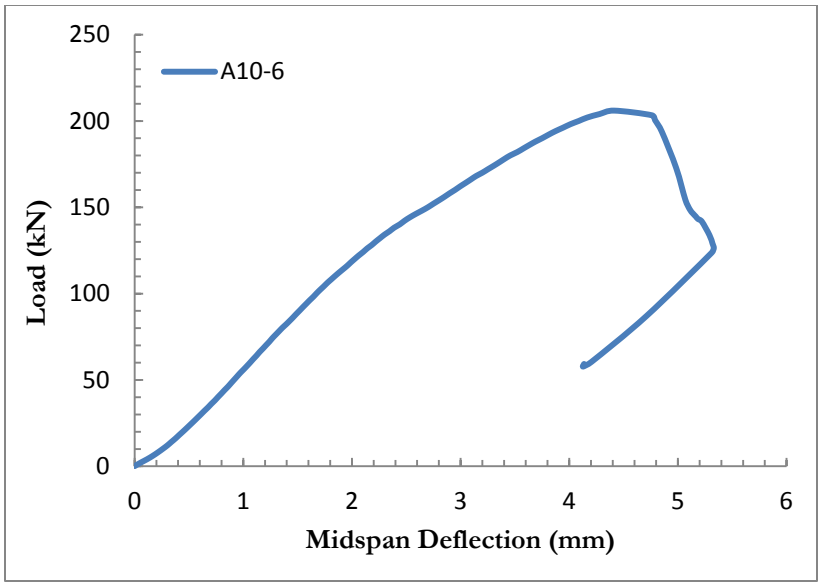

Figure A. 9: Load-midspan deflection plot for Corroded Specimen A10-6.

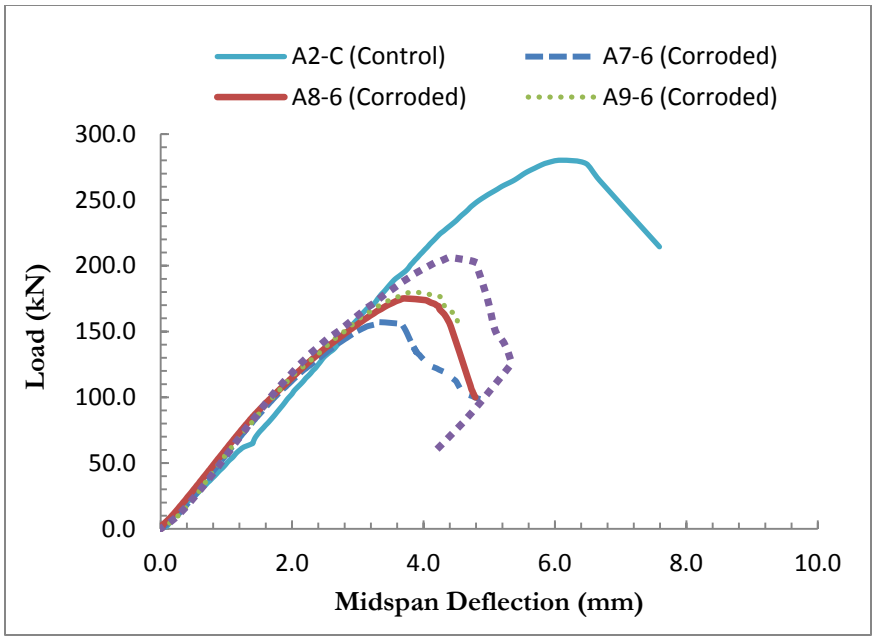

Figure A. 10: Load-midspan deflection plot for beams (Group A) corroded for 6 days.

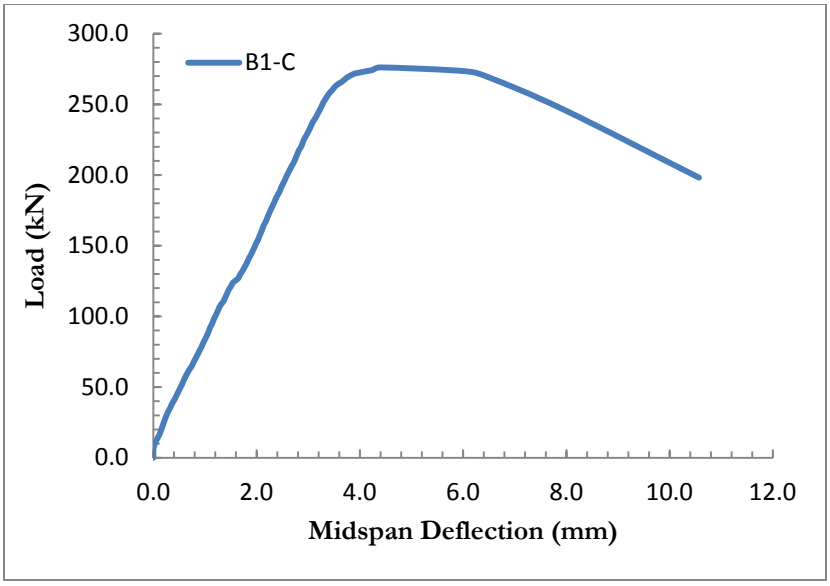

Figure A. 11: Load-midspan deflection plot for Control Specimen B1-C.

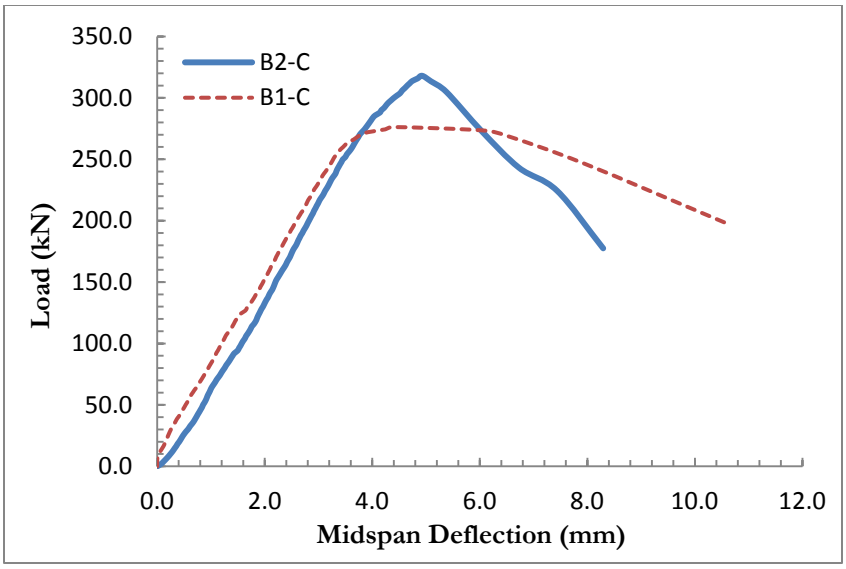

Figure A. 12: Load-midspan deflection plot for two Control Specimens from Group B.

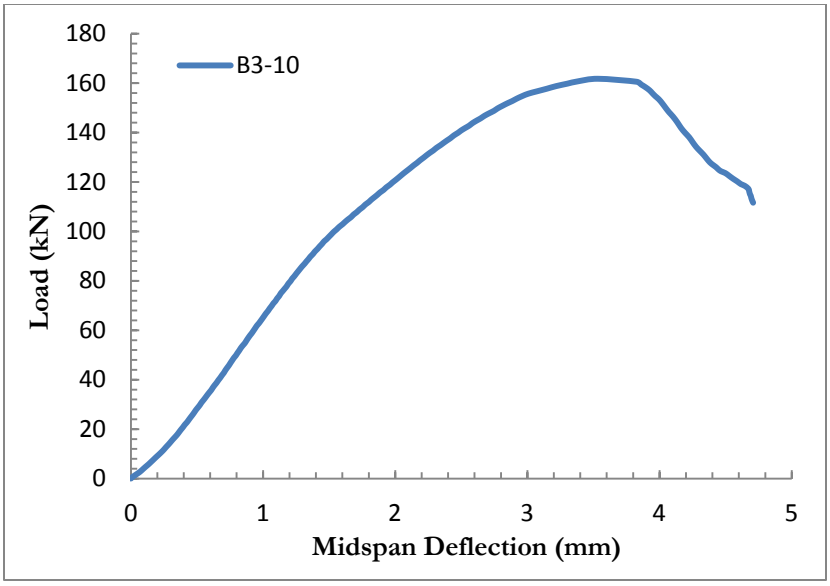

Figure A. 13: Load-midspan deflection plot for Corroded Specimen B3-10.

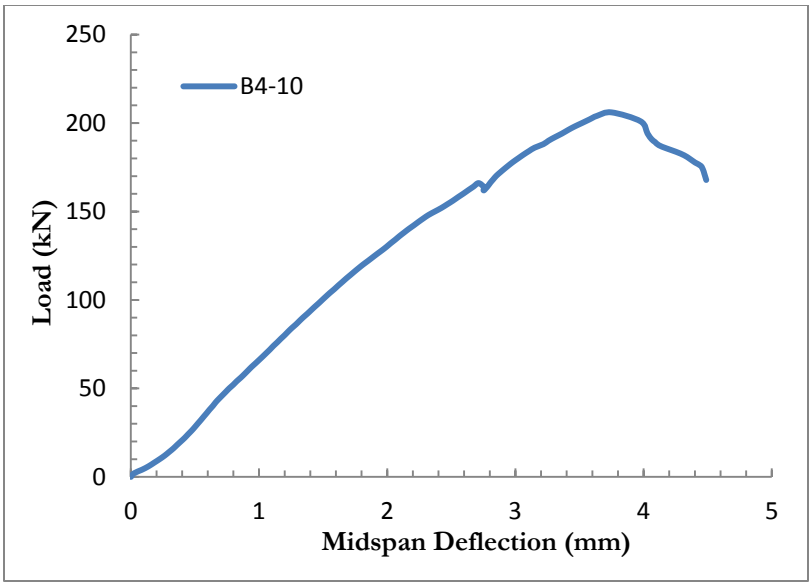

Figure A. 14: Load-midspan deflection plot for Corroded Specimen B4-10.

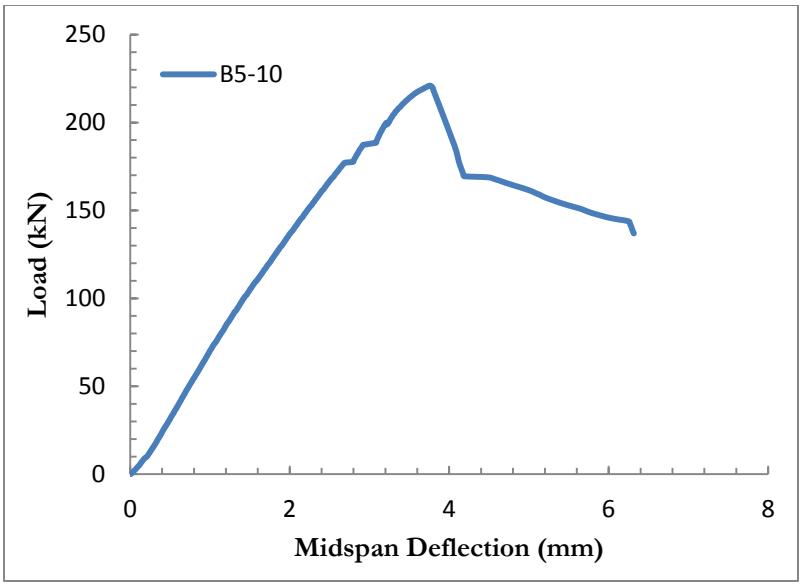

Figure A. 15: Load-midspan deflection plot for Corroded Specimen B5-10.

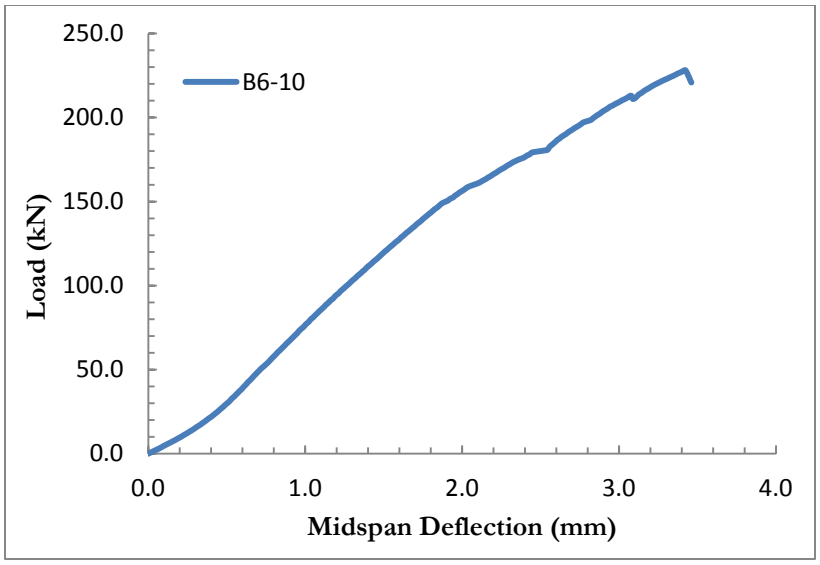

Figure A. 16: Load-midspan deflection plot for Corroded Specimen B6-10.

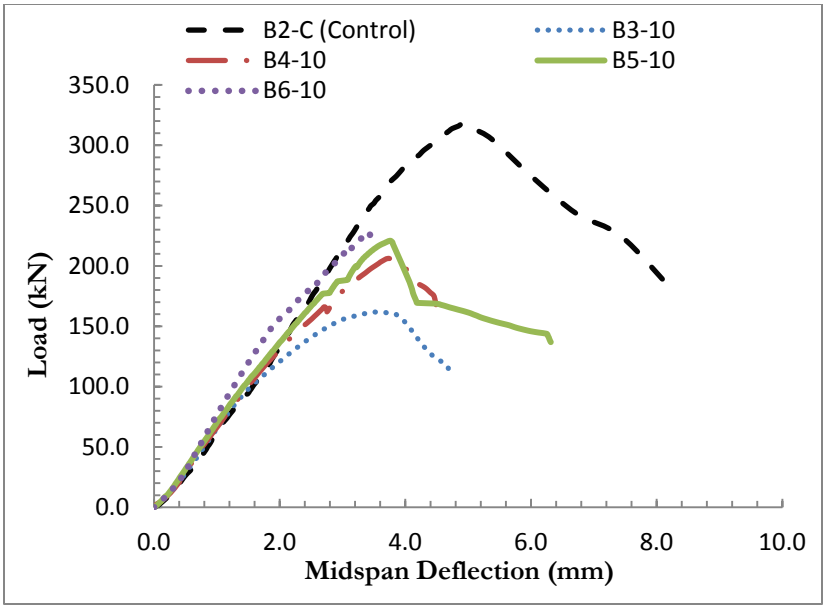

Figure A. 17: Load-midspan deflection plot for beams (Group B) corroded for 10 days.

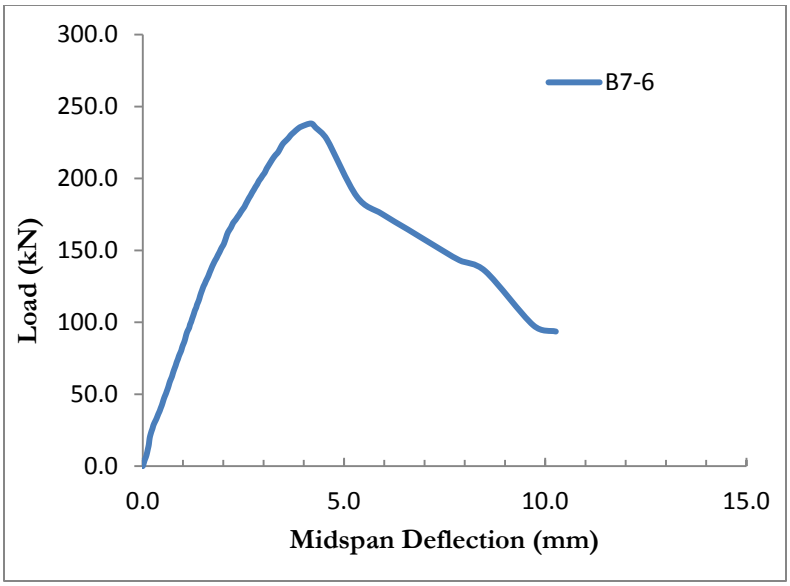

Figure A. 18: Load-midspan deflection plot for Corroded Specimen B7-6.

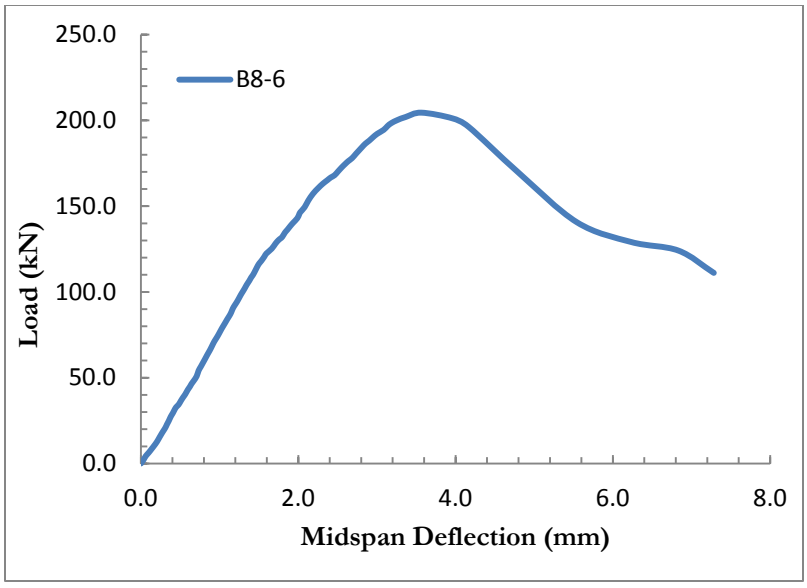

Figure A. 19: Load-midspan deflection plot for Corroded Specimen B8-6.

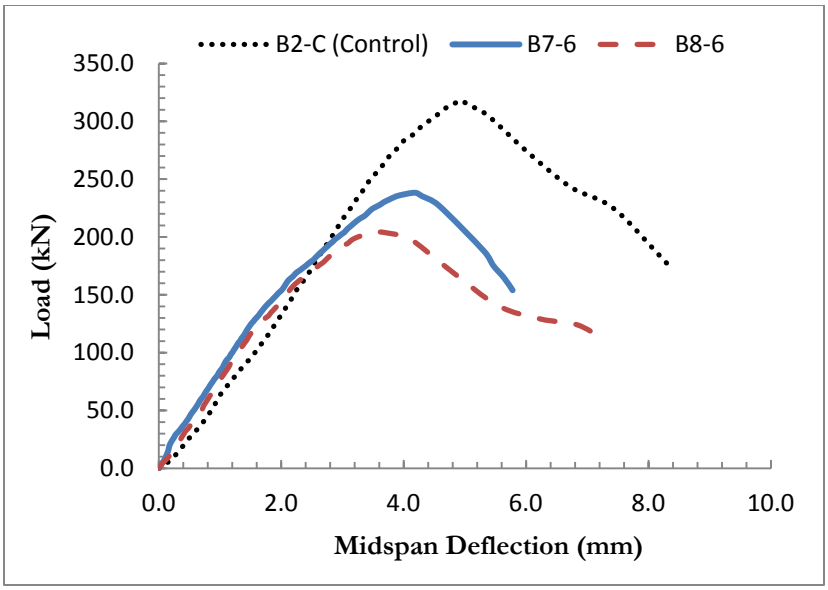

Figure A. 20: Load-midspan deflection plot for beams (Group B) corroded for 6 days.

APPENDIX B

Applications of the model

The following two examples have been presented to illustrate the application of the proposed model.

Example # 1

A reinforced concrete beam (effective depth = 220 mm, width = 160 mm, 2 legged shear reinforcement = 8 mm dia @ 100 mm c/c spacing, f_c' = 45 N/mm^2 and f_y = 500 N/mm^2) has been subjected to an active corrosion for a period of 20 years. The measured I_{corr} = 2.0 μA/cm^2. Determine the percentage residual shear strength of the beam.

Solution:

T = 20 years = 7300 days

I_{corr} = 2.0 μA/cm^2 = 0.002 mA/cm^2

$I_{corr}T = 0.002 \times 20 = 0.04\ mA - year/cm^2$

$d = 220\ mm$

$bw = 160\ mm$

Diameter of stirrups = 8 mm

$A_v = 2 \times \frac{\pi}{4} \times (D)^2 = 100.53\ mm^2$

As per ACI 318:

$$V_{thu} = V_c + V_s$$

Hence, from Eq. 4.2 and 4.3,

$$V_c = 2\sqrt{(f_c')} \times b_w \times d$$

$$V_c = 2\sqrt{6525} \times 6.3 \times 8.66 = 8814.11\ lb$$

$$= 8814.11 \times 4.448 = 39205.18\ N$$

$$V_c = 39.21\ kN$$

$$V_s = \frac{A_v f_y d}{s} = \frac{100.53 \times 500 \times 220}{100} = 110583\ N\ or\ 110.6\ kN$$

$$V_{thu} = V_c + V_s$$

$$V_{thu} = 39.21 + 110.6 = \mathbf{149.81\ kN}$$

From Eq. 4.10

$$P_r = \frac{W}{F\gamma_{st}} I_{corr} = \frac{27.925 \times 10}{96487 \times 7.85 \times 1000} \times 365 \times 24 \times 60 \times 60 I_{corr}$$

$$= 11.6253 \times 0.002$$

$$= 0.02325\ mm/year$$

$$\alpha = \frac{2P_r T}{D} = 0.1162$$

From Eq. 4.12

$$A_v' = A_v(1 - \alpha)^2 = 100.53 \times \{1 - 0.1162\}^2 = 78.52\, mm^2$$

Hence,

$$V_s' = \frac{A_v' f_y d}{s} = \frac{78.52 \times 500 \times 220}{100} = 86.38\, kN$$

$$V_{th,c} = V_c + V_s'$$

$$V_{th,c} = 39.21 + 86.38 = \mathbf{125.6\ kN}$$

Now, from Eq. 5.3, correction factor R_v is calculated as:

$$I_{corr}T = 0.002 \times 20 = 0.04\, mA - year/cm^2$$

$$\frac{A_v}{ds} = \frac{100.53}{220 \times 100} = 0.00457$$

$$R_v = 1 - \{0.88 \times (0.04)^{0.132} \times (0.00457)^{0.154}\} = 0.749$$

From Eq. 5.1, the predicted residual shear strength of the beam is calculated as:

$$\boldsymbol{V_{res} = R_v V_{th,c} = 0.749 \times 131.35 = 98.38\ kN}$$

Percentage residual shear strength of the beam is:

$$\boldsymbol{R(\%) = \frac{V_{res}}{V_{thu}} \times 100 = \frac{98.38}{149.81} \times 100 = 65.7\%}$$

Example # 2

Specify the permissible limit of I_{corr} so that the shear strength of a beam (effective depth = 220 mm, width = 160 mm, 2 legged shear reinforcement = 8 mm dia @ 100 mm c/c spacing, f_c' = 45 N/mm^2 and f_y = 500 N/mm^2) would not fall below 85% due to reinforcement corrosion during a period of 40 years.

Solution:

T = 40 years

$I_{corr} = ?$

Diameter of stirrup = 8 mm

R = 85%

$A_v = 2 \times \frac{\pi}{4} \times (D)^2 = 100.53\ mm^2$

$d = 220\ mm$

$bw = 160\ mm$

As per ACI 318:

$V_{thu} = V_c + V_s$

Hence, from Eq. 4.2 and 4.3,

$V_c = 2\sqrt{(f_c')} \times b_w \times d$

$V_c = 2\sqrt{6525} \times 6.3 \times 8.66 = 8814.11\ lb$

$= 8814.11 \times 4.448 = 39205.18\ N$

$V_c = 39.21\ kN$

$$V_s = \frac{A_v f_y d}{s} = \frac{100.53 \times 500 \times 220}{100} = 110583\ N\ or\ 110.6\ kN$$

$$V_{thu} = V_c + V_s$$

$$V_{thu} = 39.21 + 110.6 = \mathbf{149.81\ kN}$$

$$R(\%) = \frac{V_{res}}{V_{thu}} \times 100 = 85\ (given)$$

$$\Rightarrow V_{res} = 0.85 \times V_{thu} = 0.85 \times 149.81 = 127.34\ kN$$

From Eq. 4.10

$$P_r = \frac{W}{F\gamma_{st}} I_{corr} = \frac{27.925 \times 10}{96487 \times 7.85 \times 1000} \times 365 \times 24 \times 60 \times 60 I_{corr}$$

$$= 11.6253 \times I_{corr}\ mm/year$$, where I_{corr} is in mA/cm^2

$$\alpha = \frac{2P_r T}{D} \Rightarrow \alpha = \frac{2 \times 11.6253 I_{corr} \times 40}{8} = 116.25 I_{corr}$$

$$\Rightarrow I_{corr} = 0.0086\ \alpha \quad \text{(i)}$$

From Eq. 5.3,

$$R_v = 1 - \left\{0.88 \times\ (0.0086\ \alpha \times 40)^{0.132}\ \times \left(\frac{100.53}{220 \times 100}\right)^{0.154}\right\}$$

$$= 1 - (0.3334 \times \alpha^{0.132})$$

From Eq. 5.1,

$$V_{th,c} = \frac{V_{res}}{R_v} = \frac{127.34}{1 - (0.3334 \times \alpha^{0.132})} \quad \text{(ii)}$$

From Eq. 4.12

$$A_v' = A_v(1 - \alpha)^2 = 100.53 \times (1 - \alpha)^2\ mm^2$$

$$V_s' = \frac{A_v' f_y d}{s} = \frac{100.53 \times (1-\alpha)^2 \times 500 \times 220}{100} = 110583 \times (1 - \alpha)^2$$

$$V_{th,c} = V_c + V_s' = 39.21 + 110583 \times (1 - \alpha)^2 \quad \text{(iii)}$$

From Eqs. (ii) and (iii):

$$\frac{127.34}{1-(0.3334 \times \alpha^{0.132})} = 39.21 + 110583 \times (1 - \alpha)^2$$

Solving the above equation by trial and error, the value of α is calculated as:

$$\alpha = 0.963$$

Substituting the value of α in Eq. (i), the value of I_{corr} is calculated as:

$$\boldsymbol{I_{corr} = 0.0086 \times 0.963 = 0.0083\ mA/cm^2}$$ **or 8.3** $\boldsymbol{\mu A/cm^2}$

VITAE

NAME : Ashhad Imam

NATIONALITY : Indian

PERMANENT ADDRESS : Mohalla Muslim Road,

P.O. & District: Nawada,

Pin Code: 805110, Bihar, India.

PRESENT ADDRESS : P.O. Box 8653, Student Housing,

Kfupm, KSA.

EMAIL : ashhad.ce@gmail.com

PHONE NO : +966561986745

EDUCATIONAL QUALIFICATIONS

Master of Science in Civil Engineering (Structures)

Feb, 2010 – May 2012

King Fahd University of Petroleum & Minerals,

Dhahran, Saudi Arabia.

Bachelor of Technology (Civil Engineering)

Aug. 2005 – June 2009

Jamia Millia Islamia, New Delhi, India.